

DISSERTATION

THE HYDROMETEOROLOGICAL SUSTAINABILITY OF *MISCANTHUS* × *GIGANTEUS*
AS A BIOFUEL CROP IN THE US MIDWEST

Submitted by

Gavin R. Roy

Department of Atmospheric Science

In partial fulfillment of the requirements

For the Degree of Doctor of Philosophy

Colorado State University

Fort Collins, Colorado

Fall 2016

Doctoral Committee:

Advisor: Christian Kummerow

David Randall
Elizabeth Barnes
Jeffrey Niemann
Christa Peters-Lidard

Copyright by Gavin R. Roy 2016

All Rights Reserved

ABSTRACT

THE HYDROMETEOROLOGICAL SUSTAINABILITY OF *MISCANTHUS × GIGANTEUS* AS A BIOFUEL CROP IN THE US MIDWEST

Miscanthus × giganteus (*M. × giganteus*) is a dense, 3-5 m tall, productive perennial grass that has been suggested to replace corn as the principal source of biofuel for the US transportation industry. However, cultivating a regime of this water-intensive rhizomatous crop across the US Midwest may not be agronomically realistic if it is unable to survive years of low precipitation or extreme cold wintertime soil temperatures, both of which have previously killed experimental crops. The goal of this research was to use a third-generation land surface model (LSM) to provide a new assessment of the hypothetical biogeophysical sustainability of a regime of *M. × giganteus* across the US Midwest given that, for the first time, a robust and near-complete dataset over a large area of mature *M. × giganteus* was available for model validation. Modifications to the local hydrology and microclimate would necessarily occur in areas where *M. × giganteus* is adapted, but a switch to this biofuel crop can only occur where its intense growing season water usage (up to 600 mm) and wintertime soil temperature requirements (no less than -6° C) are feasibly sustainable without irrigation.

The first step was to interpret the observed turbulent and ecosystem flux behavior over an extant area of mature *M. × giganteus* and replicate this behavior within the SiB3 third-generation LSM (Simple Biosphere Model, version 3). A new vegetation parameterization was developed in SiB3 using several previous empirical studies of *M. ×*

giganteus as a foundation. The simulation results were validated against a new, robust series of turbulent and ecosystem flux data taken over a four-hectare experimental crop of *M. × giganteus* in Champaign, IL, USA from 2011-2013.

Wintertime mortality of *M. × giganteus* was subsequently assessed. It was proposed that areas with higher seasonal snowfall in the US Midwest may be favorable for *M. × giganteus* sustainability and expansion due to the significant insulating effect of snow cover. Observations of snow cover and air and soil temperatures from small experimental plots of *M. × giganteus* in Illinois, Wisconsin, and the lake effect snowbelt of southern Michigan were analyzed during several anomalously cold winters. While a large insulating effect was observed, shallow soil temperatures were still observed to drop below laboratory mortality temperature thresholds of *M. × giganteus* during periods of snow cover. Despite this, *M. × giganteus* often survived these low temperatures, and it is hypothesized that the rate of soil temperature decrease might play a role in wintertime rhizome survival.

The domain was expanded in SiB3 to cover the US Midwest, and areas defined as cropland were replaced with the developed *M. × giganteus* surface parameterization. A 14-year uncoupled simulation was carried out and compared to an unmodified simulation in order to gauge the first-order hydrometeorological sustainability of a large-scale *M. × giganteus* regime in this area in terms of simulated productivity, evapotranspiration, soil water content, and wintertime cold soil temperature. It was found that *M. × giganteus* was biogeophysically sustainable and productive in a relatively small portion of the domain in southern Indiana and Ohio, consistent with a small set of previous studies and ultimately in

disagreement with the theory that *M. × giganteus* could reliably replace corn in areas such as Illinois and Iowa as a profitable and sustainable biofuel crop.

ACKNOWLEDGMENTS

I would like to express profound appreciation to my advisor, Prof. Chris Kummerow, for seeing me through the undertaking of this research. While grass and corn typically aren't on his plate he was generous in taking me on when I came to him as a grant-funded student, and his subsequent advice and guidance have been outstanding. Thank you to Prof. Jorge Ramirez and the I-WATER program at Colorado State University for making this interdisciplinary research possible. As a young atmospheric science student I never would have thought that I would be taking classes in hydrology and soil science, let alone thoroughly enjoying them. A huge, resounding thank you goes to Dr. Ian Baker, who always, always dropped what he was doing when I swung by his office to pick his brain or ask him to walk me through something new. He never once asked for a single thing in return for his valuable time.

Drs. Elizabeth Barnes, Dave Randall, Jeff Niemann, Christa Peters-Lidard, Doug Pennington, Gregg Sanford, Kurt Thelen, Eva Joo, and Carl Bernacchi are all gratefully acknowledged for helpful discussions and correspondences throughout the completion of this research. Gratitude is extended to Carl Bernacchi and Doug Pennington for access to previously unpublished datasets. Thanks also go to the entire Chris Kummerow research group for helpful discussions about science and sanity. And finally, heartfelt thanks go to my loving family and friends, in particular my inspiring parents and my unerring wife, Lauren. Thank you.

This work was supported by the US National Science Foundation (No. NSF-DGE-0966346) through the NSF IGERT Integrated Water, Atmosphere, Ecosystems Education and Research (I-WATER) Program at Colorado State University.

DEDICATION

An element in the mechanics of how the human mind learns from the past makes us believe in definitive solutions – yet not consider that those who preceded us thought that they too had definitive solutions. We laugh at others and we don't realize that someone will be just as justified in laughing at us on some not too remote day.

— Nassim N. Taleb

TABLE OF CONTENTS

Abstract	ii
Acknowledgments.....	v
Dedication.....	vii
List of Tables	x
List of Figures.....	xi
1. Introduction.....	1
1.1. Motivation.....	1
1.2. Research Approach.....	6
1.3. Structure of Dissertation.....	7
2. Parameterizing and modeling turbulent and ecosystem fluxes of <i>Miscanthus × giganteus</i> using the SiB3 model.....	9
2.1. Introduction.....	9
2.2. Methods	11
2.2.1. Simple Biosphere Model.....	11
2.2.2. Site description and flux/meteorological measurements	12
2.2.3. <i>M. × giganteus</i> parameterization.....	14
2.3. Results and Discussion.....	18
2.3.1. Meteorological and crop conditions.....	18
2.3.2. Latent heat flux.....	20
2.3.3. Carbon budget.....	23
2.3.4. Performance during the 2012 US Midwest drought	26
2.4. Conclusions	30
3. The role of lake effect snow cover in reducing the susceptibility of <i>Miscanthus × giganteus</i> to extreme cold soil temperatures in Michigan	33
3.1. Introduction.....	33
3.1.1. <i>M. × giganteus</i> as a viable biofuel.....	33
3.1.2. Strategic propagation methods of <i>M. × giganteus</i>	34
3.1.2.1. Bounds of <i>M. × giganteus</i> sustainability in the US Midwest.....	34
3.1.2.2. Strategic in situ management methods of <i>M. × giganteus</i>	36
3.1.3. Michigan as a favorable region for <i>M. × giganteus</i> propagation.....	37
3.1.3.1. Opportunity cost of land.....	37
3.1.3.2. Snowpack insulation	38
3.1.4. Objective.....	41
3.2. Methodology.....	42
3.2.1. <i>M. × giganteus</i> sites, observations, and analysis	42
3.2.2. Additional observations and analysis in Michigan	45
3.3. Results.....	47
3.3.1. Climate and meteorological observations	47
3.3.2. Time series of air temperature, soil temperature, and snow cover	49
3.3.3. Synoptic analysis	54
3.3.4. Enviro-weather stations time series and averages.....	58
3.4. Discussion.....	61

3.5. Conclusions	67
4. Areal estimates of the sustainability and hydrometeorological impacts of a <i>Miscanthus × giganteus</i> regime in the US Midwest.....	70
4.1. Introduction	70
4.2. Methods and Planned Analysis.....	72
4.2.1. Simple Biosphere model (SiB3)	72
4.2.2. Domain and forcing data	73
4.2.3. Planned analysis of turbulent and ecosystem fluxes; rainfall recycling.....	75
4.2.4. Planned analysis of wintertime soil temperatures.....	77
4.2.5. Planned analysis of soil moisture stress and equilibrium	78
4.3. Results and Discussion.....	80
4.3.1. Turbulent and ecosystem fluxes	80
4.3.2. Rainfall recycling	84
4.3.3. Extreme cold soil temperatures.....	87
4.3.4. Soil moisture stress and equilibrium.....	90
5. Discussion and Conclusions.....	96
5.1. Summary	96
5.2. <i>M. × giganteus</i> viability; limitations.....	98
5.3. Future work	101
5.4. Final remarks	102
References	103

LIST OF TABLES

Table 1: Measurements and information of eddy covariance and meteorological instrumentation used over experimental plots at EBI, Champaign, IL.....	14
Table 2: Parameters modified from productive grassland (Biome 6) to represent <i>M. × giganteus</i> in SiB3	15
Table 3: <i>M. × giganteus</i> site data: location, timeframe, survival, and hydrometeorological observation sources.....	43
Table 4: December through February (DJF) temperature/snowfall averages and observations at three <i>M. × giganteus</i> sites	48
Table 5: Average absolute difference of 5cm soil and 2m air temperature with and without snow cover from January 1 to March 8, 2009	54
Table 6: Sites characterized by soil moisture stress, GPP, and likelihood of cold soil temperatures 2011-2013	93

LIST OF FIGURES

Figure 1: A mature stand of <i>M. × giganteus</i>	3
Figure 2: Three past proposals of favorable regimes for <i>M. × giganteus</i> propagation.....	5
Figure 3: The values of monthly parameterized LAI and fPAR from 2011-2013 in SiB3, unmodified and <i>M. × giganteus</i> parameterizations	16
Figure 4: SiB3 rooting distribution of productive grassland (biome 6) and the new <i>M. × giganteus</i> parameterization in SiB3	17
Figure 5: Monthly average temperature anomaly (left) and accumulated precipitation (right) at Champaign, IL, 2011-2013.....	19
Figure 6: April through September 2011-2013 diurnal average of turbulent fluxes at Champaign, IL, simulation vs. observations.....	22
Figure 7: Daily patterns (“fingerprint” plots) of observed, simulated, and differenced latent heat flux (LE) over <i>M. × giganteus</i> at EBI in Champaign, IL from 2011- 2013.....	23
Figure 8: April through September 2011-2013 diurnal average of carbon fluxes at Champaign, IL, simulation vs. observations.....	24
Figure 9: As in Figure 7 but for gross primary productivity	25
Figure 10: As in LE fingerprint plots of Figure 9 but for 2012 only	27
Figure 11: Daily time series from 2009 through 2013 of the modeled soil moisture stress coefficient of <i>M. × giganteus</i> and productive grassland at Champaign, IL	28
Figure 12: As in GPP fingerprint plots of Figure 9 but for 2012 only.....	29
Figure 13: Yearlong time series from an idealized model of 2m air temperature, 10cm soil temperature, and presence of snow cover.	38
Figure 14: Visible satellite imagery of lake effect convection over Michigan.....	40
Figure 15: 1951–1980 mean annual snowfall (cm) in Michigan.....	41
Figure 16: Four experimental <i>M. × giganteus</i> monitoring sites	44
Figure 17: Location of selected stations from Michigan State University's Enviro- weather network.....	46
Figure 18: Hourly time series of soil and air temperature from January 1 to March 8, 2009 at each of the four experimental <i>M. × giganteus</i> sites.....	50
Figure 19: Hourly time series of soil and air temperature from January 1 to March 8, 2014 at Arlington, Hickory Corners, and East Lansing	51
Figure 20: Surface weather maps over the contiguous US, 13–16 January 2009	56
Figure 21: Time series of surface weather maps over the contiguous US 25 February to 3 March 2009	57
Figure 22: CoCoRAHS observations of snowfall depth in Michigan on 25 February and 27 February 2009	58
Figure 23: Time series of soil temperature at 12 Enviro-weather stations in Michigan and at the experimental <i>M. × giganteus</i> plot in Champaign, Illinois from January 1 to March 8, 2009	59
Figure 24: Distributions of hourly observed soil temperature (12 selected Enviro- weather stations) by snow depth during seven consecutive winters in Michigan.....	61

Figure 25: Areal surface soil moisture content in the Eastern US on January 10 of 2009 and 2014	66
Figure 26: Map of all sites in the domain characterized as cropland within SiB3	74
Figure 27: Average difference in gross primary productivity across the domain between the <i>M. × giganteus</i> simulations and the unmodified simulations of SiB3 from July through September of 2011-2013	80
Figure 28: Same as Figure 27 but during JAS 2012 only.....	82
Figure 29: Average difference in latent heat flux across the domain between the <i>M. × giganteus</i> simulations and the unmodified simulations of SiB3 from July through September of 2011-2013.....	83
Figure 30: Same as Figure 29 but during JAS 2012 only.....	84
Figure 31: Number of years from 2000-2013 with at least one hourly simulated soil temperature below A) -3°C at 8cm, B) -6°C at 8cm, C) -3°C at 18cm, and D) -6°C at 18cm.....	88
Figure 32: Average annual hours from 2000-2013 with a simulated soil temperature below A) -3°C at 8cm, B) -6°C at 8cm, C) -3°C at 18cm, and D) -6°C at 18cm.....	89
Figure 33: Average hours of extreme soil moisture stress experienced by <i>M. × giganteus</i> at each site in SiB3 from July through September of 2011-2013	91
Figure 34: Average hours of extreme soil moisture stress experienced by <i>M. × giganteus</i> at each site in SiB3 during July 2012.....	92
Figure 35: Time series of soil moisture stress (rstfac2) calculated by SiB3 from 2011-2013 at each of the four sites marked in Figure 26.....	94

CHAPTER 1

Introduction

1.1 Motivation

As the production of energy from fossil fuels becomes increasingly contentious, renewable alternatives are being sought to satisfy increasing energy demands. One such renewable energy source is biofuel, particularly in countries such as the United States, which has ample land and a strong agricultural sector. A biofuel strategy, which entails the growth and harvesting of specific crops to be chemically converted into liquid ethanol, has existed in Europe and the United States since the middle of the twentieth century (Lewandowski et al., 2000). Liquid ethanol is currently the only renewable energy strategy that could provide fuel in a form compatible with existing energy strategies, namely liquid petroleum in the transportation sector (Heaton et al., 2010).

The Energy Independence and Security Act (EISA), passed by the US Congress in 2007 (US House, 2007), stipulated that 36 billion gallons (bga) of ethanol per year must be produced domestically by 2022. EISA also specified that 21 bga of these 36 bga must be cellulosic ethanol. Converting ethanol from cellulosic sources entails the utilization of a plant's stalks, stems, and leaves, together known as *stover*. This is in contrast with the majority of corn ethanol production (14 bga produced in the US in 2015; RFA, 2016), which uses just sugars concentrated in the kernels. Both corn ethanol and cellulosic ethanol production entail a significant amount of water and energy resources. Thus, the expected impact of ethanol production on these systems must be properly understood before being fully implemented.

In the US and Europe, the most efficient biofuel plant, i.e. that which grows the most cellulosic biomass per unit surface area, is a grass called *Miscanthus × giganteus* (hereafter *M. × giganteus*) (Dohleman and Long, 2009; Heaton et al., 2010; Arundale, R.A., 2012). *M. × giganteus* (Figure 1) is a tall (3-5m) and dense grass that originated in eastern Asia as a sterile hybrid of *Miscanthus sinensis* and *Miscanthus sacchariflorus*. It was introduced in the US in the 1930s as an ornamental plant for landscaping and golf courses. As a sterile hybrid, *M. × giganteus* is propagated not by seed but by the lateral growth of rhizomes. Another distinguishing feature from corn is that *M. × giganteus* is a perennial crop. In late autumn of each year *M. × giganteus* senesces, returning important nutrients such as nitrogen to the soil and leaving its stalks, stems, and leaves starchy and brown. It is after senescing that *M. × giganteus* is harvested for its biomass to be converted into cellulosic ethanol, typically in late fall or early winter once the ground has hardened to support the weight of machinery. Requiring no replanting, *M. × giganteus* then sprouts anew from its rhizomes in early spring.



Figure 1: A mature stand of *M. × giganteus* on Sept. 2, 2013 in Leamington, southern Ontario, Canada (42°N, 82.5°W).

Economic studies have affirmed the advantages of *M. × giganteus* in terms of its production capability and low input growing strategy. Heaton et al. (2008) asserted that *M. × giganteus* can be expected to produce an average of 260% more biomass per hectare than corn and 240% more than switchgrass (*Panicum virgatum*), another cellulosic alternative to corn. Jain et al. (2010) likewise found *M. × giganteus* to yield over twice as much biomass as switchgrass in the lower Midwest. Factoring in production cost, opportunity cost of land, and transportation cost, this resulted in a “breakeven price” of *M. × giganteus* that was competitive with corn in many areas (Jain et al., 2010). *M. × giganteus* does well on both established cropland and marginal land and requires little maintenance after the initial planting of the rhizomes, i.e. it needs no sowing each spring nor does it demand fertilization (Heaton et al., 2008; McIsaac et al., 2010; Arundale et al., 2014). Since *M. ×*

giganteus can be harvested any time after it has completely senesced, including in the winter, *M. × giganteus* farming could also provide a viable wintertime farming activity and economic boom for participating farmers. It is also sustainable long-term: farms in Europe that have been growing the same *M. × giganteus* crop for over 30 years have continued to report yields that are uniformly within 90% of their original production amounts (Schill, 2007).

Largely because of its exceptional production per unit surface area, Heaton et al. (2008) asserted that if every acre of land currently devoted to corn for ethanol production were converted to *M. × giganteus*, the EISA 36 bga of ethanol per year could be achieved instantly. Such a broad regime of land use/land cover change (LULCC) could affect the local and downstream microclimate. LULCC affects the local climate through alterations in the radiative balance – changes in surface albedo, heat fluxes, atmospheric water vapor content, surface hydrology, and carbon dioxide exchange. While not adequately assessed as a global average, Pielke et al. (2011) asserted that where LULCC has been intensive, “the regional impact is likely, in general, to be at least as important as greenhouse gas and aerosol forcings.” *M. × giganteus* differs fundamentally from corn (*Zea mays*) due to its perennial nature, commencing growth earlier in the season and senescing later in the fall while growing taller and denser during the summer. The effects of these significant phenological differences are hypothesized to be non-negligible.

A final decision will eventually need to be made regarding whether or not to implement (and likely subsidize) a switch to *M. × giganteus* on a large scale in the US. If a switch is indeed implemented, it will be of critical importance to understand the bounds of *M. × giganteus* sustainability such that its annual chance of survival and profitability far

exceed its chance of failure, even during years of extreme climatological outliers. Such research as described above has contributed insight into the location of the western boundary of *M. × giganteus* sustainability in the US Midwest given water limitations. Research on the southern US bounds of *M. × giganteus* sustainability has focused on the quantity of damaging overly-hot growing season days (Kiniry et al., 2013; Song et al., 2014) and the annual lack of a killing frost, necessary as an impulse for *M. × giganteus* to senesce or “brown down” in the winter, thereby returning vital nutrients to the rhizomes for growth the following year (Christian et al., 2009). From these hypothetical bounds have arisen several propositions of the geographical boundary of *M. × giganteus* sustainability in the Midwest, the results of which are shown in Figure 2.

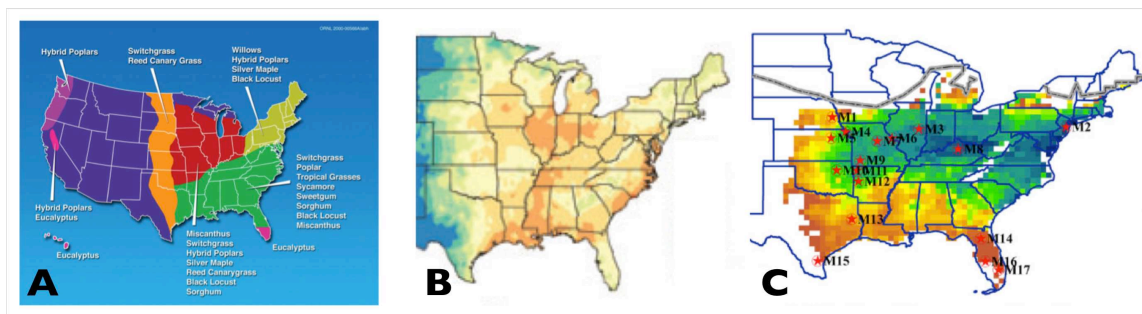


Figure 2: Three past proposals of favorable regimes for *M. × giganteus* propagation. A) US DoE, 2006 (*M. × giganteus* zone in red and green); B) Miguez et al., 2002 (*M. × giganteus* zone in orange and dark yellow); C) Song et al., 2014 (*M. × giganteus* zone in blue and dark green).

In contrast to these efforts to characterize and prevent the mortality of *M. × giganteus* due to water limitations and heat stress, a considerably smaller amount of research has focused on the mortality of *M. × giganteus* due to extreme cold soil temperatures, which can kill rhizomes during winter dormancy. Extreme post-harvest cold has several times been a principal cause of death during the establishment of *M. ×*

giganteus experimental field sites, including the almost complete mortality of the University of Illinois Urbana-Champaign (UIUC) Energy Farm site in the winter of 2008–09 (Heaton et al., 2010; Zeri et al., 2011) that disrupted a number of planned bioenergy crop comparison studies. Other mass die-offs have occurred in northern Michigan (Song et al., 2014; D. Pennington, personal communication, 2015) and in central Wisconsin during the winter of 2008–09 (Heaton et al., 2010; G. Sanford, personal communication, 2015). In Europe, where *M. × giganteus* has been an experimental biofuel crop since at least 1992 (Heaton et al., 2008), a mass winter die-off occurred in Sweden (56°N; 93% loss) and Denmark (56.5°N; 100% loss) following a June 1997 planting. Such events indicate that the probability of extreme cold soil temperatures during any given winter must likewise be factored into determining the bounds of *M. × giganteus* sustainability in the US. Such an approach, essentially a limitation on the northern bounds of sustainability, up until now has not been taken.

1.2 Research Approach

It was the main objective of this research to provide an updated estimate of the sustainability of *M. × giganteus* in the US Midwest. For the first time, this could be done using a third-generation land surface model in conjunction with a new, robust observational dataset over a mature field of *M. × giganteus*. The following questions were posed and addressed over the course of this project:

- How can a vegetation parameterization in SiB3 be developed that captures the diurnal and annual cycles of *M. × giganteus* turbulent and ecosystem fluxes, particularly given

no precedent for accurately modeling a crop with such intense water usage and productivity?

- 2012 was an anomalous year in the US Midwest: record warmth and *M. × giganteus* growth in March (Joo et al., 2016) and record drought in July (Mallya et al., 2013). Can SiB3 accurately represent *M. × giganteus* behavior during climatologically average years as well as its behavior during the climate extremes of 2012?
- *M. × giganteus* rhizomes have been killed due to extreme cold soil temperatures numerous times. Could areas in the US Midwest with cold temperatures but relatively high seasonal snowfall insulate shallow soil layers enough to motivate preferential cultivation in those areas?
- Applying a developed vegetation parameterization, which includes cold susceptibility, to all cropland areas in the Midwest, what are the realistic areal bounds of *M. × giganteus* biogeophysical sustainability, and how do these compare to previous estimates?
- In areas where *M. × giganteus* is modeled to be robust and productive, will the vigorous transpiration of a large-scale *M. × giganteus* regime result in changes in the local microclimate and downstream rainfall recycling ratio?

1.3 Structure of Dissertation

This dissertation is organized and presented as follows: Chapters 2 and 3 address two behaviors of *M. × giganteus* that are important to adequately model in order to assess its hypothetical sustainability on a large-scale: susceptibility to drought and susceptibility to cold. Chapter 2 delves into the former by cataloguing the development of a growing

season surface parameterization for *M. × giganteus* within SiB3. Discussed is the large experimental crop that was used to validate the results at a point, and a special focus is placed on the climatological extremes of 2012. Chapter 3 moves into the cold soil temperature susceptibility of *M. × giganteus*, examining previous cases of crop mortality in conjunction with meteorological variables such as air temperature and snow cover. A new theory of rhizome mortality is conjectured and a unique management strategy proposed. Chapter 4 discusses the application of the vegetation parameterization developed in Chapter 2 and the cold soil temperature threshold of Chapter 3 to all areas of cropland in the US Midwest using SiB3 in order to understand the hypothetical behavior of *M. × giganteus* across this area. A resultant recommendation on the bounds of *M. × giganteus* sustainability is proffered. Chapter 5 summarizes these results and unifies them with a perspective on the efficacy of *M. × giganteus* as a cellulosic ethanol crop in the US, in addition to addressing the potential limitations of this research approach.

After the introduction to this dissertation presented in Chapter 1, Chapters 2 and 3 can be read as stand-alone papers with individual introductions and conclusions. Chapter 2 draws heavily from a completed manuscript that has been conditionally submitted to *Agricultural and Forest Meteorology* as Roy and Baker (2016). Chapter 3 comprises the majority of a single-author journal article published by *Cold Regions Science and Technology* as Roy (2016). Chapter 4 will be submitted for publication as Roy et al. (2016) upon incorporating empirical *M. × giganteus* yield data to validate the discovered model results; this data is being compiled by a collaborator at Iowa State University. As such, the Chapter 4 conclusions are presented alongside the dissertation conclusions, remarks, and future work recommendations outlined in Chapter 5.

CHAPTER 2

Parameterizing and modeling turbulent and ecosystem fluxes of *Miscanthus × giganteus* using the SiB3 model

2.1 Introduction

In the US and Europe, the most efficient biofuel plant, i.e. that which grows the most cellulosic biomass per unit surface area, is a grass called *Miscanthus × giganteus* (hereafter *M. × giganteus*) (Dohleman and Long, 2009; Heaton et al., 2010; Arundale, R.A., 2012). *M. × giganteus* is a tall (3-5m) and dense grass that originated in eastern Asia as a sterile hybrid of *Miscanthus sinensis* and *Miscanthus sacchariflorus*. As a sterile hybrid, *M. × giganteus* is propagated not by seed but by the lateral growth of rhizomes and, unlike corn (*Zea mays*), is a perennial crop. Largely because of its exceptional production per unit surface area, Heaton et al. (2008) asserts that if every acre of land currently devoted to corn for ethanol production were converted to *M. × giganteus*, the EISA 36 bga of ethanol per year could be achieved today.

Such a broad regime of land use/land cover change (LULCC) could affect the local and downstream microclimate. LULCC affects the local climate through alterations in the radiative balance – changes in surface albedo, heat fluxes, atmospheric water vapor content, surface hydrology, and carbon dioxide exchange (Pielke et al., 2011). However, a great source of uncertainty about *M. × giganteus* is its biogeophysical sustainability. For example, using three different methods to estimate evapotranspiration – an observational residual energy balance approach (Hickman et al., 2010), an observational water budget estimation (McIsaac et al., 2010), and a model-based approach (VanLoocke et al., 2010) – it

is asserted that compared to existing vegetation, *M. × giganteus* locally increases season-long evapotranspiration at a point in Illinois by 343 mm, 104 mm, and 50 mm, respectively. VanLoocke et al. (2010) is the first to address large-scale hydrologic change, asserting that statistically significant regional water loss to the atmosphere only occurs when the fractional coverage of *M. × giganteus* in the US Midwest exceeds 50% of existing cropland. It is expected that this extra water vapor lost to the near surface atmosphere would meaningfully alter the ratio of latent heat flux to sensible heat flux. It is therefore hypothesized that such a shift to *M. × giganteus* could lead to a moister and cooler near-surface atmosphere in some areas.

The objective of this study was to develop a robust *M. × giganteus* parameterization for use within the Simple Biosphere Model (SiB3; Sellers et al., 1996a; Baker et al., 2008; Baker et al., 2013). This parameterization, which would be the first of its kind in a third-generation land surface model, will be crucial in assessing the hypothetical hydrometeorologic sustainability of *M. × giganteus* across the US Midwest, particularly in areas with low and/or overly variable seasonal precipitation. Such a parameterization could likewise be extended for use in a coupled regional atmospheric circulation model, allowing for a realistic estimate of the influence of *M. × giganteus* on local and downstream precipitation and near-surface temperature and humidity to be assessed where it is asserted to be sustainable.

The *M. × giganteus* parameterization developed in this study is based on measurements from a climatologically diverse span of three years (2011 – 2013) in Champaign, Illinois, in the Corn Belt of the US Midwest, where a four-hectare experimental plot of *M. × giganteus* has been cultivated and extensively observed since 2008 by the

Energy Biosciences Institute (EBI) of the University of Illinois at Champaign-Urbana (Zeri et al., 2011). The use of this robust multiyear observational dataset, the first from a field large enough to reduce observational fetch from exterior vegetation, was critical to the understanding, interpretation, and capture of not only the seasonal cycles of behavior in fluxes, moisture, and trace gases such as carbon dioxide over mature *M. × giganteus*, but also the behavior around the mean annual cycle, particularly during years of extreme drought.

2.2 Methods

2.2.1 Simple Biosphere model

The Simple Biosphere model (SiB; Sellers et al., 1986) was introduced in 1986 with the intent of providing a lower boundary for General Circulation models. The model provided the necessary exchange of energy, moisture and momentum with the atmosphere, but with a level of biophysical complexity that made the model useful to ecologists as well. SiB simulates photosynthesis using enzyme kinetics following Farquhar et al. (1980) and couples photosynthesis to stomatal conductance and energy and moisture exchange using Collatz et al. (1991, 1992). SiB was updated to incorporate satellite observations of vegetation phenology (SiB2; Sellers et al., 1996a, 1996b), and soil/snow processes based on the Community Land Model (CLM; Dai et al., 2003) and a prognostic Canopy Air Space (CAS; Vidale and Stöckli 2005) in another update (SiB3; Baker et al., 2003; Baker et al., 2008), the version used in the present research.

SiB has been coupled to GCMs (Sato et al., 1989), mesoscale models (Denning et al., 2003; Nicholls et al., 2004; Wang et al., 2007; Corbin et al., 2008, 2010) as well as in single-

point mode in grasslands (Colello et al., 1998; Hanan et al., 2005), midlatitude forests (Baker et al., 2003; Schaefer et al., 2008) and tropical forests (Baker et al., 2008, 2013; Schaefer et al., 2008). SiB has performed at or near the top in Model Intercomparison Studies (MIPS; Schwalm et al., 2010) and has a proven track record as a land surface parameterization.

SiB3 simulations in the present research were initialized in 1979 with saturated soil and a 30-minute time step, forced by 6-hourly global $1^\circ \times 1^\circ$ meteorological analysis datasets produced by the National Centers for Environmental Prediction (NCEP Reanalysis-2: Kalnay et al., 1996; Kanamitsu et al., 2002). Forcing data input variables were temperature, pressure, precipitation, wind, and solar radiation. Analysis of turbulent and ecosystem fluxes began January 2011 (32-year spin-up period), extending through December 2013.

2.2.2 Site description and flux/meteorological measurements

The experimental plots of *M. × giganteus* and productive grassland used in this study for model verification are located at the Energy Biosciences Institute (EBI) Energy Farm near the University of Illinois at Urbana-Champaign in Champaign, IL, USA. This area of the US Midwest experiences winters with temperatures well below freezing, but also experiences warm to hot summers (daily averages 20 °C - 30 °C) with relatively high precipitation (Angel, 2016). The growing season begins in mid- to late-April and mean annual precipitation is 1042mm.

Replicate plots of *M. × giganteus* and a mixture of native prairie grasses were planted in spring 2008 in 200 m × 200 m stands; see Zeri et al. (2011) for a complete list of

native prairie species. After experiencing near complete mortality during the winter of 2008-2009 due to extreme cold (Roy, 2016; Zeri et al., 2011), these stands were replanted in early 2010. Because *M. × giganteus* takes two to three years to reach productive maturity (Heaton et al., 2010), it is therefore considered that these stands were fully mature by 2012, although for the sake of this study, observations from the arguably mature experimental crops in 2011 were also examined and used. No fertilizer was applied to either crop (Zeri et al., 2011).

The observations taken from this site compose the longest and most complete biogeophysical dataset ever developed over a large spatial coverage of mature *M. × giganteus*. Half-hourly meteorological and 10 Hz turbulent flux measurements were taken from stations located in the exact center of each of these stands. **Error! Reference source not found.** has a complete list of measurements, frequency, and instrumentation. 10 Hz ecosystem fluxes were calculated and quality-controlled as outlined in Joo et al. (2016), including gap-filling (Reichstein et al., 2005; Zeri et al., 2011) and the exclusion of data during times of low fetch, i.e. a data footprint beyond the influence of the plots (as in Hsieh et al., 2000).

Table 1: Measurements and information of eddy covariance and meteorological instrumentation used over experimental plots at EBI, Champaign, IL, USA. Flux measurements were taken at a temporal frequency of 10 Hz and post-processed as in Joo et al. (2016); all data were quality-checked by EBI and made available at half-hourly resolution.

<i>Measurements</i>	<i>Instrument</i>	<i>Specifications</i>
CO₂ flux, Latent heat flux, Sensible heat flux, Friction velocity, Wind speed	Three-dimensional sonic anemometer	81000VRE, R.M. Young Company, Traverse City, MI, USA
	Open path infrared gas analyzer	LI-7500 and LI-7500A, LI-COR Biosciences, Lincoln, NE, USA
2 m air temperature, 2 m relative humidity	Temperature and relative humidity probe	HMP-45C, Campbell Scientific, Logan, UT, USA
Upwelling and downwelling shortwave and longwave radiation, net radiation	Net radiometer	CNR1, Kipp & Zonen, Netherlands
Canopy surface temperature	Infrared radiometer	SI-121 and SI-111, Apogee Instruments, USA
Upwelling and downwelling photosynthetically active radiation	Quantum sensor	LI-190, LI-COR Biosciences, Lincoln, NE, USA

2.2.3 *M. × giganteus* parameterization

To model the turbulent and ecosystem fluxes of this tall, dense crop over the 0.1° x 0.1° grid cell collocated with the EBI site in Champaign, IL, a set of biophysical parameters for a new biome at this site was derived from the existing, unmodified parameterization of a productive grassland (Biome 6) in SiB3. The productive grassland parameterization was considered a good baseline for parameterizing *M. × giganteus* due to its phenological similarity, timing of emergence and senescence, areal coverage, and local climate tolerance. The *M. × giganteus* parameterization was developed as delineated henceforth and in Table 2. All modifications were based on a mechanistic understanding of C4 crops such as *M. ×*

giganteus, as well as empirical measurements from existing experimental *M. × giganteus* plots.

Table 2: Parameters modified from productive grassland (Biome 6) to represent *M. × giganteus* in SiB3. ¹ Joo et al. (2016); ² Sellers et al. (1992); ³ Monti and Zatta (2009); ⁴ Mann et al. (2012); ⁵ Sellers et al. (1989)

Parameter	SiB3 variable	Productive grassland	<i>M. × giganteus</i>
Leaf area index (LAI)	zlt	see Figure 3 ¹	
Fraction of photosynthetically active radiation (fPAR)	fpar	see Figure 3 ²	
Rooting depth	rootd	3.0 m	2.0 m ^{3,4}
Rooting profile	kroot	see Figure 4 ^{3,4}	
Soil moisture uptake method	(begtem.F90) ⁵	~ from layer with highest root density	~ from layer with highest water content
Half-point high temperature of photosynthesis	hhti	313 K	323 K ¹

The modification of parameterized LAI from 2011-2013 is shown in Figure 3a. LAI was empirically measured at EBI weekly or biweekly (Joo et al., 2016) during each growing season 2011-2013. As such, these LAI values are unique by year and substituted weekly MODIS-derived LAI in each year's respective parameterization. In order to maintain the consistency of LAI with the fraction of photosynthetically active radiation (fPAR) at this site in SiB3, these empirical *M. × giganteus* LAI values were used to generate corresponding fPAR values per the two-stream approximation model of Sellers et al. (1992), as seen in Figure 3b.

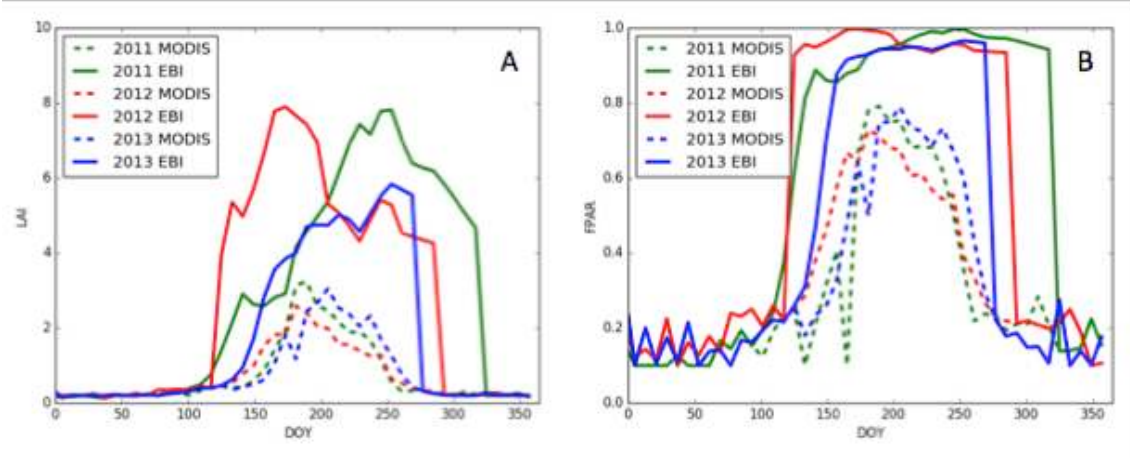


Figure 3: The values of monthly parameterized LAI (A) and fPAR (B) in 2011 (green), 2012 (red), and 2013 (blue). The unaltered seasonal cycle of these values at the Champaign, IL point is represented with a dashed line while the new parameters derived from EBI field observations of *M. × giganteus* are represented with a solid line. LAI was directly observed by Joo et al. (2016) while fPAR values are calculated using the two-stream approximation of Sellers et al. (1992).

The parameterized *M. × giganteus* root distribution was developed per Monti and Zatta (2009) and Mann et al. (2012), which charted mature, unirrigated *M. × giganteus* roots in Italy and California, respectively. It can be seen in Figure 4 that the root structure of *M. × giganteus* is much shallower than the productive grassland parameterization of SiB3 (2.0 m vs. 3.5 m), with a majority of the *M. × giganteus* roots concentrated between 0 cm and 30 cm, assuming the crop is rainfed, as opposed to irrigated (Mann et al., 2012). Additionally, *M. × giganteus* roots in SiB3 are modified to be able to draw water from any of the ten soil layers in which there is some fraction of the rooting distribution in that layer, i.e., irrespective of root density (Baker et al., 2008).

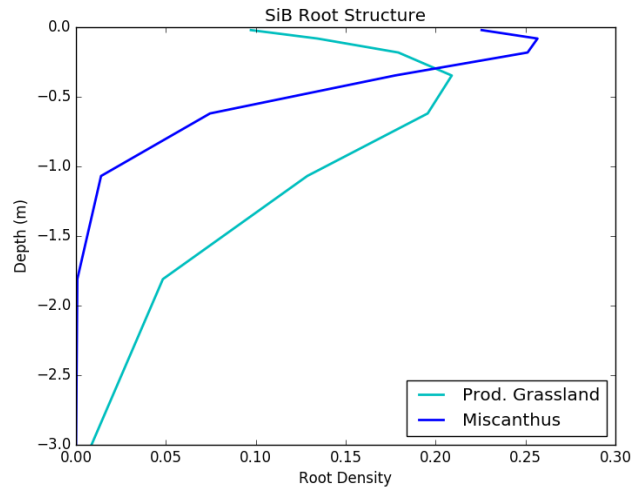


Figure 4: SiB3 rooting distribution of productive grassland (biome 6) and the new *M. × giganteus* parameterization. The former has a maximum depth of 3.5 m while the latter has a maximum depth of 2 m and has a much higher overall root density in the top 50 cm. Observations are from Monti and Zatta (2009) as well as Mann et al. (2012).

The *M. × giganteus* parameterization was also modified to allow for a greater heat tolerance than productive grassland per the recent findings of Joo et al. (2016). This study identified the tendency of an experimental crop of *M. × giganteus* at EBI in Champaign, IL to maintain a high stomatal conductance during extreme drought conditions despite an extremely high vapor pressure deficit and eventually limited soil moisture, likely an unsustainable trait that solely arose because *M. × giganteus* is a hybrid plant and may lack various beneficial evolutionary survival strategies. Just as with soil moisture stress, SiB3 also limits the transpiration permitted by the leaf surface in tandem with the near-surface atmospheric temperature (heat stress). In accordance with these recent findings, the half-point high temperature of photosynthesis (hhti) was raised by 10 K, from 313 to 323 K. This meant that with an ambient air temperature of 323 K, potential transpiration would be scaled to half of the value that it would otherwise be. It should be noted that while temperatures this high have never been recorded at Champaign, EBI experimental *M. ×*

giganteus has never been categorically proven to react to extreme heat stress, keeping stomatal conductance high and respiring at temperatures greater than 313 K (40 °C) given sufficient soil moisture (see Joo et al., 2016).

2.3 Results and Discussion

2.3.1 Meteorological and crop conditions

In general, 2011 and 2012 can be characterized as anomalously warm years, while 2013 was slightly cooler than average at Champaign, IL (Figure 5; Angel, 2016). In 2012, above-average temperatures were recorded in every month except September and October; it was also the warmest spring on record at Champaign (1902 to present), with a March/April/May (MAM) mean daily high temperature 9.5 °C warmer than average. 2011 and 2012 both had a warm July and August: while mean maximum summer temperatures reach a climatological average of 30 °C at Champaign, temperatures of 35 °C were observed multiple times in these years, and temperatures higher than 40 °C were recorded several times in 2012. In contrast, the mean June/July/August (JJA) temperature in 2013 was 0.6 °C below average and the 2013 annual temperature was 0.3 °C below average.

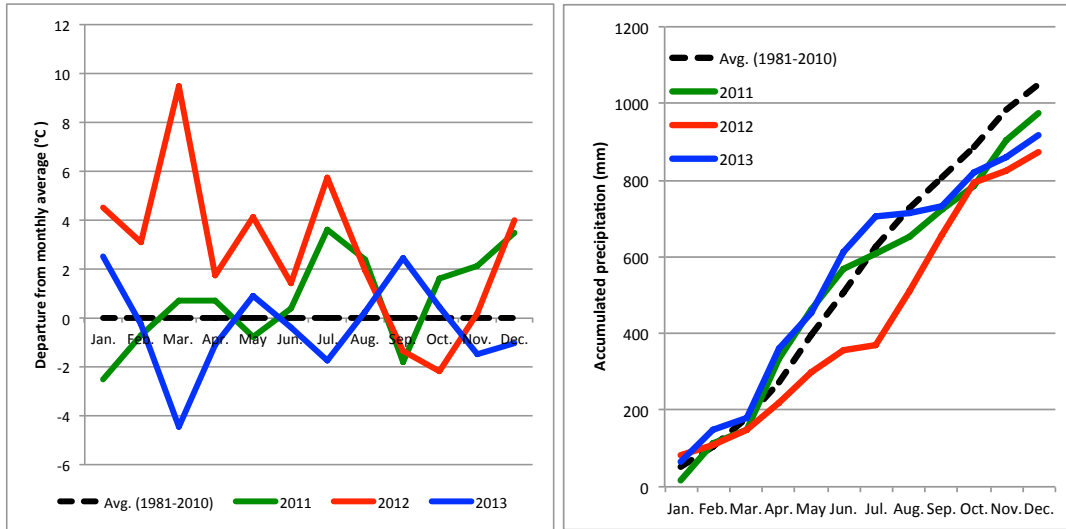


Figure 5: Monthly average temperature anomaly (left) and accumulated precipitation (right) at Champaign, IL in 2011 (green), 2012 (red), and 2013 (blue). Data is from the state climatologist office for Illinois (Angel, 2016).

All three years recorded below average annual precipitation, although both 2011 and 2013 had above-average precipitation in the spring (Figure 5). 2012 experienced the contrary: extremely below-average rainfall from January through July, totaling 381mm, or 59% of the 1981-2010 climatological average precipitation of 626mm (Angel, 2016). Slightly above-average rainfall was then observed from August 2012 until the end of the year. This drought in the US Midwest in 2012 (Mallya et al., 2013) occurred in conjunction with the aforementioned period of anomalously high temperatures (greater than 40°C) at Champaign, leading to a combination of severe drought stress and heat stress for crops in the region.

Joo et al. (2016) discussed that during the 2012 drought, other nearby crops such as switchgrass (*Panicum virgatum*) and a tall grass prairie mixture (Zeri et al., 2011) survived, but registered a decline in evapotranspiration (ET) and net ecosystem productivity (NEP). This was likely due to an expected phenological response mechanism evolved by

anisohydric plants to survive droughts: the gradual closing of stomata in times of high leaf-level gradients of atmospheric vapor pressure deficit (Gentine et al., 2016; Sinclair et al., 2005; Maroco et al., 1997). The EBI plots of *M. × giganteus* used in this study also survived all three summers, but showed a much different phenological response, maintaining open stomata through the peak of the drought and thereby using as much as 11mm water per day. *M. × giganteus* ET and NEP started to see a decline after approximately DOY200 (July 20), which was hypothesized to be due to the depletion of most of the soil water available to the deeper roots of *M. × giganteus*. This may have been due to *M. × giganteus* tending toward a more isohydric growth strategy (Gentine et al., 2016), but it was also hypothesized by Joo et al. (2016) that this response was a manifestation of a lack of a drought adaptation strategy in *M. × giganteus*, being a recent sterile hybrid between two different species. The depletion of rooting zone soil moisture in 2012 potentially then led to a slightly subpar growing season in 2013 for *M. × giganteus* at EBI in terms of NEP, despite average climatic conditions. This rapid depletion of soil moisture also led to an abnormally large latent heat flux and carbon flux over *M. × giganteus* during this time, which provided an opportunity to test the robustness of the SiB3 *M. × giganteus* parameterization and performance, detailed in the following sections in conjunction with the presentation of flux observations.

2.3.2 Latent heat flux

The goal of the present research is to develop a model parameterization of *M. × giganteus* that accurately represents the turbulent and ecosystem flux behavior observed in the real world, i.e. over an existing experimental crop. This parameterization could be extended to model the extent to which the near-surface atmosphere in the US Midwest may

be affected by the possible increased evapotranspiration due to a regime of *M. × giganteus* being grown for biofuel instead of a relatively more water-conservative crop such as *Zea mays* or *Panicum virgatum*. Because total evapotranspiration is proportional to the surface latent heat flux, it is instructive to focus on observed and SiB3 modeled turbulent fluxes over these three very different years, 2011 through 2013, for which data over mature *M. × giganteus* exists at EBI.

The average calculated and observed diurnal cycle of turbulent fluxes from 1 April through 30 September 2011-2013 is shown in Figure 6, with the productive grassland simulation on the left and the *M. × giganteus* simulation on the right. For both biomes, the timing of the diurnal cycle of all fluxes was captured by SiB3. The average net radiation (Rnet) and sensible heat flux (H) of *M. × giganteus* were adequately reproduced by the model, while during the afternoon, the latent heat flux (LE) seemed to be systematically slightly overestimated and the ground heat flux (G) underestimated, particularly over *M. × giganteus*. One possible reason for this was that the *M. × giganteus* surface parameterization potentially over-represented vegetation, contributing to an increase in expected evapotranspiration and a decrease in the expected ground interception of solar radiation.

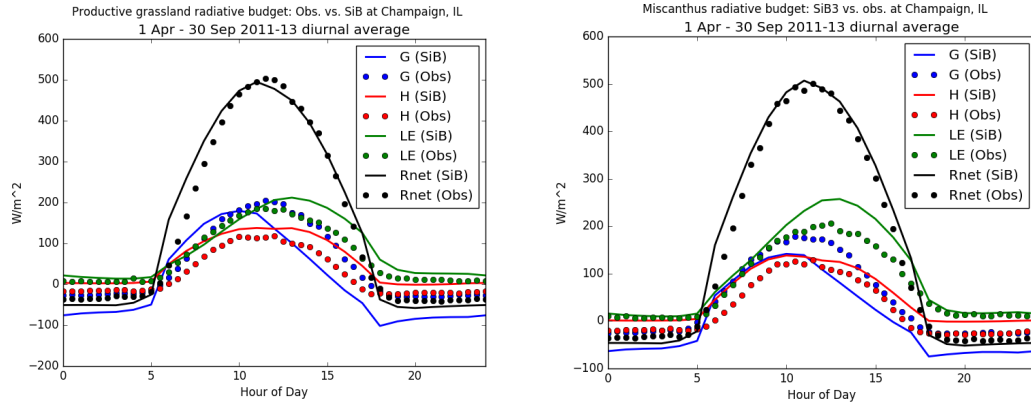


Figure 6: April through September 2011-2013 diurnal average of turbulent fluxes over productive grassland and *M. × giganteus* at Champaign, IL, simulation (SiB3, solid lines) vs. observations (EBI, dotted lines): net radiation (Rnet), latent heat flux (LE), sensible heat flux (H), and ground heat flux (G). Rnet and H were simulated well, while LE and G exhibited a persistent afternoon overestimation and underestimation, respectively.

Figure 7 is a fingerprint plot of the hourly observed and simulated LE at Champaign, IL from 2011 through 2013. LE can be used to estimate diurnal and seasonal crop evapotranspiration (Bonan, 2013; e.g. VanLoocke et al., 2010). SiB3 was able to represent well the seasonal patterns of LE, including the timing of spring emergence and fall senescence of *M. × giganteus* vegetation. As seen in Figure 7, the bulk of the modeled overestimation of *M. × giganteus* LE was during local afternoon, particularly throughout the growing season of 2011, in May and June 2012, and August 2013. LE was underestimated throughout the entire day in July and August 2012 (during the 2012 drought in the US Midwest), often by greater than 200 W/m². During the period of peak vapor pressure deficit in July 2012 (Joo et al., 2016), SiB3 modeled expected LE values at times greater than 600 W/m², or approximately 7mm of evapotranspiration per day by *M. × giganteus* (Bonan, 2013). During this same period, a peak daily water usage of 11mm was observed by Joo et al. (2016), however, while observations of LE over *M. × giganteus* at EBI were quality-controlled and gap-filled, many unrealistic values of observed LE appear in the

dataset, including several instances of LE greater than 600 W/m^2 before sunset or after sunrise.

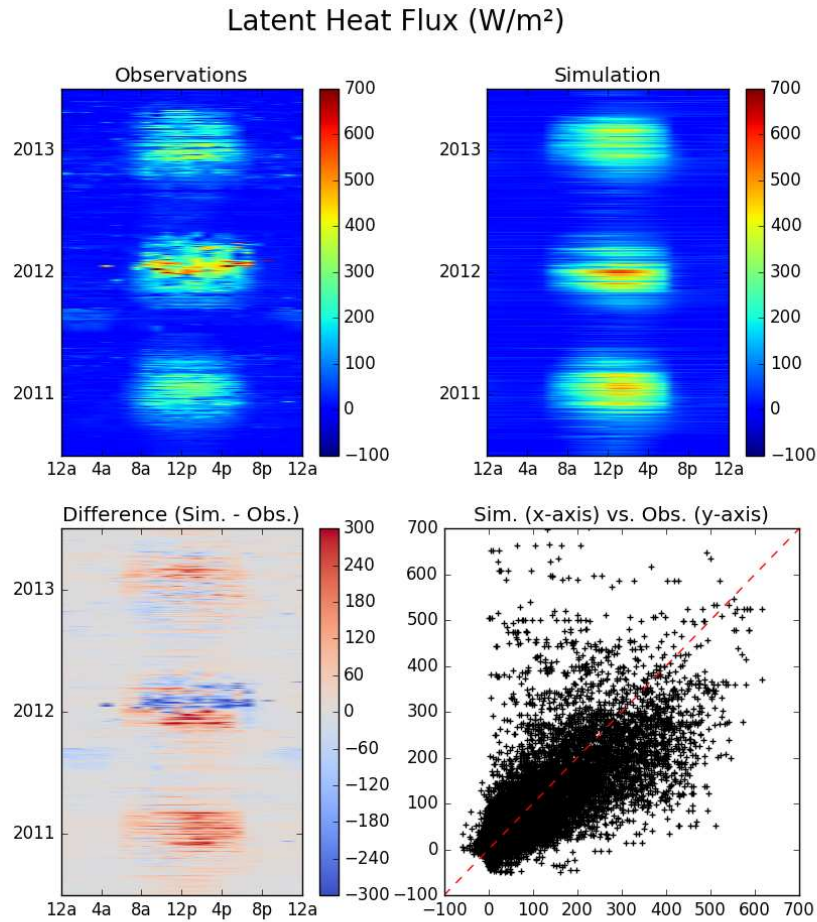


Figure 7: Daily patterns (“fingerprint” plots) of observed, simulated, and differenced latent heat flux (LE) over *M. x giganteus* at EBI in Champaign, IL from 2011 through 2013. The scatter plot in the bottom right also plots all timeframe simulation data vs. observations, with the 1:1 line shown for comparison. While EBI observations are half-hourly, data is plotted every hour to maintain consistency with SiB3 output. Fingerprint plot x-axes are the local hour at Champaign, and y-axes are the year, with ticks centered on DOY182, the first day of July in non-leap years (note that 2012 was a leap year, however). The difference plot is calculated such that positive values indicate an overestimation by SiB3, i.e. simulation – observations.

2.3.3 Carbon budget

The average calculated and observed diurnal cycles of gross primary productivity (GPP), respiration (Resp), and net ecosystem exchange (NEE) from 1 April through 30 September 2011-2013 are shown in Figure 8. Again, SiB3 was able to accurately represent

the timing of the diurnal carbon flux cycle on average. GPP was underestimated by an average of 13% and NEE by 30% between 1000 and 1800 local time, the daily period of peak temperature and plant photosynthesis. The magnitude of the average diurnal cycle of respiration was well-captured.

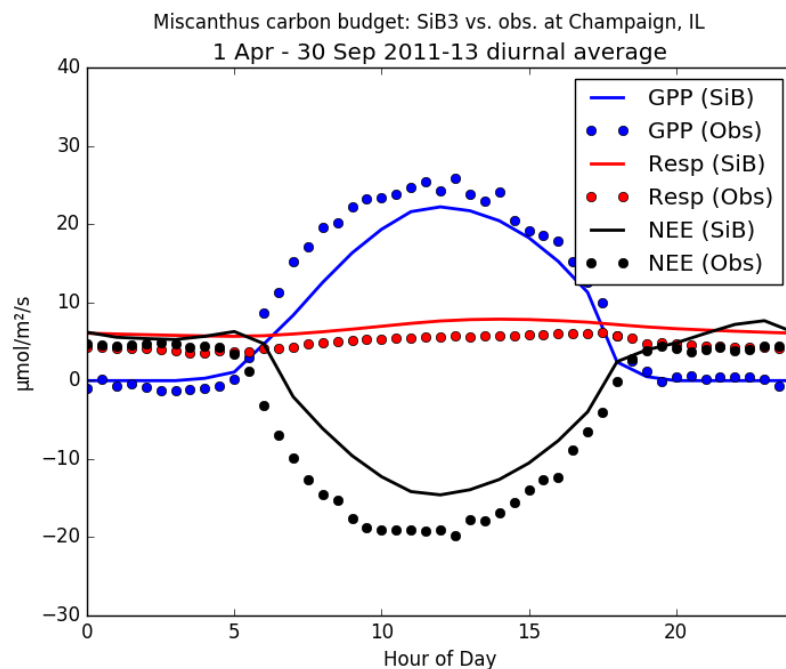


Figure 8: April through September 2011-2013 diurnal average of carbon fluxes at Champaign, IL, simulation (SiB3, solid lines) vs. observations (EBI, dotted lines): gross primary productivity (GPP), respiration (Resp), and net ecosystem exchange (NEE). The average diurnal cycle was adequately resolved by SiB3.

Fingerprint plots of observed and simulated GPP are shown in Figure 9. Because the release of water into the atmosphere by *M. × giganteus* stomata is a necessary trade-off in primary productivity via photosynthesis, the seasonal-diurnal patterns shown here closely matched those of LE. Note that latent heat flux was quality-controlled in each of 2011, 2012, and 2013, but only gap-filled by EBI in 2012 and 2013, resulting in the missing data in 2011. GPP was simulated very well in 2011 and 2013, with absolute discrepancies rarely exceeding 10 $\mu\text{mol}/\text{m}^2/\text{s}$. The largest difference between the SiB3 simulation and EBI

observations of *M. × giganteus* again occurred in July, August, and September 2012, during and after the 2012 drought in the US Midwest. During this timeframe, SiB3 often underestimated GPP by 50 to 100%, including a period of several weeks in August 2012 when virtually zero GPP was predicted. A more detailed analysis of the model discrepancies that occurred in the summer of 2012 is outlined in the following section.

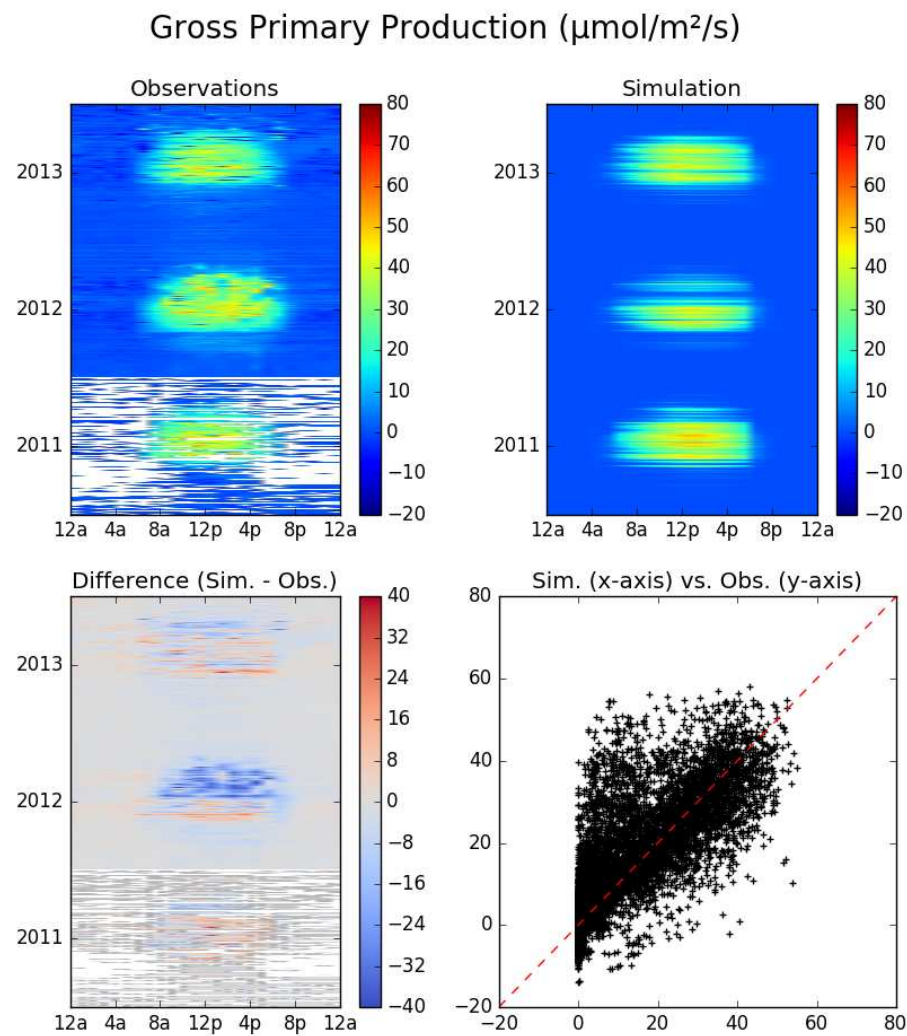


Figure 9: As in Figure 7 but for gross primary productivity (GPP). White areas in fingerprint plots indicate missing observational data.

2.3.4 Performance during the 2012 US Midwest drought

Temperature and precipitation extremes provide excellent opportunities to test the rigor of land surface models in a broad range of climatic conditions. Such extreme events are often the trigger for the mass failure of plants in various regions (e.g. Lynch et al., 2014). These extremes, not the averages, are the events that will define the boundaries of *M. × giganteus* sustainability (both biogeophysical and economic) in the US Midwest (e.g. Jain et al., 2010). In the case of *M. × giganteus* and other perennial cellulosic feedstock grasses such as *Panicum virgatum*, a single year every decade of killing drought, flood, or extreme temperature conditions could be enough to render such an agronomic biofuel strategy unviable in these regions (Jain et al., 2010; VanLoocke et al., 2012; Roy, 2016). The 2012 drought in the US Midwest, coincident with mature crops of *M. × giganteus* at EBI, provided a great opportunity to test the robustness of SiB3 in modeling the biogeophysical sustainability of *M. × giganteus*.

Figure 10 is a LE fingerprint plot over the 366 days of 2012. In general, LE was overestimated by SiB3 in the first half of the growing season (through approximately DOY200) and underestimated in the second half. March 2012 was the warmest on record at Champaign, IL (Angel, 2016) and the early emergence of *M. × giganteus* was indeed well-captured by SiB3. Modeled LE was anomalously high beginning around DOY140 (late May) and extended through the period of maximum observed atmospheric water vapor pressure deficit in July, tapering off by approximately DOY195. SiB3 then underestimated LE through approximately DOY225.

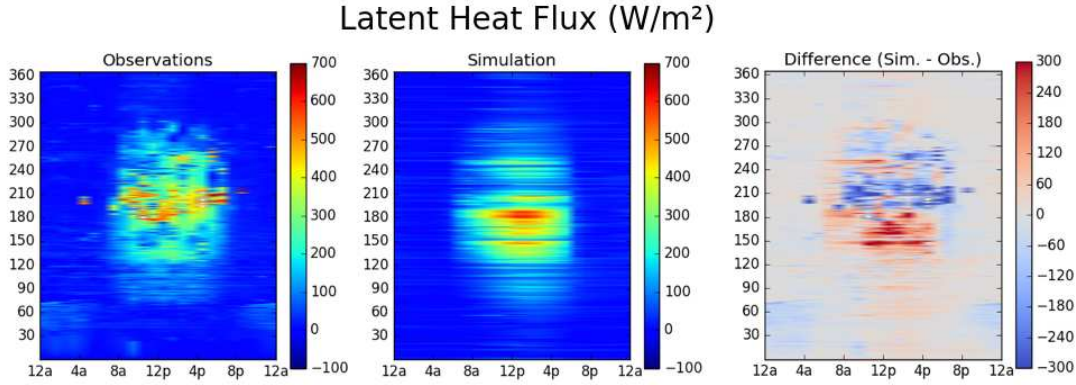


Figure 10: As in LE fingerprint plots of Figure 9 but for 2012 only, with the y-axis representing day of year (DOY). Potentially erroneous LE values can be seen in the observations, particularly before sunrise and after sunset. Seen in the SiB3 simulation plot is the extreme LE modeled in June and July followed by a near shutdown of evapotranspiration in late July and early August.

Joo et al. (2016) discussed the unusually high LE observed over this EBI plot of *M. × giganteus*, and SiB3 indeed resolved this with the new *M. × giganteus* parameterization implemented here. However, it may be the case that modeled *M. × giganteus* used ground water more quickly than the observed EBI crop, leading to a more abrupt shutdown of the photosynthetic process within the model. Stomatal resistance is the most important factor contributing to canopy transpiration (e.g. Godfrey et al., 2007) and in modeling this resistance, SiB3 implements a series of parameters that characterize the expected stress a plant may feel due to air temperature, vapor pressure deficit, and soil moisture, as discussed in the Methods section. Since the present run was uncoupled, the sole prognostic variable that may have modified this resistance in SiB3 was the calculated leaf water potential ψ_l (sometimes referred to as $rstfac2$).

Figure 11 shows daily ψ_l from the beginning of 2009 through the end of 2013, along with a yearlong running average of temperature and precipitation at Champaign, IL to give an idea of the recent climatological conditions that the area had experienced. ψ_l can essentially be thought of as a measure of the stress that the local plants modeled by SiB3

were undergoing due to lack of soil water for uptake. Notable is that the ψ_l of modeled productive grassland varied much more drastically with time and precipitation events than that of modeled *M. × giganteus*. This ability of *M. × giganteus* modeled by SiB3 to generally withstand minor drought events is that its roots may uptake water from any soil layer with equal efficiency, regardless of the proportional density of roots situated in that given layer. During minor drought or heat events, modeled *M. × giganteus* may preferentially draw water from deeper layers, thus keeping this component of total plant stress (ψ_l in the stomatal resistance equation [21], Sellers et al., 1989) stable when the shallower layers are relatively dry.

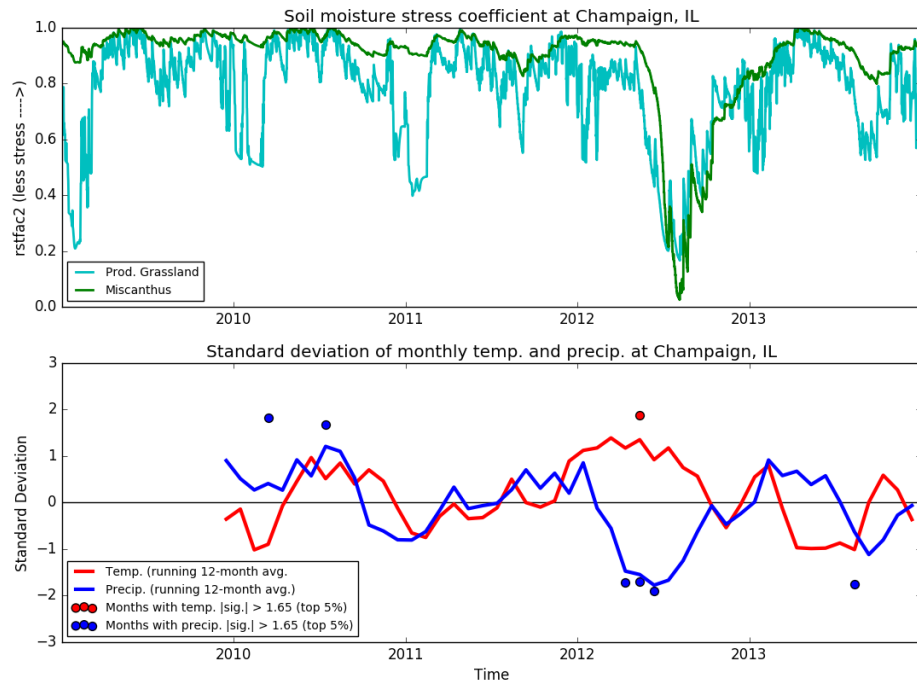


Figure 11: Daily time series from 2009 through 2013 of the modeled soil moisture stress coefficient (ψ_l or rstfac2) of *M. × giganteus* (plotted in green) and productive grassland (plotted in cyan) at the Champaign grid cell in SiB3 (top); one-year running average of monthly NLDAS-2 temperature and precipitation anomalies from the 1981-2010 time series climatological average at the same grid cell, with calculated 95th percentile extreme anomalous months indicated with dots. The *M. × giganteus* parameterization resulted in less fluctuation in ψ_l , i.e. less soil moisture stress in times of minor drought, than did the productive prairie simulation. In 2012, however, coincident with three straight

months of 95th percentile low precipitation and a month of 95th percentile high temperatures at Champaign, the simulated stress is almost total (i.e. ψ_l near zero). *M. × giganteus* then took longer to recharge the soil moisture it was modeled to have used.

However, during the anomalously hot, dry spring and summer of 2012 (one month of 95th percentile high temperatures and three months of 95th percentile low precipitation), *M. × giganteus* took longer than productive grassland in SiB3 to experience stomatal stress, but both reached extreme minimum values of ψ_l by late July, with modeled *M. × giganteus* having surpassed productive grassland in plant stress. This led directly to the sudden shutdown of the photosynthetic process in SiB3 by late July (approximately DOY210), reflected in the 2012 mid-summer gap in modeled LE seen in Figure 10 as well as in the modeled GPP during the same timeframe shown in Figure 12. This gap is not as abrupt in the observations: *M. × giganteus*, whether due to being hybrid (Joo et al. 2016) or isohydric (Gentine et al., 2016), maintains open stomata and has access to sufficient soil moisture to support transpiration during this period, albeit at a slower rate than expected.

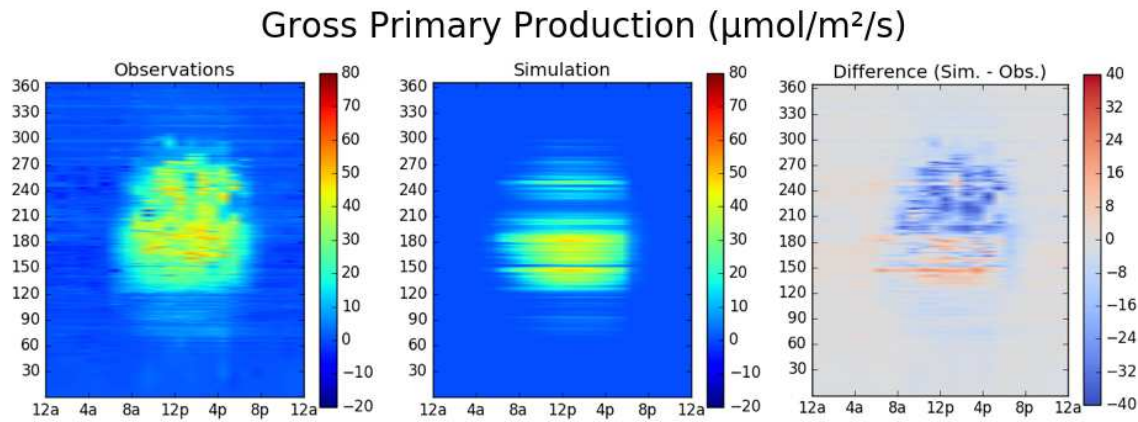


Figure 12: As in GPP fingerprint plots of Figure 9 but for 2012 only, with the y-axis representing day of year (DOY). Once again, the effects of the 2012 drought, particularly in mid-July (DOY 200) onward, can be seen in both the observations and the simulation, the principal difference being that *M. × giganteus* was still observed to be performing photosynthesis while the SiB3 simulation predicted a complete shutdown of photosynthetic activity for two weeks followed by very little productivity.

As monthly precipitation and temperatures returned to more climatologically average values for the remainder of the year, *M. × giganteus* lagged slightly behind productive grassland to regain higher values of ψ_l (i.e. lower stress), likely due to the increased time resolved by SiB3 for all soil layers to recharge their soil moisture from the surface down after having nearly depleted every layer during the drought. This modeled residual stress is in agreement with *M. × giganteus* observations of Joo et al., 2016, which found that *M. × giganteus* maintained a higher LE later into the drought than did productive grassland at Champaign, but took until the following year to recharge the excess soil moisture it had used.

2.4 Conclusions

A new empirical parameterization for *M. × giganteus* was developed and implemented within the Simple Biosphere Model (SiB3). The model was run in uncoupled mode with the new parameterization from 2011-2013 at a point in Champaign, IL and the results compared with observational data from a coincident large experimental plot of mature *M. × giganteus*. This is one of the first studies to have the luxury of using an extant biogeophysical dataset over a broad set of years of mature *M. × giganteus*, as many past observational datasets were either too short temporally, too small areally, or based on measurements of *M. × giganteus* that had not fully reached maturity. This dataset was critical to understanding not only the *M. × giganteus* seasonal cycles of turbulent fluxes, moisture, and trace gases such as carbon dioxide, but also its behavior around the mean annual cycle, particularly during the US Midwest drought of 2012.

The diurnal and seasonal timing of *M. × giganteus* evapotranspiration and productivity were well-simulated, as were the three-year average magnitudes of turbulent and carbon fluxes. Equating water lost to the atmosphere by transpiration (latent heat flux [LE]) to being a direct tradeoff for carbon acquisition from the atmosphere (gross primary productivity [GPP]), it could be expected that any errors in LE and GPP simulations should have been of approximately the same magnitude. However, it was seen that the diurnal and seasonal cycles and estimations of GPP (Figure 9) were generally modeled slightly better than LE (Figure 7), indicating future room for mechanistic improvement of the *M. × giganteus* parameterization in SiB3, potentially with a higher water use efficiency but less vegetation at the modeled surface.

Approaching this discrepancy differently: by removing 2012, an extreme drought year in the US Midwest, the average diurnal fluxes become nearly perfectly simulated. However, it is crucial to remember that climate extremes are important to adequately simulate, due to their disproportionately large influence on the long-term sustainability of perennial crops such as *M. × giganteus*. SiB3 performance in 2012 specifically was analyzed and it was discovered that modeled *M. × giganteus* used available water more rapidly than observed, shutting down evapotranspiration and productivity for approximately two weeks and greatly contributing to the underestimation of LE and GPP compared to observations. While the root structure and behavior may be further modified, more would first need to be understood about the EBI observations – the dataset is immensely beneficial, being the first of its kind, but may have erroneously measured and/or calculated latent heat flux during the 2012 drought, particularly in the early morning and evening (Figure 10).

The parameterization developed and validated here will provide a good foundation as the simulation is expanded to a broader area and the sustainability of *M. × giganteus* is tested across a large swath of the US Midwest where it has been proposed to be adopted as a cellulosic biofuel crop. Because a single year in ten of killing drought or extreme cold can disrupt *M. × giganteus* productivity for up to three years, it will be immensely important to choose wisely the areas in which large-scale crops of *M. × giganteus* will be planted, should such a renewable fuel strategy ultimately be pursued.

CHAPTER 3

The role of lake effect snow cover in reducing the susceptibility of *Miscanthus × giganteus* to extreme cold soil temperatures in Michigan

3.1 Introduction

3.1.1 *M. × giganteus* as a viable biofuel

As use of the world's fossil fuel reserves becomes increasingly more contentious, innovative alternatives continue to be sought to satisfy the world's increasing energy demands. In the United States transportation sector, an alternative method of focus has been the use of biofuels, including the conversion of dry plant matter into liquid ethanol as well as thermal-chemical conversion. This focus is largely motivated by the fact that biofuels are the only type of renewable energy that can be produced in a liquid form and are scale-compatible with existing transportation infrastructure (Heaton et al., 2010). The Energy Independence and Security Act (EISA) of 2007 (US House, 2007) calls for the domestic production of 36 billion gallons (bga) of ethanol by 2022 (up from 4.7 bga in 2007). EISA also specifies that 21 of the 36 bga ethanol must be derived from biomass sources other than corn since it would be impossible to meet the 36 bga goal using domestic corn alone (e.g. Heaton et al., 2008). A prime candidate crop for this role is asserted to be *Miscanthus × giganteus* (hereafter "*M. × giganteus*").

M. × giganteus is a dense, tall grass (3–5 meters) native to eastern Asia that is a favorable source of cellulosic ethanol due to its productivity (260% more harvestable biomass per unit surface area than corn and 280% more than switchgrass, another proposed cellulosic ethanol crop [Heaton et al., 2008]) and its low agrochemical

requirements (Kucharik et al., 2013). *M. × giganteus* is a natural sterile hybrid of *Miscanthus sinensis* and *Miscanthus sacchariflorus*, propagating by rhizome instead of by seed (Beale and Long, 1997; Dohleman and Long, 2009). It has been used in Europe as a feedstock for ethanol production for over 30 years and has shown no evidence of being an invasive species (Heaton et al., 2010).

3.1.2 Strategic propagation methods of *M. × giganteus*

To avoid mass *M. × giganteus* die-off and the agro-economic consequences of a disruption of several years, there are two ways in which it has been proposed to strategically propagate *M. × giganteus*: first, by initiating crops exclusively in areas where the climatological range of temperature and moisture make a year of unsustainability extremely unlikely (i.e. an area of stable productivity; Jain et al., 2010), and second, by the adoption of strategic in situ planting and management methods.

3.1.2.1 Bounds of *M. × giganteus* sustainability in the US Midwest

Many studies have focused on the water-limited sustainability of *M. × giganteus* (e.g. McIsaac et al., 2010; VanLoocke et al., 2012; Zeri et al., 2013). Such research has contributed insight into the location of the western boundary of *M. × giganteus* sustainability in the US Midwest given water limitations. Research on the southern US bounds of *M. × giganteus* sustainability has focused on the quantity of damaging overly-hot growing season days (Kiniry et al., 2013; Song et al., 2014) and the annual lack of a killing frost, necessary as an impulse for *M. × giganteus* to senesce or “brown down” in the winter, thereby returning vital nutrients to the rhizomes for growth the following year (Christian et al., 2009). From these hypothetical bounds have arisen several propositions of the

geographical boundary of *M. × giganteus* sustainability in the Midwest, the results of which are shown in Figure 2.

In contrast to these efforts to characterize and prevent the mortality of *M. × giganteus* due to water limitations and heat stress, a considerably smaller amount of research has focused on the mortality of *M. × giganteus* due to extreme cold soil temperatures, which can kill rhizomes during winter dormancy. Extreme post-harvest cold has several times been a principal cause of death during the establishment of *M. × giganteus* experimental field sites, including the almost complete mortality of the University of Illinois Urbana-Champaign (UIUC) Energy Farm site in the winter of 2008–09 (Heaton et al., 2010; Zeri et al., 2011) that disrupted a number of planned bioenergy crop comparison studies. Other mass die-offs have occurred in northern Michigan (Song et al., 2014; D. Pennington, personal communication, 2015) and in central Wisconsin during the winter of 2008–09 (Heaton et al., 2010; G. Sanford, personal communication, 2015). In Europe, where *M. × giganteus* has been an experimental biofuel crop since at least 1992 (Heaton et al., 2008), a mass winter die-off occurred in Sweden (56°N; 93% loss) and Denmark (56.5°N; 100% loss) following a June 1997 planting; during this time the minimum 5cm soil temperature reached –5.4°C and –4.5°C, respectively (Clifton-Brown and Lewandowski, 2000). Nearby *M. × giganteus* stands in the United Kingdom (51.8°N) and Germany (48.7°N) experienced complete survival during the same winter, with 5cm minimum soil temperatures reaching –1.2°C and –2.8°C respectively. In a laboratory test, Clifton-Brown and Lewandowski (2000) found that freezing *M. × giganteus* rhizomes to a temperature of –3°C began to induce mortality and that at –3.5°C, half of the rhizomes had died. Peixoto et al. (2015) found that *M. × giganteus* rhizomes tolerated temperatures as

low as -6.5°C when lowered 1°C per hour in a laboratory freezing experiment, and several specific strains tolerated temperatures as low as -14°C when the temperature was lowered more slowly (1°C per day). Rosser (2012) notes that rarely did stands suffering 10% or greater mortality have yields in the following year that were sufficient to compensate for the loss.

3.1.2.2 Strategic in situ management methods of *M. × giganteus*

A set of *M. × giganteus* propagation strategies calls for the adoption of different planting techniques in areas with a greater likelihood of extreme cold winter temperatures in order to better insulate the rhizomes and prevent mortality. While Clifton-Brown and Lewandowski (2000) report a standard rhizome planting depth of 5cm in early European *M. × giganteus* stands, the standard practice in the US is now a planting depth of 10cm. This depth was first employed in Illinois in 2002 (Heaton et al., 2008) and was confirmed by Pyter et al. (2010) in a separate trial to be the planting depth which produced the greatest quantity of biomass after a single year's growth.

Pennington (2011) suggests that propagating *M. × giganteus* via plugs (i.e. with a small, viable existing shoot and root structure established in a greenhouse and micro-propagated within a block of soil), instead of via rhizomes, significantly reduces mortality and increases yield during the first two years of growth. Plazek et al. (2011) likewise observed decreased mortality in *M. × giganteus* plugs versus rhizomes, although only during the first year of growth, emphasizing the importance of mitigating winter temperature stress during the establishment year. However, Boersma and Heaton (2014) asserts that during *M. × giganteus* establishment in Iowa from 2009 to 2011, no significant

difference in yield or winter mortality was observed between the two propagation methods; moreover, *M. × giganteus* losses from failure to survive initial establishment outweighed *M. × giganteus* losses due to winter die-off by a factor of 20 during this time.

Kucharik et al. (2013) used a dynamic ecosystem model to show that as little as 2.5cm (1in) of post-harvest field residue was enough to raise the annual minimum 10cm soil temperatures by 1–3°C compared to bare soil across Iowa, Wisconsin, and Illinois, and 5cm of residue (enough to raise 10cm temperatures 2–5°C) virtually eliminated the risk of 10cm soil temperature reaching –3°C in Iowa, Illinois, Michigan, Kansas, and all states farther south. It is mentioned that leftover residue/stubble not only insulates the surface soil layer from radiative cooling but also preferentially traps snow, which insulates the soil even further; this is supported by Benoit et al. (1986).

3.1.3 Michigan as a favorable region for *M. × giganteus* propagation

3.1.3.1 Opportunity cost of land

Several studies analyzing the economic requirements and viability of a *M. × giganteus* regime in the US have been undertaken (e.g. Khanna et al., 2008; Jain et al., 2010; Xie et al., 2013). Notably, Jain et al (2010) developed a county-level budget of and switchgrass production costs in the Midwest. Michigan was found to be the state with the lowest opportunity cost of land for a corn-soybean rotation. It is asserted that in regards to the opportunity cost of land for *M. × giganteus*, Michigan is second to Missouri. The hypothetical *M. × giganteus* yield in Michigan was found to have a breakeven price for profitability of \$79–128 per ton of dry matter, comparable to Iowa but slightly higher than

that of Illinois, Indiana, Ohio, and Missouri due to the modeled risk of cold mortality in Michigan.

3.1.3.2 Snowpack insulation

Just as it takes little crop residue to decrease soil heat loss in the winter per Kucharik et al. (2013), the insulating effects of snowpack are also significant. The thermal conductivity of snow is one-third to one-fifth that of mineral soil; therefore, less heat is transferred by conduction to a colder atmosphere when the ground is snow-covered (Figure 13). Specifically, Geiger (1965) found that it takes 7.5cm of snow to dampen the daily range of surface soil temperature by fifty percent, and Sharatt et al. (1992) and Isard and Schaezl (1995) analyzed empirical data to conclude that 15cm of snow is sufficient to achieve a steady state soil temperature. In Finland, the lowest observed 10cm soil temperature under a non-vegetated surface and at least 30cm of snow during several weeks of temperatures below -20°C was -1.5°C (Sutinen et al., 2008).

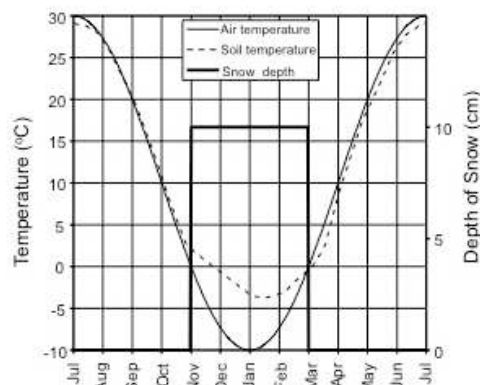


Figure 13: Yearlong time series from an idealized model of 2m air temperature (thin solid line), 10cm soil temperature (dashed line), and presence of snow cover (thick solid line). Soil temperature is modeled to remain warmer than the sub-freezing air temperature during periods of snow cover. Bonan, 2013.

It is hypothesized that regions that are characterized not only by relatively high annual snowfall but also by continuous snowpack coverage are less likely to experience threateningly low shallow soil temperatures for *M. × giganteus* (i.e. less than -3°C). Areas that experience regular lake effect snowfall fit these criteria, and one such area in particular is the west coast of Michigan's Lower Peninsula due to the impact of lake effect snow from the Great Lakes of North America. When cold air aloft behind a cold front travels over the relatively warmer water of the Great Lakes, vigorous convection can occur that results in bands of heavy snowfall downwind (Figure 14 and Bluestein, 1993). These annual winter conditions over the Great Lakes result in the highest average seasonal snowfall totals recorded in the US apart from mountain locations (Climate Source, 2015). In Michigan specifically, Figure 15 demonstrates the influence of steady lake effect snow on average annual snowfall, with many areas along Michigan's western coast receiving over double the snowfall of inland locations just 50 to 100km farther east. The effects of this continuous snowpack were outlined by a study of 5cm soil temperatures in Michigan over the course of five climatologically disparate winters (Isard and Schaetzl, 1998): most of western Michigan's topsoil layers remained unfrozen during all or nearly all of the winters, while more inland and southern locations (i.e. beyond the influence of lake effect snow) experienced hard freezes every year.

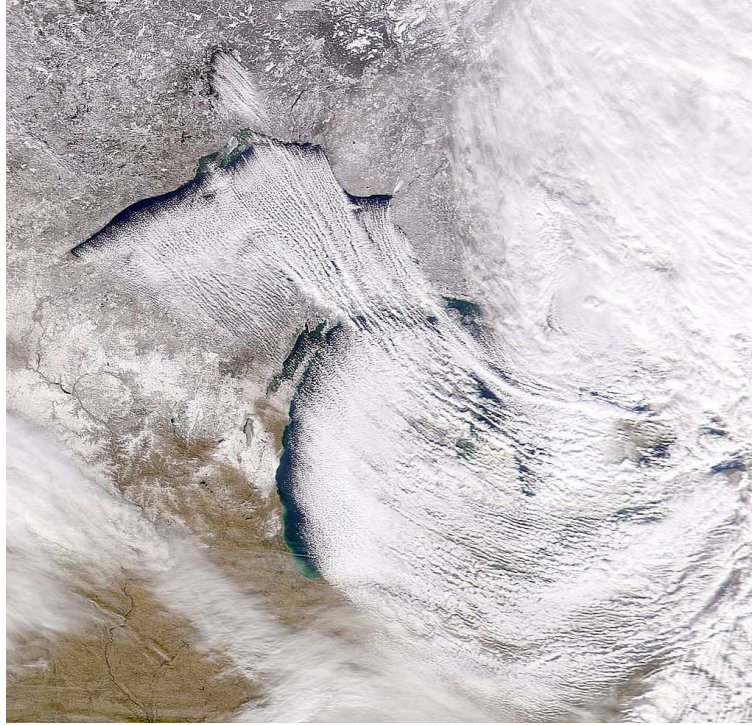


Figure 14: Visible satellite imagery of lake effect convection over Michigan on November 30, 2004. Nemiroff and Bonnell, 2015.

Analyses of empirical and modeled climate and soil data in Michigan specifically show that soil temperature is more dependent upon snowpack depth and persistence than upon air temperature (Isard and Schaetzl, 1998). Schaetzl and Tomczak (2001) found that two barren sites in central Michigan experienced soil freezing to depths greater than 20cm, but two nearby sites protected by leaf litter and a thin but continuous snowpack in a forest setting did not freeze below 3cm. Isard and Schaetzl (1995) modeled the forty-year average minimum monthly soil temperature in the Lower Peninsula of Michigan and found it to be 1.7°C warmer at the lake effect snowbelt site than at the non-snowbelt site along the same latitude less than 42km apart. Enhanced snowfall also contributes to a favorable increase in soil moisture recharge at the beginning of the temperate growing season (Johnsson and

Lundin, 1991; Hinkel et al., 1997; Sutinen et al., 2008). This augmented, continuous infiltration of snowmelt also aids in the decomposition of residue from the previous year, delivering an increase in nutrients to the soil below (Schaetzl et al., 2005).

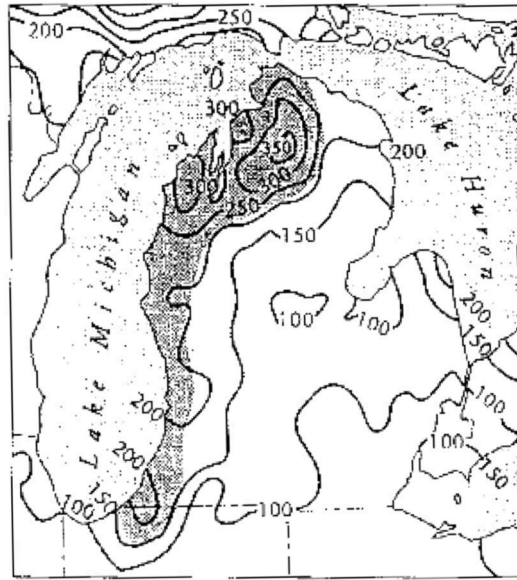


Figure 15: 1951–1980 mean annual snowfall (cm) in Michigan. Lake effect snowbelt is shaded in gray. Isard and Schaetzl, 1998.

3.1.4 Objective

It has been asserted that cold temperatures during the winter of 2008–2009 led to the mass mortality of *M. × giganteus* at experimental sites in Champaign, Illinois and Arlington, Wisconsin (Heaton et al., 2010; Zeri et al., 2011; G. Sanford, personal communication, 2015). However, *M. × giganteus* crops in southwest Michigan experienced near total survival during this time period despite being established in the same manner (Zeri et al., 2011; D. Pennington, unpublished data, 2015). This study seeks to use observations to explore and test the hypothesis that the prevalence of lake effect snow in

the Lower Peninsula of Michigan may reliably insulate the 0-10cm soil layer and meaningfully reduce the local wintertime mortality of *M. × giganteus* rhizomes. This possible preferential survival, coupled with low opportunity costs of land, would render southern Michigan a favorable area for future propagation of *M. × giganteus*.

3.2 Methodology

3.2.1 *M. × giganteus* sites, observations, and analysis

Four experimental *M. × giganteus* sites were analyzed during the winter of 2008–2009 and the winter of 2013–2014. The details of each site are presented in Table 3 and their locations shown in Figure 16. Each of the four sites, in addition to having an experimental first-year *M. × giganteus* crop, has an automated weather station either collocated or within 5km that measures 2m air temperature and 5cm soil temperature (soil heat flux plates [Illinois, Michigan; Zeri et al., 2011] and chromel-constantan thermocouples [Wisconsin; Kucharik et al., 2013]). While 10cm is the standard planting depth of *M. × giganteus* rhizomes, analysis at these sites was at a depth of 5cm to maintain consistency, since not all stations have soil temperature measurements at 10cm. All hydrometeorological data at each site have undergone quality control and gap-filling according to the methods of each collection agency (Zeri et al., 2011; Bland and Wayne, 2015; Olsen et al., 2015), and data availability ranges from 2008 to the present at the Wisconsin and Michigan stations and from 2008-2013 at the Illinois station. For this reason, the Illinois station was analyzed only during the winter of 2008-2009. Snow cover data from the state climatologists of Illinois and Wisconsin (Angel, 2015; Young, 2015), as

well as assimilated satellite and ground observations (SNODAS) in Michigan developed by the National Oceanic and Atmospheric Administration (NOAA) National Operational Hydrologic Remote Sensing Center (NOHRSC, 2004), were used as a proxy for station snowfall data since snowfall is not measured automatically. A synoptic weather analysis was also undertaken to further explain snow cover and soil temperature observations in the winter of 2008-2009.

Table 3: *M. × giganteus* site data: location, timeframe, survival, and hydrometeorological observation sources. References: [1] Zeri et al., 2011 and Zeri et al., 2013; [2] Thelen et al., 2009; [3] Heaton et al., 2010; [4] G. Sanford, personal communication, 2015; [5] D. Pennington, unpublished data, 2015; [6] Bland and Wayne, 2015; [7] Olsen et al., 2015; [8] Angel, 2015; [9] Young, 2015; [10] Snow data assimilation System (SNODAS): NOHRSC, 2004.

Site	Winters Analyzed	Survival >70%	Data: Weather/Soil	Data: Snow Depth
Champaign, Illinois (40.06°N, 88.20°W)	2008-09	No ¹	Energy Biosciences Institute: Champaign ¹	in situ ⁸
Arlington, Wisconsin (43.31°N, 89.38°W)	2008-09 2013-14	No ^{2,3,4} Yes ⁴	University of Wisconsin Extension Ag. Weather station: Arlington ⁶	in situ ⁹
Hickory Corners, Michigan (42.41°N, 85.37°W)	2008-09 2013-14	Yes ^{1,5} Yes ⁵	Enviro-weather station: Hickory Corners ⁷	SNODAS ¹⁰
East Lansing, Michigan (42.67°N, 84.49°W)	2008-09 2013-14	Yes ^{1,5} Yes ⁵	Enviro-weather station: East Lansing ⁷	SNODAS ¹⁰

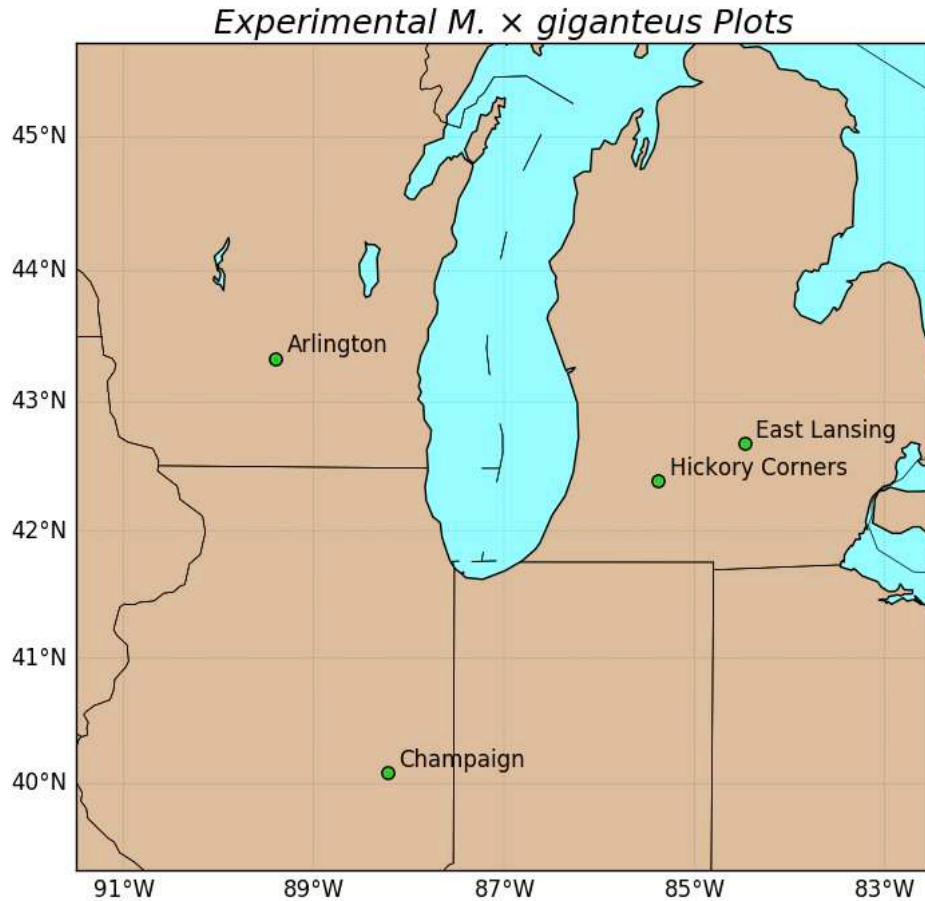


Figure 16: Four experimental *M. × giganteus* monitoring sites: Champaign, Illinois (University of Illinois), Arlington, Wisconsin (University of Wisconsin), and East Lansing and Hickory Corners, Michigan (Michigan State University). In 2009, the sites at Champaign and Arlington suffered near complete mortality while the sites in Michigan experienced near complete survival.

The hourly time series of air and soil temperatures at the four stations was compared during times of snow cover greater and less than 2.5cm (1in) during the winters of 2008-2009 and 2013-2014. Additionally, in order to test the degree that snow cover insulated the soil at these sites, the average absolute hourly difference of soil and air temperature during snow cover and no snow cover was calculated along with 5th and 95th percentile hourly values. To test if the two datasets were statistically different, two-sample t-tests were performed after avoiding autocorrelation by appropriately reducing the temporal frequency of the temperature data by a factor of the e-folding time of the time

series. Since the snow vs. no snow temperature datasets were assumed to be of different size and variance, normalization via the central limit theorem was employed followed by Welch's *t*-test. The dataset pairs were expected to pass at a level of $\alpha=0.01$ or lower to be considered statistically significant.

3.2.2 Additional observations and analysis in Michigan

To assess on a greater spatial scale the effects of lake effect snow cover on soil insulation in the Lower Peninsula of Michigan, air and soil temperature analysis was expanded to include data from the Enviro-weather (EW) Michigan observation network (Olsen et al., 2015). 12 EW stations were selected (Figure 17) for comparison of time series differences in 2m air temperature and 5cm soil temperature during periods of snow cover and no snow cover (again, in order to maintain consistency, 5cm data was used instead of 10cm [standard *M. × giganteus* rhizome depth], since 10cm soil temperature is not measured at all sites). These 12 specific stations were selected due to their data availability 2008-present, as well as their diversity in location: four stations within 10km of Lake Michigan ("lakeside"), six stations 10–100km from Lake Michigan ("near-lake"), and two stations in southeast Michigan ("inland") that are situated well beyond the principal lake effect snowbelt.

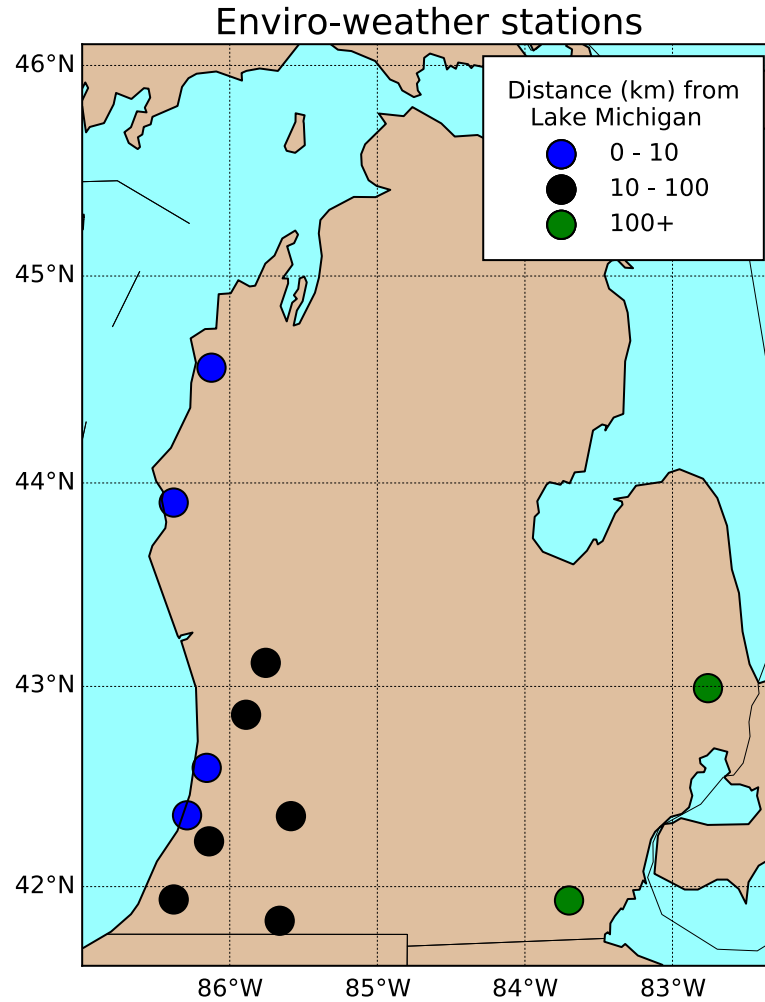


Figure 17: Location of selected stations from Michigan State University's Enviro-weather network. Blue dots represent lakeside stations, black dots represent near-lake stations, and green dots represent inland stations chosen for this study.

In order to expand the comparison of soil temperatures during times of snow cover vs. no snow cover to include the 12 EW sites during DJF 2008-2015, areal snow cover data of a higher spatial resolution than climatologist and airport observations were needed. In this analysis, data from the NOHRSC SNOw Data Assimilation System (SNODAS) were used

(NOHRSC, 2004). These data, available over the timeframe of study at a resolution of 1km in the US, incorporate downscaled predictions from numerical weather prediction models into a physically-based, energy- and mass-balanced snow model, also assimilating satellite, aircraft, and ground observations, to predict various snow cover parameters including snow water equivalent and snow depth. EW stations were matched to their corresponding NOHRSC data grid cell and were subsequently binned by snow depth in increments of 2.5cm. The mean soil temperature, 1st and 99th percentile temperatures, and outliers were calculated from the observations within each of these snow depth bins. The results from these seven consecutive winters in Michigan broaden the spatial and temporal range of evidence as to whether increased snow depth may lead to a robust, decreased likelihood of 5cm soil temperature reaching each experimental mortality threshold of *M. x giganteus*: –3°C (Clifton-Brown and Lewandowski, 2000; hereafter referred to as **CL2000**) and –6°C (rounded from –6.5°C; Peixoto et al., 2015; hereafter referred to as **PFS2015**).

3.3 Results

3.3.1 Climate and meteorological observations

Both the winters of 2008–2009 and 2013–2014 had below average temperatures and above average snowfall across most of the Midwest, although Champaign recorded below average snowfall during 2008–2009 (US NOAA National Climatic Data Center 1981–2010 U.S. climate normals: Arguez et al., 2012). Table 4 summarizes the 1981–2010 average winter temperatures and snowfall in Champaign, Arlington, and East Lansing alongside in situ observations from the winters of 2008–2009 and 2013–2014.

Table 4: December through February (DJF) temperature/snowfall averages and observations at three *M. × giganteus* sites (Arguez et al., 2012).

	<i>Avg. DJF temp. (°C)</i>	08–09 DJF temp. (°C)	13–14 DJF temp. (°C)	<i>Avg. DJF snow (cm)</i>	08–09 DJF snow (cm)	13–14 DJF snow (cm)
Champaign, IL	–2.3°C	–3.7°C	–4.2°C	67	42	110
Arlington, WI	–7.4°C	–9.8°C	–12.8°C	130	209	132
E. Lansing, MI	–3.5°C	–6.2°C	–7.3°C	130	213	173

Champaign, Illinois, the location of the experimental cropping site of the UIUC Energy Farm in the east-central part of the state, has an average December through February (hereafter DJF) temperature of –2.3°C and an average seasonal snowfall of 67cm. The winter of 2008–2009 was the 28th coldest on record in Illinois; Champaign recorded an average DJF temperature of –3.7°C (1.4°C below average) and a total seasonal snowfall of 42cm (25cm below average). The winter of 2013–2014 was the 9th coldest on record in Illinois; Champaign recorded an average DJF temperature of –4.2°C (1.9°C below average) and a total seasonal snowfall of 110cm (43cm above average).

Arlington, Wisconsin, the location of the experimental cropping site of the Great Lakes Bioenergy Research Center, is located in southern Wisconsin, 30km north of Madison. Arlington’s average DJF temperature is –7.4°C and average seasonal snowfall is 130cm. The winter of 2008–2009 was the 18th coldest on record in Wisconsin; Arlington recorded an average DJF temperature of –9.8°C (2.4°C below average) and a total seasonal snowfall of 209cm (79cm above average). The winter of 2013–2014 was the 4th coldest on record in Wisconsin; Arlington recorded an average DJF temperature of –12.8°C (5.4°C below average) and a total seasonal snowfall of 132cm (2cm above average).

East Lansing, Michigan, the location of one of the experimental *M. × giganteus* cropping sites of Michigan State University (MSU), is located along the eastern fringe of the southern Michigan lake effect snowbelt. East Lansing has a similar climate to Hickory Corners, Michigan, which lies 80km to the southwest and is another MSU experimental *M. × giganteus* site. East Lansing's average DJF temperature is -3.5°C and average seasonal snowfall is 130cm. The winter of 2008–2009 was the 20th coldest on record in Michigan; East Lansing recorded an average DJF temperature of -6.2°C (2.7°C below average) and a total season snowfall of 213cm (83cm above average). The winter of 2013–2014 was the 10th coldest on record in Michigan; East Lansing recorded an average DJF temperature of -7.3°C (3.8°C below average) and a total season snowfall of 173cm (43cm above average). East Lansing also broke its own record for most consecutive days of snow cover during this winter, with 110 consecutive days with at least 2.5cm (1in) of snow on the ground from late December 2013 to late March 2014 (Hoepner, 2014).

3.3.2 Time series of air temperature, soil temperature, and snow cover

The following time series show hourly 2m air temperature, hourly 5cm soil temperature, and hourly presence (binary) of at least 2.5cm snow cover from January to early March of 2009 (Figure 18) and 2014 (Figure 19) at the four stations. Figure 19 does not include data from Champaign due to lack of data availability at this particular *M. × giganteus* site. In all of these diagrams, blue shading indicates time periods of snow cover greater than or equal to 2.5cm.

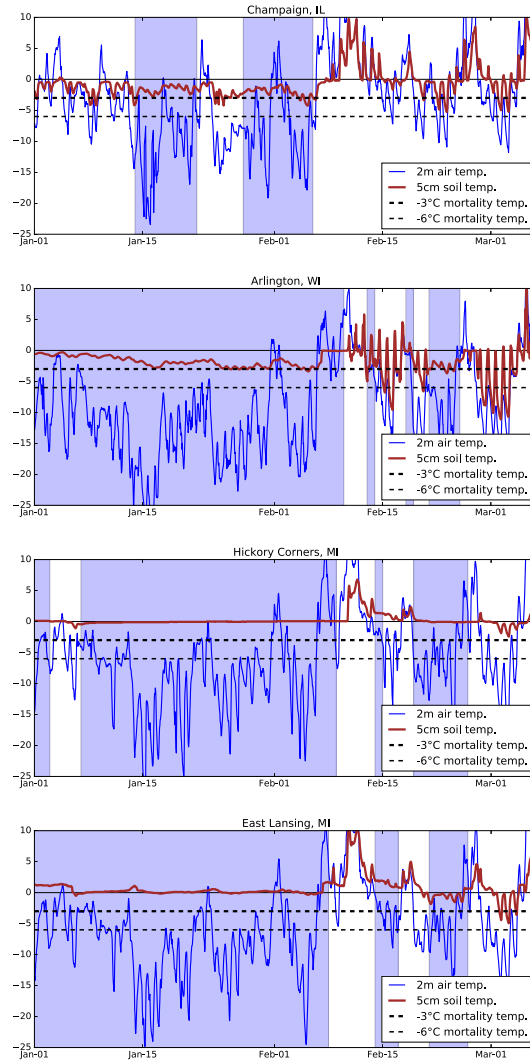


Figure 18: Hourly time series of soil and air temperature from January 1 to March 8, 2009 at each of the four experimental *M. × giganteus* sites. “Windows” of blue shading represent at least 2.5cm of snow cover on the ground. Dotted black lines indicate -3°C , and -6°C , the laboratory mortality temperatures of *M. × giganteus* observed by CL2000 and PFS2015, respectively. Near-complete mortality occurred at the sites of the first two time series, while near-complete survival occurred at the last two. It can be seen that soil temperature more readily fluctuated with air temperature during periods of no snow cover. Only the second time series (Arlington, WI) registered soil temperatures below the -6°C threshold of PFS2015.

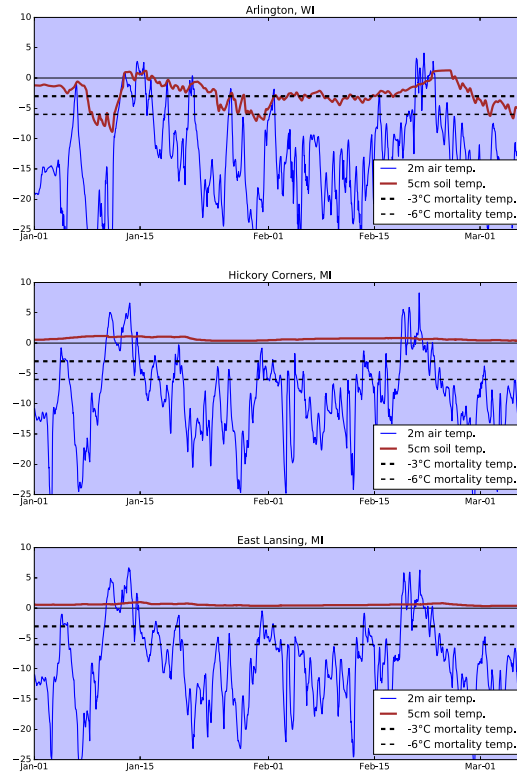


Figure 19: Hourly time series of soil and air temperature from January 1 to March 8, 2014 at Arlington, Hickory Corners, and East Lansing. “Windows” of blue shading represent at least 2.5cm of snow cover on the ground. Dotted black lines indicate -3°C , and -6°C , the laboratory mortality temperatures of *M. x giganteus* observed by CL2000 and PFS2015, respectively. Snow cover persisted for the entirety of each of these time series, and all sites experienced complete survival, although the Arlington time series still shows that soil temperatures dropped below both mortality thresholds.

At Champaign in 2009, the temperature remained above the CL2000 threshold of -3°C with snow cover on the ground except for a short interval in early February. Outside of these windows of snow cover, the 5cm soil temperature dropped below -3°C on ten separate occasions, but never dropped below the PFS2015 threshold of -6°C . In Arlington, snow cover persisted from January 1 to February 10 in 2009 and the 5cm soil temperature, while below freezing, remained at or above -3°C during this stretch. However, in the four intervals from February 10 onward during which there was no snow cover at Arlington, soil temperatures dropped well below -6°C at night and typically rebounded to above-

freezing soil temperatures during the day despite below-freezing air temperatures. Additionally, despite uninterrupted snow cover during the same timeframe in 2014 at Arlington, the soil temperature dropped below -6°C on seven separate occasions. It is possible that these variations, unseen in the Michigan time series in January through March of 2014, were due to instrument error, however no data quality control issues were reported by the Wisconsin State Climatology Office during this time frame (Young, 2015).

In 2009 at Hickory Corners, MI, insulating snow cover during most of January and early February caused the 5cm soil temperature to remain near 0°C despite air temperatures that were often below -20°C . This snow cover persisted until February 9, at which point a stretch of above-freezing temperatures caused the snow to melt. Two days later the phase change to liquid water was complete to a depth of 5cm, allowing the additional heat input from the unseasonably warm surface air to contribute to warming the soil rather than to the latent heat absorption that accompanies melting. Schaetzl and Tomczak (2001) likewise observed this phenomenon of shallow soil temperature lagging behind atmospheric temperature due to the latent heat requirements of the phase changes of water, manifested by a “flatlining” of temperature until all water at that depth is either completely liquid or completely frozen. Once this is achieved, the temperature can more freely fluctuate with the atmospheric temperature, assuming no snow cover and minimal residue. Another weeklong snowfall event at Hickory Corners in late February brought the 5cm soil back to the freezing point but no further, at which point the heat loss to the atmosphere was balanced by heat transfer from the relatively warmer ground below. However, with no snow cover at Hickory Corners in early March 2009, the 5cm soil temperature dropped below freezing and approached -3°C , the CL2000 laboratory

mortality temperature of *M. × giganteus*. At Hickory Corners in 2014 the scenario was quite different: despite the winter being much colder than average, the 5cm soil temperature remained at or above freezing for the duration of the timeframe of study.

In East Lansing, conditions were similar to Hickory Corners during both winters. In early March 2009, East Lansing recorded 5cm soil temperatures slightly below -3°C due to cold temperatures and no protective snow cover, however, the crop almost completely survived. In addition to the 5cm soil temperature not dropping below the -6°C PFS2015 mortality threshold in 2009, it is also a possibility that the slightly deeper but unobserved 10cm (standard rhizome depth) soil temperature remained above the -3°C CL2000 mortality threshold as well.

Table 5 shows the average absolute difference between 2m air temperature and 5cm soil temperature at each of the four sites from January 1 to March 8, 2009 during times of snow cover and no snow cover. Also included are the 5th and 95th percentile absolute difference values, i.e. 90% of the absolute temperature differences lie between these two values. It can be seen that there was a greater average difference between air and soil temperature during periods of snow cover. The soil-air absolute differences were also greater during extreme cold events with snow on the ground, seen in the 95th percentile values. Each of the four dataset pairs presented (two snow cover scenarios at four sites) are calculated to pass Welch's *t*-test with a p-value lower than the significance level $\alpha = 0.01$, indicating that the means of the absolute soil-air temperature differences are statistically different. This suggests that snow cover provided a meaningful insulating effect at each of these four sites during this timeframe.

Table 5: Average absolute difference of 5cm soil and 2m air temperature with and without snow cover from January 1 to March 8, 2009. Numbers in parentheses are the 5th and 95th percentile absolute differences, respectively, i.e. 90% of the absolute temperature differences lie between these two values. Each pair of complete datasets is calculated to pass Welch's *t*-test with a p-value lower than $\alpha = 0.01$, indicating that absolute soil-air temperature differences during periods of snow cover were statistically higher than during periods of no snow cover over this time frame.

Site	$ T_{\text{soil}} - T_{\text{air}} $ (°C), 2.5+ cm snow cover	$ T_{\text{soil}} - T_{\text{air}} $ (°C), < 2.5cm snow cover	Difference in means passed <i>t</i> - test at $p < 0.01$?
Champaign, IL	7.6 (0.8, 16.8)	3.9 (0.3, 8.7)	Yes
Arlington, WI	9.5 (1.1, 19.3)	2.8 (0.3, 10.7)	Yes
Hickory Corners, MI	9.0 (1.7, 20.5)	5.7 (0.6, 13.2)	Yes
East Lansing, MI	8.3 (1.6, 19.3)	4.8 (0.4, 10.1)	Yes

3.3.3 Synoptic analysis

At all four of these experimental *M. × giganteus* sites in early 2009, the timing of snowfall and cold air masses appears to play a large role in crop survival. The majority of cold temperature events in boreal winter in the US Midwest are associated with high-pressure systems that originate in Canada and move southward behind low-pressure systems that sweep northeastward across the eastern half of the US (Bluestein, 1993). These low-pressure systems are accompanied by a southward-stretching cold front and precipitation centered on the low-pressure system, extending in bands southward along the front. If temperatures are cold enough, this precipitation falls as snow. It is this snow cover that often protects against the cold temperatures that follow behind such frontal passage.

A series of surface weather maps in Figure 20 and Figure 21 show two mid-latitude systems that brought precipitation and cold temperatures to the Upper Midwest in early 2009. During the first event (13–16 January 2009), 5cm soil temperatures at each of the

four *M. × giganteus* sites of focus remained above the CL2000 *M. × giganteus* mortality temperature of -3°C . During the second event (25 February – 3 March 2009), 5cm soil temperatures at all sites but one (Hickory Corners) did not, and at Arlington the soil temperature reached below the PFS2015 mortality threshold of -6°C . Figure 20 extends from 13–16 January 2009 during and after the passage of a cold front in the eastern half of the US. The dashed light blue line represents the location of the 0°C surface isotherm at 0700 Eastern Standard Time (EST). A low-pressure system moved through the Upper Midwest on January 13 followed by another faster-moving low on January 14, which brought significant snow to the region. Over the following two days, cold, high-pressure air from Canada moved southward across the region. This onset of snow cover and subsequent cold temperatures can be seen in the meteorological data of the four experimental *M. × giganteus* sites in Figure 18. The shallow soil layers remained above -3°C likely due to the snow cover during this time period.

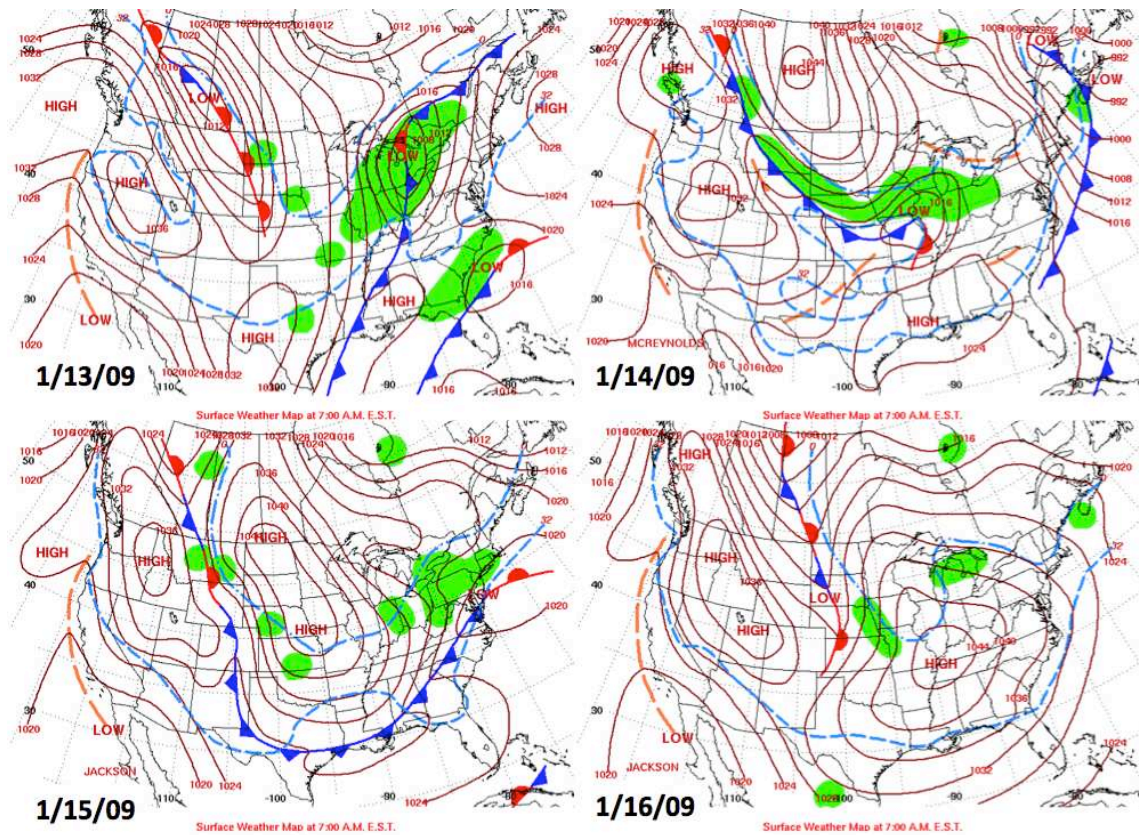


Figure 20: Surface weather maps over the contiguous US, 13–16 January 2009. The southernmost dashed light blue line represents the 0°C surface isotherm. Passage of a low pressure system in the US Midwest is seen, immediately followed by a high pressure system which brought well below-freezing air to the region.

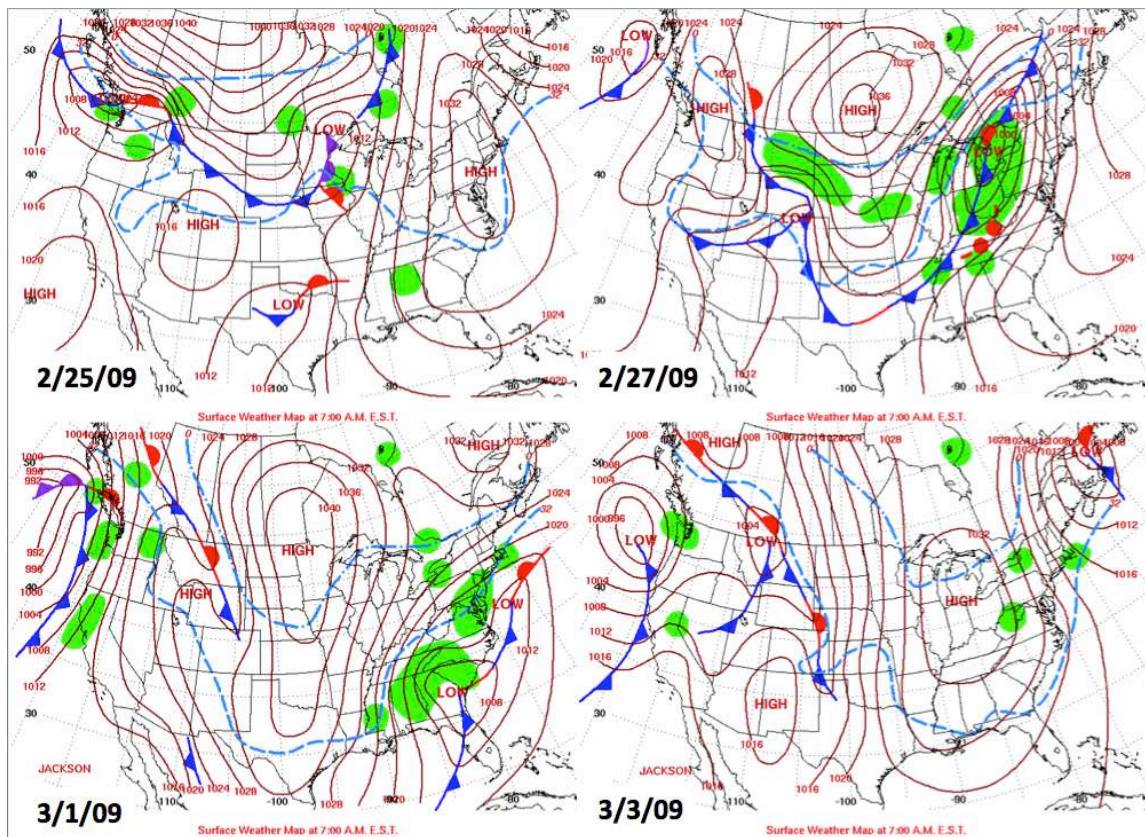


Figure 21: Time series of surface weather maps over the contiguous US 25 February to 3 March 2009. The southernmost dashed light blue line represents the 0°C surface isotherm. Passage of a low pressure system in the US Midwest is seen, ahead of which the surface temperatures were warm enough to melt existing snow cover. Following this passage, a high pressure system set in, which brought well below-freezing temperatures to the region.

In contrast, Figure 21 is a series of surface maps from 25 February to 3 March 2009: during 25 – 27 February a much slower-moving low-pressure system traversed the Upper Midwest, providing additional time to advect warmer air from the south northward ahead of the front, which caused significant melting and also caused the majority of the associated precipitation to reach the surface as rain, not snow. Figure 22 shows CoCoRaHS observations of this melting and lack of subsequent snow cover in southern Michigan. Behind this cold front, a high-pressure system once again moved in, which led to a series of three clear, cold nights. With no protective snow cover, enhanced radiative cooling of the surface led to the

coldest 5cm soil temperatures of the year from 1 – 4 March at each of the sites despite nighttime low air temperatures during this timeframe remaining much warmer than the coldest air temperatures experienced in 2009. It is this latter type of system, with complete snowmelt immediately succeeded by a snow-less cold front and subsequent high-pressure regime, that may pose the biggest wintertime threat to *M. × giganteus* crops in the US Midwest.

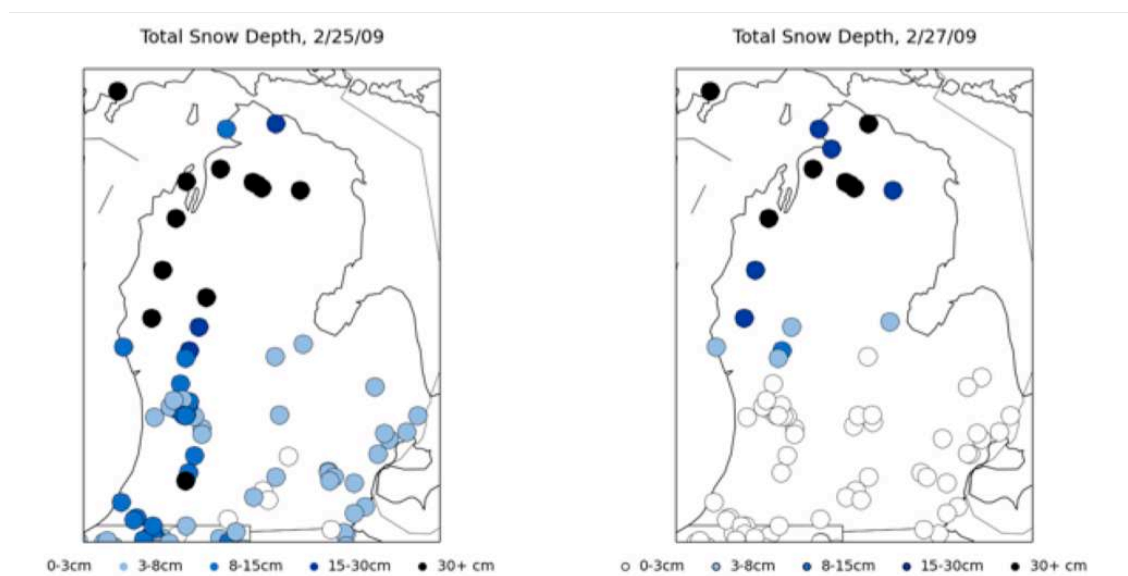


Figure 22: CoCoRAHS observations of snowfall depth in Michigan on 25 February and 27 February 2009. Snowmelt caused by the southerly surge of warm air ahead of the low pressure system is reflected in diminished snow depths on 27 February, with white dots representing zero snow cover.

3.3.4 Enviro-weather stations time series and averages

Figure 23 shows the time series of 5cm soil data from each of the 12 stations plotted against the same data from Champaign from January 1 to March 8, 2009, with the EW station time series color-coded by proximity to the lake (see Figure 17). It can be seen that Champaign's shallow soil temperature was colder and more variable than any of the EW

sites. In fact, throughout the timeframe of focus only one EW site (an inland site) reached a temperature below the CL2000 *M. x giganteus* mortality threshold of -3°C . The time series average 5cm soil temperatures for the lakeside stations, near-lake stations, inland stations, and Champaign, respectively, were 0.98°C , 0.85°C , 0.07°C , and -0.51°C . The average difference between soil temperature and air temperature was virtually identical across the three EW regimes: between 5.7°C and 6.0°C . Meanwhile, the average soil-air temperature difference in Champaign was much lower, at 2.3°C .

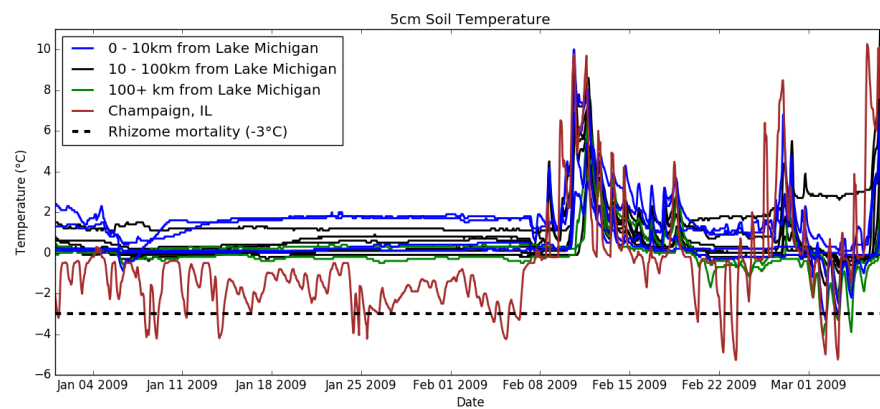


Figure 23: Time series of soil temperature at 12 Enviro-weather stations in Michigan and at the experimental *M. x giganteus* plot in Champaign, Illinois from January 1 to March 8, 2009, color coded by proximity to Lake Michigan. While the soil temperatures of every lakeside and near-lake station remained well above the CL2000 -3°C mortality threshold throughout the winter, both of the inland stations and the Champaign *M. x giganteus* site experienced soil temperatures below this threshold on at least three separate occasions during this time period.

Figure 24 is a box-and-whisker diagram of 5cm soil temperature vs. snow depth in seven consecutive winters (DJF) 2008-2015 at the 12 EW stations. Soil temperatures are binned in increments of 2.5cm of snow cover and there are at least 50 soil temperature observations at each of the snow depths shown. The mean soil temperature was 2.5°C with no snow cover, 2.2°C with 2.5cm of snow cover, and between 0.6°C and 1.1°C for every

other snow depth. None of the sites recorded a 5cm soil temperature below -3°C from 0-12.5cm of snow cover, but from 15-32.5cm of snow cover there were multiple instances of 5cm soil temperature dropping below -3°C. It should be noted that the soil temperature sensor at each of the EW sites used in this study is located beneath a surface cover of grass (Olsen et al., 2015), which may have also led to a positive temperature bias when compared to the *M. × giganteus* sites with varying amounts of post-harvest residue. It should likewise be considered that these data were taken at 5cm as opposed to the standard rhizome planting depth of 10cm. No 5cm soil temperatures at or below -6°C were observed at any of these sites during this time frame.

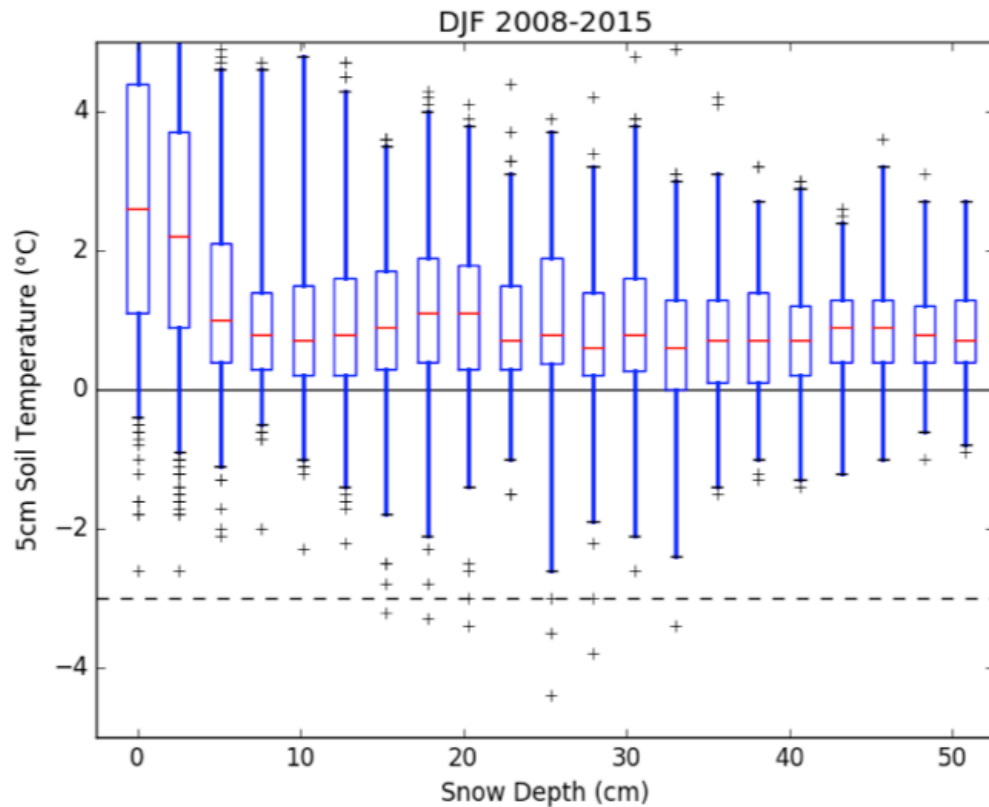


Figure 24: Distributions of hourly observed soil temperature (12 selected Enviro-weather stations) by snow depth (NOHRSC) during seven consecutive winters (DJF 2008-2015) in Michigan. There at least 50 soil temperature observations of each snow depth shown. At each depth, the box represents soil temperatures within the 1st and 99th percentile, the red bar represents the mean soil temperature, and '+' markers represent outliers. Also plotted as horizontal lines are 0°C (solid; freezing temperature of water) and -3°C (dashed; CL2000 laboratory mortality temperature of *M. × giganteus*). From 2008-2015 at the 12 stations, seven instances of the 5cm soil temperature dropping below -3°C were recorded with 15-32.5cm of snow cover, while zero such instances were recorded under 0-12.5cm snow cover. Zero instances of 5cm soil temperature dropping below -6°C (PFS2015 laboratory mortality temperature of *M. × giganteus*) were recorded.

3.4 Discussion

In Champaign, cold air temperatures during periods of no snow cover during the 2008–2009 winter contributed to soil temperatures dropping below the CL2000 mortality threshold of -3°C, potentially triggering the mass mortality of the *M. × giganteus* crop at

this site. Arlington experienced approximately the same amount of days with snow cover as the two Michigan sites during the 2008-2009 winter but had slightly lower air temperatures and recorded much lower extreme cold soil temperatures during periods of no snow cover, which led to mass mortality of *M. × giganteus*. In Michigan, first-year *M. × giganteus* crops experienced near total survival in both years. Additionally, at each of Champaign, Arlington, and East Lansing, the winter of 2013–2014 was colder than the winter of 2008–2009. In Arlington and East Lansing, the winter of 2013–2014 was also less snowy than the winter of 2008–2009. Given that colder air temperatures and shallower depths of snow cover are physically expected to contribute to colder shallow soil temperatures, it is concomitantly expected that the winter of 2013–2014 experienced higher first-year *M. × giganteus* mortality than the winter of 2008–2009. But in fact, at Arlington, while air temperatures dropped below -6°C frequently in both winters, *M. × giganteus* planted in 2008 experienced a near total die-off due to cold exposure during the winter of 2008–2009 but *M. × giganteus* planted in 2013 experienced little to no loss during the winter of 2013–2014.

In this study there were two instances when the observed 5cm soil temperature dropped below the CL2000 -3°C threshold and yet the first-year *M. × giganteus* crop experienced greater than 70% survival entering the growing season that immediately followed. In East Lansing, this threshold was reached during the high-pressure event of early March 2009. One possible explanation for this is that the PFS2015 experimental *M. × giganteus* mortality threshold of -6°C was never reached, and perhaps this threshold is more representative of the ability of rhizomes to tolerate cold soil temperatures. Another possible explanation for this discrepancy is that *M. × giganteus* rhizomes are typically

planted at a depth of 10cm, but in this study, only the 5cm temperatures were analyzed, since the Champaign observations were only taken at that depth. It is typically expected that deeper soil temperatures are warmer than shallower temperatures in the winter, and as expected the 10cm soil temperature at East Lansing in the winter of 2009 never dropped below -3°C , reaching an absolute minimum of -1.6°C on the morning of March 3, 2009. In Arlington, despite uninterrupted snow cover during the winter of 2014, the measured 5cm temperature dipped below the PFS2015 threshold of -6°C multiple times. This also occurred at a depth of 10cm, with a seasonal minimum of -7.2°C observed on the morning of January 9, 2014. The possible conclusions are that the sensor or sensor placement was errant, the new *M. × giganteus* rhizomes in 2013 were planted deeper than 10cm, or that this particular strain of *M. × giganteus* can tolerate colder soil temperatures than previously tested. The manner in which the mortality temperature is superseded might also matter, as delineated in Peixoto et al. (2015). For example, in Arlington in 2014, the observed temperatures below -6°C were reached more gradually, whereas at the same site in 2009 there were eight diurnal episodes of rapid thawing and subsequent refreezing to well below -6°C .

It is shown here and in past studies that snow cover insulates shallow soil layers. It would follow that areas that receive more annual snowfall (such as the lake effect snowbelt of Lower Michigan) are more likely to provide cold insulation throughout the winter, an important consideration for rhizomatous perennial crops such as *M. × giganteus* that do well in warm continental climates but are susceptible to cold mortality. However, other factors that may also contribute to the preferential wintertime survival of first-year *M. × giganteus* rhizomes at these sites are the establishment practices (Pennington, 2011;

Plazek et al., 2011; Boersma and Heaton, 2014) and also residual winter surface cover at each site. That is, since bare soil is more influenced by atmospheric temperature fluctuations than soil covered by vegetation or crop residue, *M. × giganteus* stands that have been established for three or more years typically produce more above-ground biomass (Heaton et al., 2010) that may be left on the ground post-harvest to help insulate the soil (Kucharik et al., 2013). Because none of the four sites discussed in the present study have available data from side-by-side replicate plots of *M. × giganteus* of different age and winter crop residue amounts, the effects of stand age on winter survival is beyond the scope of this research but would be an intriguing area of future study.

An additional factor beyond snow cover that may influence the extent to which soil temperature is affected by extreme cold soil temperature is soil water content. Due to the higher heat capacity of water and the latent heating/cooling associated with the phase change of water, soil with higher water content will take a longer amount of time to respond to changes in air temperature (Schaetzl and Tomczak, 2001). This “flatlining” can be seen in parts of the time series of soil temperature in Figure 18, when air temperature oscillated above and below 0°C during periods of no snow cover. In general, this means that moister soils will have a decreased likelihood of reaching extreme cold temperatures at 10cm. Of the four *M. × giganteus* sites of the present study, only the Champaign, Illinois site had available soil moisture data at an adequate temporal resolution; therefore, a detailed soil moisture analysis is beyond the scope of this study. However, a facet of soil water content to note is that during the harsh winter of 2013-2014, while first-year *M. × giganteus* survived at all four sites, experimental stands of first-year *M. × giganteus* in Iowa suffered severe mortality (Boersma and Bonin, 2014). Figure 25 shows modeled surface soil

moisture percentages in January 2009 and January 2014 in the Eastern US. It can be seen that in 2009, the areal surface soil moisture near each of the present sites was ample and thus may not explain the variability in mortality. However, in 2014, Iowa was much drier than Michigan and southern Wisconsin, which may have contributed to the mortality of *M. × giganteus* in Iowa during that winter. This would be another intriguing area of future replication and study.

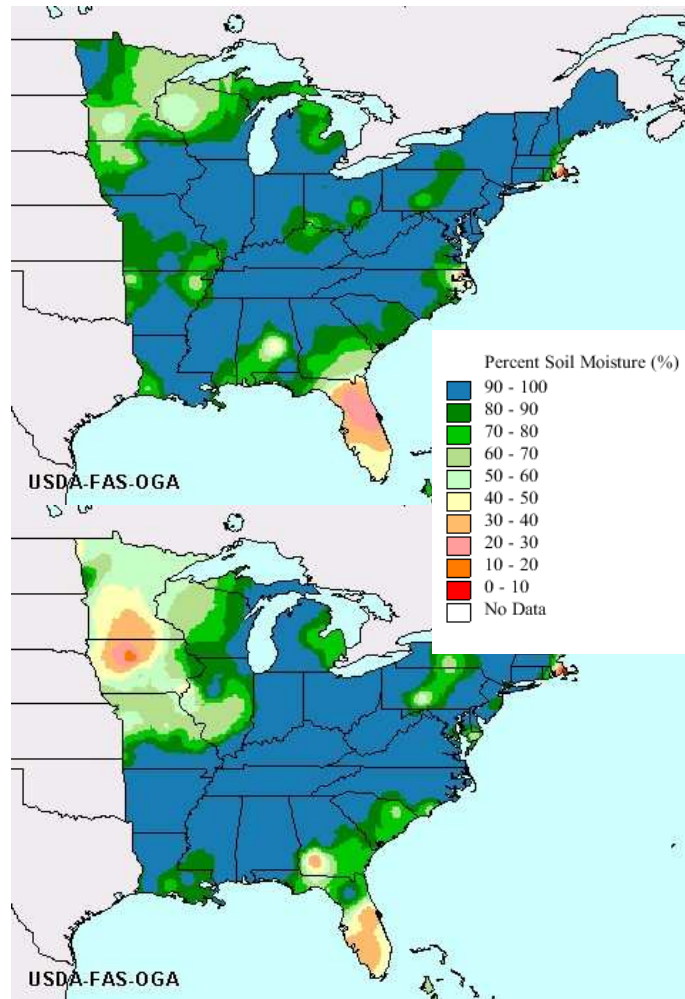


Figure 25: Areal surface soil moisture content in the Eastern US on January 10 of 2009 (top) and 2014 (bottom). Percentages were calculated using a two-layer soil moisture model, Penman-Monteith evapotranspiration, and FAO soil classification. (WMO, 2015). Soil moisture percentages in January 2009 were close to 100% throughout the majority of the area of study, while percentages in January 2014 were as low as 40% in southern Minnesota and 20% in Iowa, which allowed for soil temperatures to fluctuate more freely with the air temperature.

The soil and air temperature versus snow depth data shown in Figure 24 provide another refutation to the hypothesis that increased snow depth and persistence in Michigan's Lower Peninsula lake effect snowbelt will alone lead to a decreased likelihood of *M. x giganteus* cold mortality. Increased snow depth at the 12 selected EW stations did not

predict shallow soil temperatures. In fact, with little or no snow depth, the average soil temperature was actually higher, likely an artifact of pre-snowfall and post-snowmelt warm air events. Additionally, it is extreme cold soil temperature events, not the average of all events, that directly lead to cold-induced rhizome mortality of *M. × giganteus*, and soil temperatures below -3°C occur were recorded seven times from 2008-2015 across the 12 EW stations, each one of these instances occurring with between 15cm and 32.5cm of snow cover. This is in conflict with the idea that increased snow cover directly leads to a decreased likelihood of extreme cold soil temperatures.

Good management practices can be followed that leave enough residue to help shelter the otherwise bare soil, however this comes at the expense of losing marketable biomass, thus increasing the breakeven price of *M. × giganteus*. Another option could be to harvest and remove the entire *M. × giganteus* plant (leaving bare soil) but afterwards continuing to monitor snow depth, soil temperature, and the threat of cold-air, high-pressure systems (synoptic analysis) throughout the winter. If a complete snowmelt is forecasted to be quickly followed by a hard freeze, small acreage *M. × giganteus* farms could have enough warning time to apply an insulating layer of miscellaneous stover in preparation.

3.5 Conclusions

Lake Michigan's lake effect snowbelt is an intriguing option for large-scale expansion of *M. × giganteus* agriculture because the opportunity cost of land is low and the annual moisture supply is ample. The prevalence of orchards, another form of perennial

agriculture along the Lower Peninsula of Michigan's western coast, demonstrates this preference of perennial growth along Lake Michigan's lake effect snowbelt (Kiefer, 2015). This study used observations to explore and test the hypothesis that the prevalence of lake effect snow in the Lower Peninsula of Michigan may reliably insulate the 0-10cm soil layer and meaningfully reduce the local wintertime mortality of *M. x giganteus* rhizomes. This hypothesis was here disproven that snow cover in the western Lower Peninsula of Michigan categorically decreases the likelihood of soil temperatures lower than the *M. x giganteus* mortality threshold. Each of the four experimental sites exhibited an absolute difference in 5cm soil temperature and 2m air temperature that was statistically greater during times of at least 2.5cm snow cover than times of no snow cover. However, there were still multiple instances of the 5cm soil temperature dropping below -6°C at these *M. x giganteus* sites despite ample snow cover. The rapid melting, varying snowfall totals, and subsequent intense cold often associated with the passage of synoptic-scale systems in Michigan likewise contribute to the volatility of depending solely on snow cover to prevent *M. x giganteus* mortality. Analysis of observations at 12 additional Enviro-weather stations in Michigan over seven consecutive winters also showed instances of soil temperatures dropping below -3°C (although never below -6°C), despite being covered with 15-32.5cm of snow. These results together indicate that snow should not be exclusively relied upon to insulate shallow soil layers and improve the wintertime survival of *M. x giganteus*.

The precise instances and circumstances of past cold mortality events of *M. x giganteus* in the US Midwest will be valuable in the future parameterization of crop and land surface models in this region and in similar areas such as Southern Ontario (Canada), which has little empirical information to help test model results of the productivity and

biogeophysical effects of *M. × giganteus* on a regional scale. However, due to the lack of organized observations and dissemination of *M. × giganteus* winter survival statistics, it remains difficult to assign a universal explanation for the preferential *M. × giganteus* survival in Michigan during the winter of 2008–2009 compared to the affected Wisconsin and Illinois crops. By continuing to organize and publish the details of *M. × giganteus* sites, including establishment practices, stand age, wintertime residue, soil moisture, and mortality statistics, the circumstances of cold-induced *M. × giganteus* mortality can be more rigorously analyzed on a site-by-site level and the most favorable geographic zones for future *M. × giganteus* propagation properly adjusted.

CHAPTER 4

Areal estimates of the sustainability and hydrometeorological impacts of a *Miscanthus × giganteus* regime in the US Midwest

4.1 Introduction

The cultivation of biofuel crops, particularly corn (*Zea mays*), as a renewable energy source continues to be a common practice in the United States. The United States has ample land area and an immense agricultural sector, both of which have facilitated the large-scale implementation of biofuel crop regimes and policy.

However, as delineated in Heaton et al. (2008), there is not enough usable land in the heart of the United States agricultural belt, i.e. the US Midwest and Great Plains, to achieve the domestic biofuel production goals of the 2007 Energy Independence and Security Act (EISA; US House, 2007) using corn alone. For this reason, the perennial grass *Miscanthus × giganteus* (*M. × giganteus*) has been a crop recently touted to be a solution to this domestic ethanol production problem by numerous agricultural studies (e.g. Dohleman and Long, 2009; Heaton et al., 2010, Arundale, 2012; VanLoocke et al., 2012). *M. × giganteus* benefits from producing an immense amount of convertible biomass per unit surface area: it perennially grows to be 3-5 m tall in areas with sufficient precipitation after several years of establishment. Heaton et al. (2008) famously asserted that if all the corn being grown for biofuel in the US in 2007 were switched to *M. × giganteus*, the 2022 EISA ethanol goal would be met immediately.

Many questions have been raised about the long-term sustainability of *M. × giganteus*, however. The biggest unknown, and the one upon which the economic and

political questions lean, is the yearly biogeophysical sustainability of *M. × giganteus*. Simply put, if *M. × giganteus*, which uses 39-56% more water each year than corn (McIsaac et al., 2010; Hickman et al., 2010; Le et al., 2011; VanLoocke et al., 2012), is routinely stilted or killed due to drought or extreme cold, as it has recently been shown to do (Zeri et al., 2011; Zeri et al., 2013; Roy and Baker, Chapter 2), it can not and will not be a viable renewable energy option. *M. × giganteus*, being a perennial grass that propagates by rhizome, takes two to three years to reach productive maturity (Heaton et al., 2010), and therefore just one year in ten of mortality will result in a loss of at least 20-30% of its decadal biomass potential, in addition to the financial toll of purchasing and replanting new rhizomes.

It is therefore summarily important to understand the realistic bounds of *M. × giganteus* sustainability in the US. Without an existing large-scale regime of *M. × giganteus* in the US, such understanding must come from scattered experimental sites and concomitant mechanistic modeling that can accurately reproduce the behavior observed at these sites (e.g. yield, leaf area index, latent heat flux, carbon assimilation, rooting zone soil moisture). The results of three such modeling studies, each of which has arrived at a different estimate of its bounds of sustainability, are shown in Figure 2.

This research sought to bolster and extend the existing empirical data and modeling techniques on a large scale in order to provide an updated, realistic areal estimate of long-term *M. × giganteus* sustainability in the US Midwest and Great Plains. It was the first study to employ a third-generation land surface model (LSM), the third version of the Simple Biosphere model (SiB3). Using a first-of-its-kind *M. × giganteus* surface parameterization empirically derived and validated over Champaign, Illinois, USA as described in Chapter 2, the spatial domain was expanded to comprise 75 1-degree by 1-degree grid cells in the US

Midwest and Great Plains, where the parameterization was applied over a span of fourteen years (2000-2013). The critical possibility of *M. × giganteus* mortality due to extreme cold soil temperatures each winter was also included in such an estimate for the first time. (see Roy, 2016 and Song et al., 2014). The hours and instances of mortality-inducing drought and cold indicated by SiB3 were tracked and mapped. Additionally, the modified local soil moisture equilibrium modeled by SiB3 was characterized at four contrasting sites in the domain via examination of the evolution of calculated stomatal stress due to dry soil. The joint results of these analyses and insights resulted in an updated estimate of the bounds of *M. × giganteus* sustainability in the US Midwest, which will contribute to a conclusive and imminently necessary decision as to whether or not *M. × giganteus* should be implemented as a large-scale biofuel crop in the US.

4.2 Methods and Planned Analyses

4.2.1 Simple Biosphere model (SiB3)

The Simple Biosphere model (SiB; Sellers et al., 1986) was introduced in 1986 with the intent of providing a lower boundary for General Circulation models. The model provided the necessary exchange of energy, moisture and momentum with the atmosphere, but with a level of biophysical complexity that made the model useful to ecologists as well. SiB simulates photosynthesis using enzyme kinetics following Farquhar et al. (1980) and couples photosynthesis to stomatal conductance and energy and moisture exchange using Collatz et al. (1991, 1992). SiB was updated to incorporate satellite observations of vegetation phenology (SiB2; Sellers et al., 1996a, 1996b), and soil/snow processes based on the Community Land Model (CLM; Dai et al., 2003) and a prognostic Canopy Air Space

(CAS; Vidale and Stöckli 2005) in another update (SiB3; Baker et al., 2003), the version used in the present research.

SiB has been coupled to GCMs (Sato et al., 1989), mesoscale models (Denning et al., 2003; Nicholls et al., 2004; Wang et al., 2007; Corbin et al., 2008, 2010) as well as in single-point mode in grasslands (Colello et al., 1998; Hanan et al., 2005), midlatitude forests (Baker et al., 2003; Schaefer et al., 2008) and tropical forests (Baker et al., 2008, 2013; Schaefer et al., 2008). SiB has performed at or near the top in Model Intercomparison Studies (MIPS; Schwalm et al., 2010) and has a proven track record as a land surface parameterization.

4.2.2 Domain and forcing data

The domain of the present research is centered over the US Midwest, extending from 81°W to 95°W and 36°N to 48°N. The SiB3 biome classification has a 100 km (1°) cartesian grid resolution across the globe; all 100 km by 100 km grid cells in the domain classified as cropland within SiB3 (DeFries and Townshend, 1994) were selected and are shown in Figure 26. 75 sites fit this criterion.

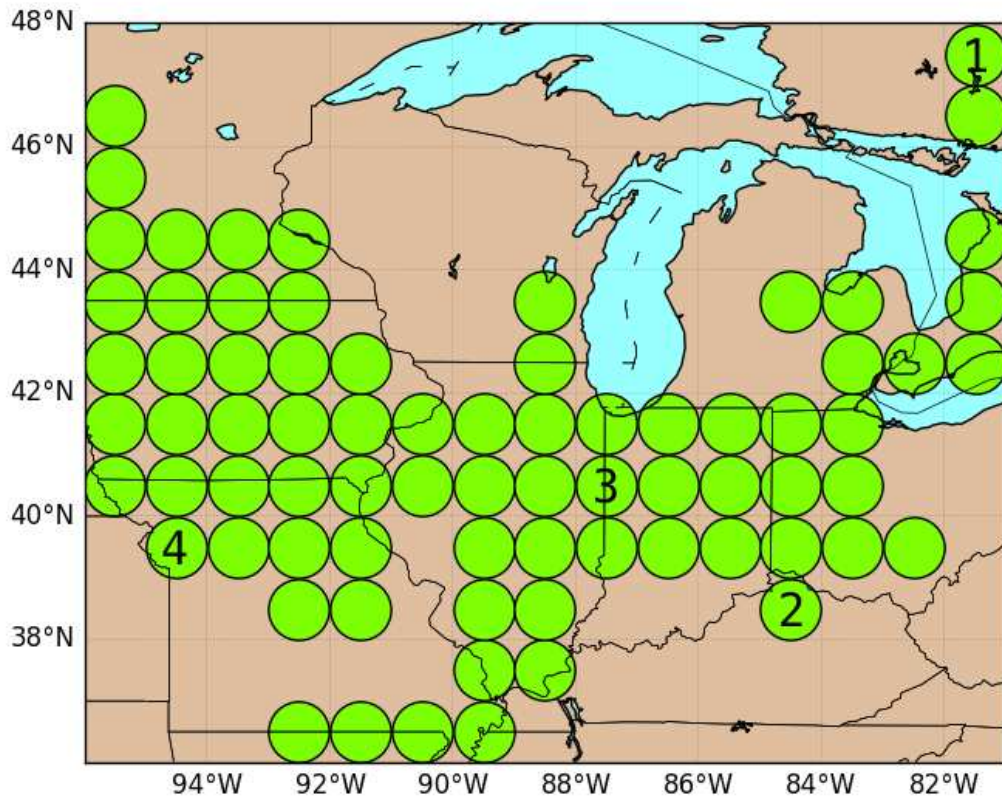


Figure 26: Map of all sites in the domain characterized as cropland within SiB3 (75 total). While the biome classification is 1 degree by 1 degree, SiB3 is run at the 0.1 degree by 0.1 degree (10 km by 10 km) center of each cell as described in Methods. The four numbered cells are the sites of detailed soil moisture analysis, discussed in Results and Discussion.

In the present study, SiB3 was executed twice at the 10 km by 10 km center of each of the 75 sites in the domain, once unmodified and once substituting the *M. × giganteus* parameterization developed by Roy and Baker (Chapter 2) from 2011 through 2013 in order to simulate a switch to this cropping regime. Empirically-based parameter modifications included a higher leaf area index and fraction of photosynthetically active radiation, a deeper and more efficient rooting structure, and weaker stomatal resistance during times of significant heat stress (see Table 2). This same *M. × giganteus*

parameterization developed at Champaign, Illinois (Figure 26, site 3) was assumed to represent the potential *M. × giganteus* growing behavior and timing that would be observed at each site. There was no communication amongst the grid cells and the simulations were uncoupled, i.e. biogeophysical modifications at the surface were not permitted to modify the atmosphere.

Both SiB3 simulations at each site were initialized in 1979 with saturated soil and a 21-year spin-up period ending 31 December 1999; the time step was 30 minutes and the simulations were forced by 6-hourly global $1^{\circ} \times 1^{\circ}$ meteorological analysis datasets produced by the National Centers for Environmental Prediction (NCEP Reanalysis-2: Kalnay et al., 1996; Kanamitsu et al., 2002). Forcing data input variables were temperature, pressure, precipitation, wind, and solar radiation. Analysis of soil moisture temperature began January 2000 and analyses of turbulent and ecosystem fluxes began January 2011 (32-year spin-up period), extending through December 2013 and described in the following section.

4.2.3. Planned analysis of turbulent and ecosystem fluxes; rainfall recycling

Employing the *M. × giganteus* parameterization originally developed in Roy et al. (2016), the goal of this research was to accurately simulate the photosynthetic processes of *M. × giganteus* that would be observed in the US Midwest and to use the flux estimates of carbon and water as a metric to gauge the potential longer-term sustainability of *M. × giganteus* across the domain. Gross primary productivity (GPP) as a metric of representing the exchange of atmospheric carbon for water through the stomata of vegetation is directly proportional to transpiration, and evapotranspiration, or the sum of the transpiration of

plants and the evaporation of water from both the ground and the vegetation surface, is proportional to the total latent heat flux (LE). It is therefore instructive to analyze SiB3 modeled LE during the time frame of focus in order to understand how a hypothetical water-intensive *M. × giganteus* regime may affect the local hydrology, near-surface atmosphere, and possibly local rainfall recycling rates and downstream precipitation.

SiB3 was run twice at each of the 75 sites, once with the surface parameterization unmodified and once with the *M. × giganteus* parameterization of Roy and Baker (Chapter 2) implemented in the final three years of the simulation (2011 to 2013). Analyzed were the hourly calculated GPP and LE averaged over July/August/September (JAS): these are typically the peak growing months of *M. × giganteus*, during which time the highest seasonal amount of carbon and water is exchanged with the atmosphere by the plant (Heaton et al., 2010; Joo et al., 2016). At the 75 sites the average difference in GPP and LE between the two runs was calculated and the results presented in map form. Also emphasized was the outsized influence of the 2012 drought on the three-year average GPP and LE by calculating the average site differences during JAS 2012 alone. The fact that meteorological data from this strong drought is present in an otherwise climatologically average dataset was considered a fortuitous occurrence, understanding that the climatological extremes, not the long-term averages, are the critical factor in establishing the bounds of crop sustainability.

This study did not include the coupling of SiB3 to an atmospheric general circulation model in order to ascertain how changes in surface fluxes due to a large regime of *M. × giganteus* may affect the local atmosphere. However, there exists a considerable body of past observations and simulations addressing the possible extent of irrigation effects on

the local and downstream atmosphere (particularly precipitation and rainfall recycling) in the US Midwest and Great Plains (e.g. Harding and Snyder, 2012b; Zaitchik et al., 2013; Huber et al., 2014). The present simulated LE was analyzed in conjunction with these previous studies, giving insight into the likelihood of a moister near-surface atmosphere induced by a broad-scale *M. × giganteus* regime. Evapotranspiration estimates derived from calculated LE at the 75 sites were compared to past estimates of the local rainfall recycling ratio and a conclusion was made as to whether the intense water use of *M. × giganteus* has the ability to be partially offset by increased precipitation across the domain, i.e. a more rapid hydrologic cycle.

4.2.4 Planned analysis of wintertime soil temperatures

Extreme post-harvest cold has several times been the principal cause of death during the initial establishment (first year) of *M. × giganteus* experimental field sites in the US, including the almost complete mortality of the newly planted University of Illinois Urbana-Champaign (UIUC) Energy Farm site in the winter of 2008–09 (Heaton et al., 2010; Zeri et al., 2011) that disrupted a number of planned bioenergy crop comparison studies. Other mass die-offs in the US have occurred in northern Michigan (Song et al., 2014) and central Wisconsin (Heaton et al., 2010). In Sweden and Denmark, a notable and well-observed mass-mortality of first-year crops occurred after having experienced minimum 5cm soil temperatures -5.4°C and -4.5°C , respectively (Clifton-Brown and Lewandowski, 2000). In a laboratory test, Clifton-Brown and Lewandowski (2000) found that freezing young *M. × giganteus* rhizomes to a temperature of -3°C began to induce mortality and that at -3.5°C , half of the rhizomes had died. However, Peixoto et al. (2015) found that *M. ×*

giganteus rhizomes tolerated temperatures as low as -6.5°C when lowered 1°C per hour in a laboratory freezing experiment, and several specific strains tolerated temperatures as low as -14°C when the temperature was lowered more slowly (1°C per day).

To contribute to the determination of the hypothetical bounds of *M. × giganteus* sustainability, 14 years of modeled soil temperatures at the 8cm node (second layer) and 18cm node (third layer) of SiB3's telescoping soil representation were analyzed to determine how many of these years experienced at least one instance of temperatures below -3°C and -6°C at these depths. This was used as an analog to the overall risk for die-off in any given establishment year. It is assumed that after the first year, rhizomes are hardy enough to survive temperatures as low as -6°C (Peixoto et al., 2015). Additionally calculated was the average amount of time spent below these thresholds in each layer over the 14 years. The second and third soil layers of SiB3 were again examined due to the recent shift in standard rhizome planting depth from 5cm to 10cm (Clifton-Brown and Lewandowski, 2000; Pyter et al., 2010). It must also be noted that SiB3 does not calculate the insulating effect of any post-harvest residue intentionally left on the field to shelter shallow soil layers as in Kucharik et al. (2013).

4.2.5 Planned analysis of soil moisture stress and equilibrium

The evolution of simulated soil moisture from 2011-2013 in the unmodified and modified runs of SiB3 was analyzed to determine the areal differences in *M. × giganteus* sustainability given its increased water usage over existing crops. It was hypothesized that a new equilibrium in rooting zone soil moisture would be reached as in Georgescu et al. (2011) such that the average annual soil moisture would be lower for simulated *M. ×*

giganteus but still capable of supporting the transpiration and productivity of the modeled vegetation due to its deeper roots and perhaps a slightly greater average stomatal resistance throughout the year.

In areas with greater precipitation, i.e. farther east in the present domain, the *M. × giganteus* soil moisture equilibrium was expected to be closer to the unmodified equilibrium due to ample soil moisture, perhaps resulting in diminished runoff. The model metric used for soil moisture was the leaf water potential variable ψ_l , implemented in the stomatal resistance scheme of SiB3 as in Sellers et al. (1989). This variable ψ_l , henceforth referred to as *rstfac2*, represents the transpiration stress (i.e. limitation on water exchange with the atmosphere) that the modeled vegetation “feels” due to lack of soil water. This dynamic variable ranges from 0 to 1, with 0 representing complete limitation and 1 representing no limitation, i.e. completely open stomata. *Rstfac2* is standardly limited to 0.10 in SiB3, but was lowered to 0.01 during the present runs to capture the extreme depletion of soil water by *M. × giganteus* during times of extreme heat and vapor pressure deficit (Roy and Baker, Chapter 2). Joo et al. (2016) observed such soil moisture depletion by *M. × giganteus* during the 2012 US Midwest drought and attributed *M. × giganteus*’s lack of a drought-response mechanism (i.e. the closing of stomata and wilting of the plant) to it being a recent and poorly adapted hybrid grass (in contrast to an evolved, robust, drought-tolerant grass such as *Panicum virgatum*, commonly known as switchgrass).

4.3 Results and Discussion

4.3.1 Turbulent and ecosystem fluxes

Figure 27 shows the hourly average difference in gross primary productivity (GPP) between the *M. × giganteus* runs and the unmodified runs of SiB3 at each of the 75 sites during July through September (JAS) 2011-2013. These were the years for which empirical leaf area index measurements were available at Champaign, Illinois, which were used to tune the parameterization employed here on a broader scale as described in Roy and Baker (Chapter 2). As a metric for the rate of carbon exchange with the atmosphere, the integral of which is accumulated biomass, the units of GPP are micromoles per square meter per second ($\mu\text{mol}/\text{m}^2/\text{sec}$). During this three-year period the majority of the domain was modeled to experience increased productivity under a *M. × giganteus* regime, with the exception of central Minnesota and Ontario.

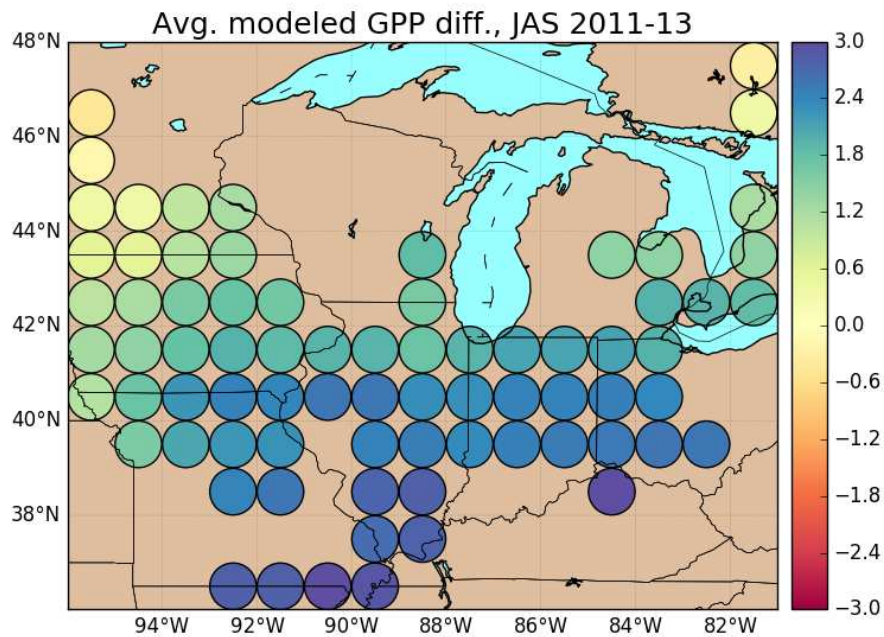


Figure 27: Average difference in gross primary productivity (GPP; units $\mu\text{mol}/\text{m}^2/\text{sec}$) across the domain between the *M. × giganteus* simulations and the unmodified simulations of SiB3 from July through September of 2011-2013. Bluer colors indicate greater average productivity under a *M. × giganteus* regime.

However, as the US Midwest drought of 2012 put a strain on existing water-intensive agriculture, the modeled switch to an even more water-intensive *M. × giganteus* regime in JAS 2012 showed a resulting average GPP that was well below the unmodified average GPP at virtually all of the sites west of Indiana. This can be seen in Figure 28. Comparing these two timeframes, it can also be seen that the average GPP in areas farther east in the domain are less affected by the drought, which matches the pattern of precipitation recorded during this time (Mallya et al., 2013). Central Minnesota recorded the largest decline in the modeled difference in average GPP between the modified and unmodified regimes during these two timeframes, indicating a large sensitivity to decreased soil water availability to maintain transpiration. During this same period, the sites in central Ontario were modeled to experience virtually no decrease in average differenced GPP between the drought year and the overall three-year timeframe, JAS 2011-2013. This may indicate that although drought was less of a concern there during the years of study, the long-term mean temperature and rainfall there are still not sufficient to support an extremely productive and water-intensive crop such as *M. × giganteus*.

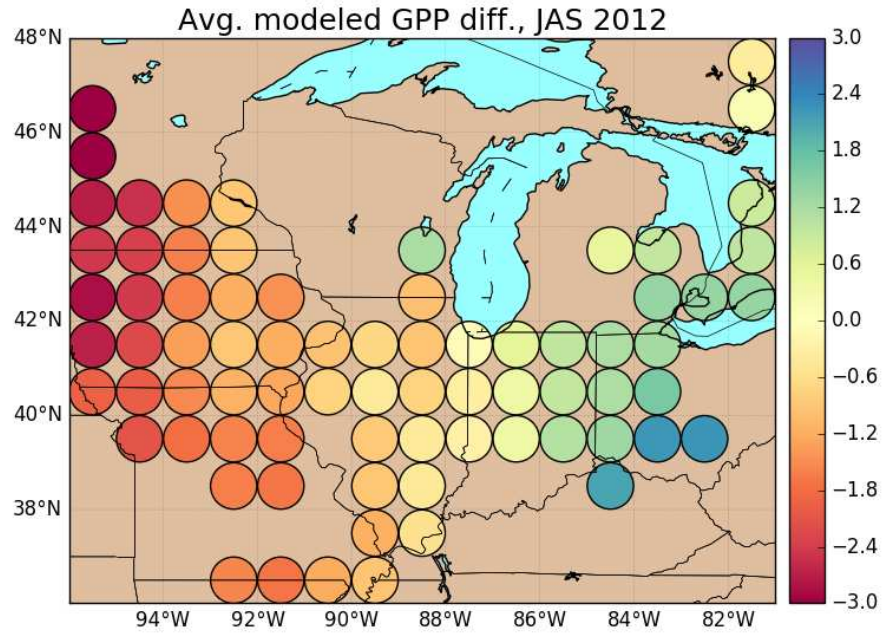


Figure 28: Same as Figure 27 but during JAS 2012 only.

To investigate the possible local and downstream hydrometeorological effects of this water-intensive crop, modeled latent heat flux (LE) was analyzed as an analog for evapotranspiration. Figure 29 shows the average hourly difference in LE between the *M. × giganteus* simulation and the unmodified simulation during JAS 2011-2013 at each of the 75 sites. Figure 30 is the same except for during JAS 2012. Important to note is the difference in color scales between the two plots, where the range is larger during the drought year of 2012 in order to capture the higher magnitude differences during this time.

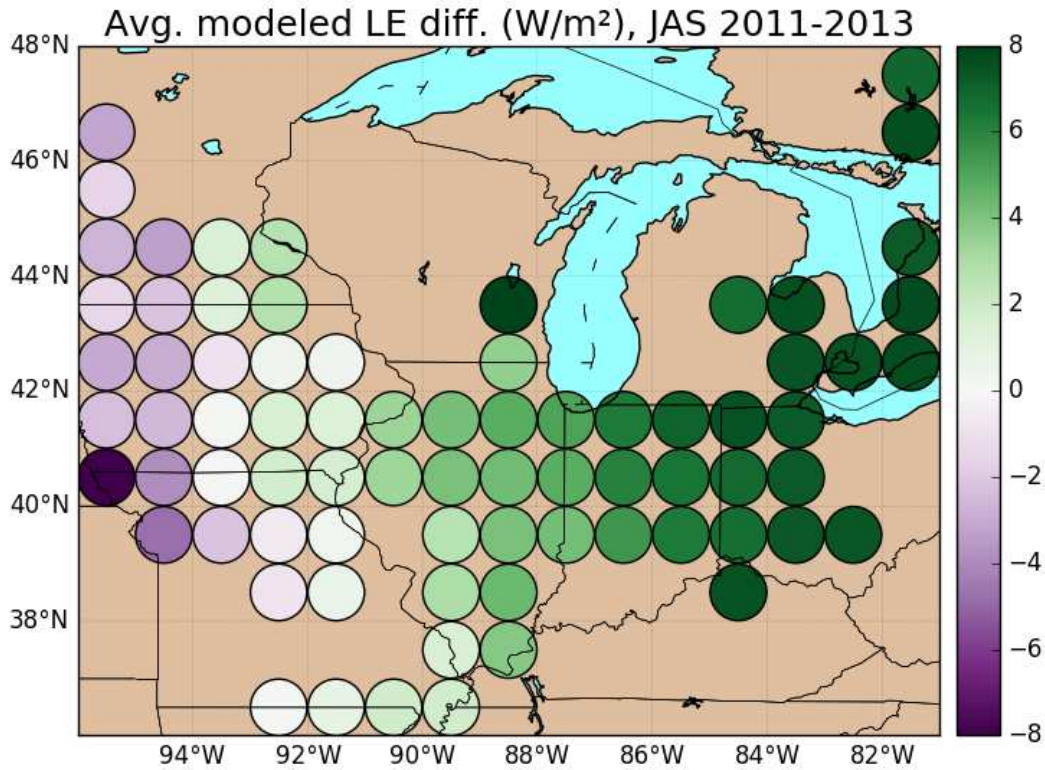


Figure 29: Average difference in latent heat flux (LE; units W/m^2) across the domain between the *M. × giganteus* simulations and the unmodified simulations of SiB3 from July through September of 2011-2013. Greener colors indicate higher average LE under a *M. × giganteus* regime.

It can be seen in Figure 29 that over the period of JAS 2011-2013, all sites in Illinois and eastward were calculated to experience a net increase in LE. This indicates sufficient water on average to satisfy the rooting zone soil moisture updraw of *M. × giganteus*. The average modeled LE increase was nearly 10 W/m^2 at sites farther east in the domain, particularly Ohio and Ontario. Examining LE during JAS 2012 in Figure 30 it is seen that Illinois was calculated to experience a net decrease in LE, as were all areas westward, where strong decreases indicate insufficient soil moisture to maintain productivity. Areas in eastern Indiana, Ohio, Michigan, and Ontario still registered a net increase in LE, although the magnitude was much smaller than the decrease observed at sites farther west

in the domain. This validates the idea that drought years have an inherently outsized influence on the long-term average LE, GPP, and crop survival. It may also be expected that years with abnormally high precipitation would not experience concomitant sharp increases in LE and GPP, but would influence *M. × giganteus* sustainability by instead recharging the rooting zone soil moisture and increasing the water availability for use the following year. This approach of diagnosing sustainability by examining the seasonal soil moisture recharge, depletion, and overall equilibrium is discussed in Section 4.3.4.

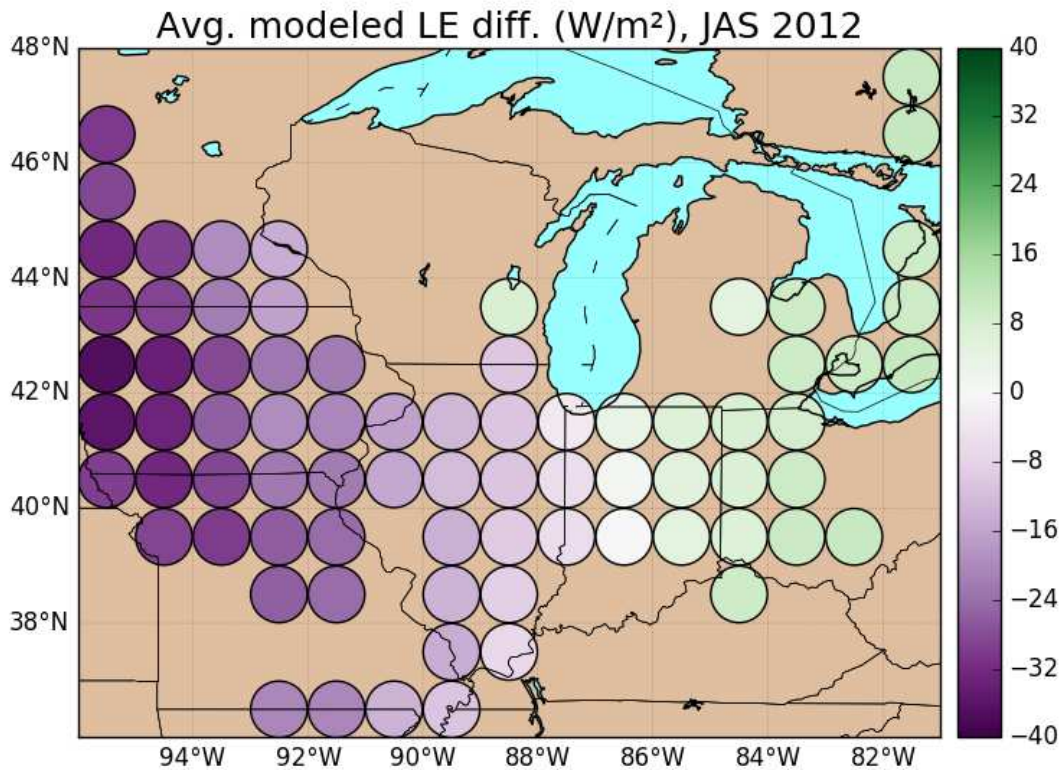


Figure 30: Same as Figure 29 but during JAS 2012 only and with a larger absolute color scale (-40 to 40 W/m²).

4.3.2 Rainfall recycling

With an increased average LE observed in part of the domain, even during the drought month of July 2012, the next goal was to estimate the expected rainfall recycling

ratio of a water-intensive regime of *M. × giganteus*. Once again, this was motivated by the idea that an intensifying of the water cycle via more intense transpiration could generate a positive feedback cycle of sustainability, generating increased precipitation and therefore more available soil moisture for downstream crops, increasing their productivity and reducing their drought-induced mortality. Without the ability to couple SiB3 to a general circulation model such as the Weather Research and Forecasting (WRF) model (Skamarock et al., 2008), studies of similar land use and land cover change (LULCC) were examined as analogs. A LULCC scenario that has been researched and quantified and that is similar to what could hypothetically be observed with *M. × giganteus* is the contribution of irrigation in the US Great Plains, to downstream precipitation and rainfall recycling over the last 100 years. Just as Georgescu et al. (2009 and 2011) employed WRF to simulate atmospheric feedbacks caused by a more vegetated surface, many studies used WRF to specifically simulate the atmospheric response to enhanced irrigation in the central US.

Harding and Snyder (2012a, 2012b) found there to be non-negligible increases in near-surface water vapor mixing ratio (via LE analysis), near-surface temperature (via sensible heat flux [H] analysis), and precipitation totals due to extensive pivot irrigation in the Ogallala Aquifer region. Growing season increases in precipitation totals were the most robust in July and the least robust in September, and were the most robust when the soil was already very wet and the least robust when the soil was very dry. Overall regional evapotranspiration increased by 4% and precipitation by 1% (with local increases up to 20%), although only 15% of the water evaporated in the region returned to the same aquifer area as rainfall (i.e. a 15% rainfall recycling ratio).

Zaitchik et al. (2013) examined three soil moisture-precipitation feedback mechanisms (two positive, one negative) and subsequently ran three WRF simulations with temporal soil moisture assumptions (unchanging moisture, dynamic moisture, and dynamic moisture with dynamic albedo). While the implementation of dynamic albedo made little difference, allowing the soil moisture to vary based on precipitation inputs contributed to a cycle of increased precipitation intensity (although not frequency), supporting the hypothesis that the soil moisture-precipitation feedback system is principally dominated by positive feedbacks on a local scale. Huber et al. (2014) ran WRF in July with stationary vegetation and a constantly saturated surface over cropland in the US Great Plains, which is unrealistic in standard irrigation practice but was assumed for the sake of studying the sensitivity and bounds of the effects of irrigation on turbulent fluxes and precipitation. This region saw a 90% average increase in LE and a 46% (25.9 mm) increase in downwind precipitation. Lu et al. (2015) ran WRF coupled with a LSM (CLM4crop) and compared a stationary vegetation scheme to a dynamic vegetation scheme across the US. An irrigation scheme was also implemented. It was found that this land surface model overestimated LAI (crop growth) and thus crop water usage, leading to a 40.8% increase in LE. It was therefore worse than the control. However, partitioning of the surface energy budget was greatly improved.

From this rainfall recycling research and the results of the present research using SiB3, several hypotheses were made about the possible effects of a *M. × giganteus* regime on precipitation and rainfall recycling in the US Midwest. In addition to the 15% estimate of the rainfall recycling ratio in the US Midwest developed by Harding and Snyder (2012b), in the extreme irrigation parameterization of Huber et al. (2014), over 300mm of irrigation in

July led to a 25.9mm average increase in nearby downwind precipitation during that month (i.e. 8.6% rainfall recycling). In the present research, the 2011-2013 maximum average LE increase was approximately 8 W/m², observed in the northeastern part of the domain (Figure 29). Calculating water use via the latent heat of evaporation (Bonan, 2013), this is approximately an extra 0.28 mm of evaporation per day. This is equal to approximately 25.4 mm of additional water extracted from the ground and released into the atmosphere in JAS. Such an increase, if realized, is not likely to be statistically significant and is certainly not bolstering to *M. × giganteus* sustainability given these rainfall recycling estimates of 8-15%. Even under the poor assumption of limitless soil moisture in drier parts of the US Midwest, previous estimates of the increase in yearlong *M. × giganteus* water usage compared to corn range from 50 mm (VanLoocke et al., 2010) to 343 mm (Hickman et al., 2010). The latter would likely still fail to produce meaningful increases in downstream precipitation according to the studies cited above. Moreover, should a widespread switch from corn to miscanthus occur in the US, it is unlikely that miscanthus crops would be concentrated in one area (that is, a patchwork of *M. × giganteus* would arise based on interested farmers, opportunity costs of land, etc.), and so any influences on the atmosphere would be further diluted and very likely non-significant.

4.3.3 Extreme cold soil temperatures

Figure 31 shows the number of years from 2000-2013 during which temperatures as low as -3°C and -6°C were simulated to occur at least once at 8 cm and at 18 cm in each of the 75 grid cells in the domain. Similarly, Figure 32 shows the average annual hours spent below these temperature thresholds at these depths.

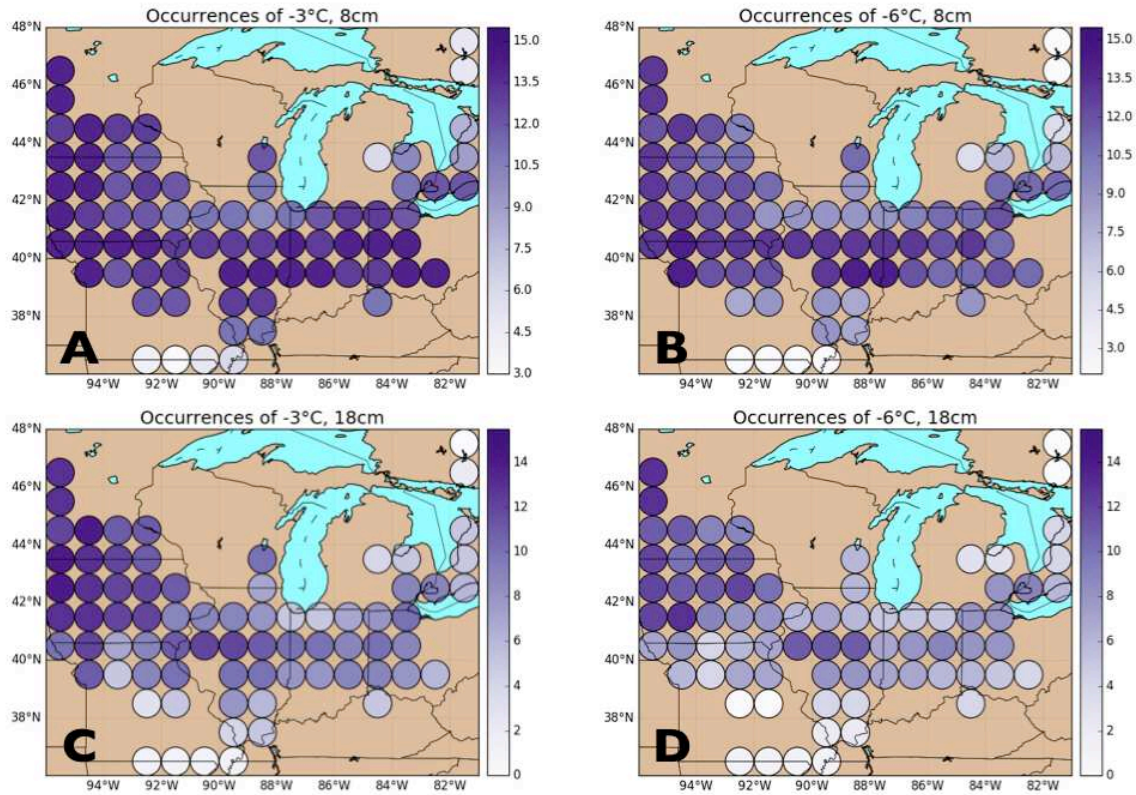


Figure 31: Number of years from 2000-2013 with at least one hourly simulated soil temperature below A) -3°C at 8cm, B) -6°C at 8cm, C) -3°C at 18cm, and D) -6°C at 18cm across the domain. These two temperatures represent the two levels of rhizome mortality (Clifton-Brown and Lewandowski, 2000; Peixoto et al., 2015; Roy, 2016) at two depths in SiB3 closest to the standard planting depth of 10cm (Pyter et al., 2010). Purpler hues represent more annual occurrences, with 14 years being the maximum possible number.

From Figure 31 it can be seen that, with the exception of the sites along the Missouri-Arkansas border and in northern Ontario, these thresholds were surpassed more often than not each winter in SiB3. Even at locations in southern Illinois, Indiana, and Ohio, temperatures lower than -3°C at 8cm were simulated to occur almost every single year from 2000-2013. At the same locations, temperatures lower than -6°C at 18cm still occurred in over half of the years. It is hypothesized that the simulated decreased likelihood of extreme cold soil temperatures in northern Ontario and central Michigan is due to lake effect snow coverage, contributing to increased insulation of the soil (Roy,

2016). The decreased likelihood of extreme cold soil temperatures in southern Missouri was expected due to the milder climate there.

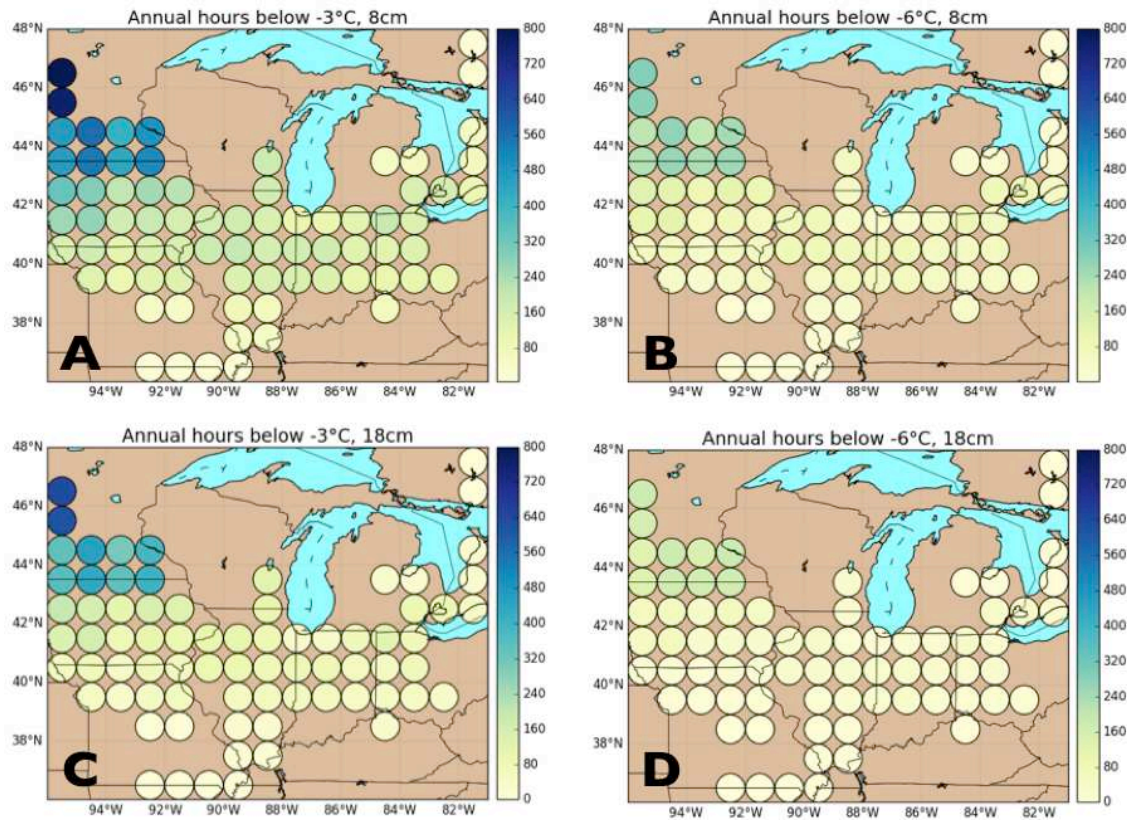


Figure 32: Average annual hours from 2000-2013 with a simulated soil temperature below A) -3°C at 8cm, B) -6°C at 8cm, C) -3°C at 18cm, and D) -6°C at 18cm across the domain. Bluer hues represent a greater average amount of time spent below these thresholds (n.b. 800 hours is equal to approximately 33 days).

Comparing Figure 31 with Figure 32 indicates that, with the exception of Minnesota and northwestern Iowa, the average annual time spent below the extreme temperature thresholds during the entire winter was approximately 120 hours or less in all scenarios except for -3°C at 8 cm. Additionally, in several field trials, first-year *M. × giganteus* rhizomes survived the winter despite experiencing calculated soil temperatures as low as -6°C. This may be explained by the lack of a post-harvest residue insulation calculation

within SiB3 (as in Kucharik et al., 2013). It may also be due to the manner in which these temperatures were experienced, as there is evidence that gradual temperature drops (instead of sharp, sudden fluctuations) may be better tolerated by the rhizomes (Peixoto et al., 2015; Roy, 2016). Future site-by-site case studies of the character of wintertime soil temperature variations will be immensely beneficial to addressing this question.

4.3.4 Soil moisture stress and equilibrium

Figure 33 again shows the areal domain of the present research, with each site shaded according to the total number of hours during 2011-2013 that SiB3 vegetation experienced extreme stress due to low soil moisture, defined as $\text{rstfac2} < 0.3$. Figure 34 is the same but only for July 2012. Further west in the domain, where average precipitation is lower, more hours are spent under extreme soil moisture stress. A peak total value of approximately 2,250 hours, or 94 total days during JAS 2011-2013, is recorded in northwestern Missouri. In central Indiana and eastward, SiB3 records zero hours of extreme soil moisture stress. In the unmodified simulation, only three sites in northwestern Missouri recorded an rstfac2 value below 0.3 during the drought of July 2012 (not shown), indicating that it was indeed the switch to a *M. × giganteus* parameterization that led to the high frequency of extreme soil moisture stress values seen in Figure 34.

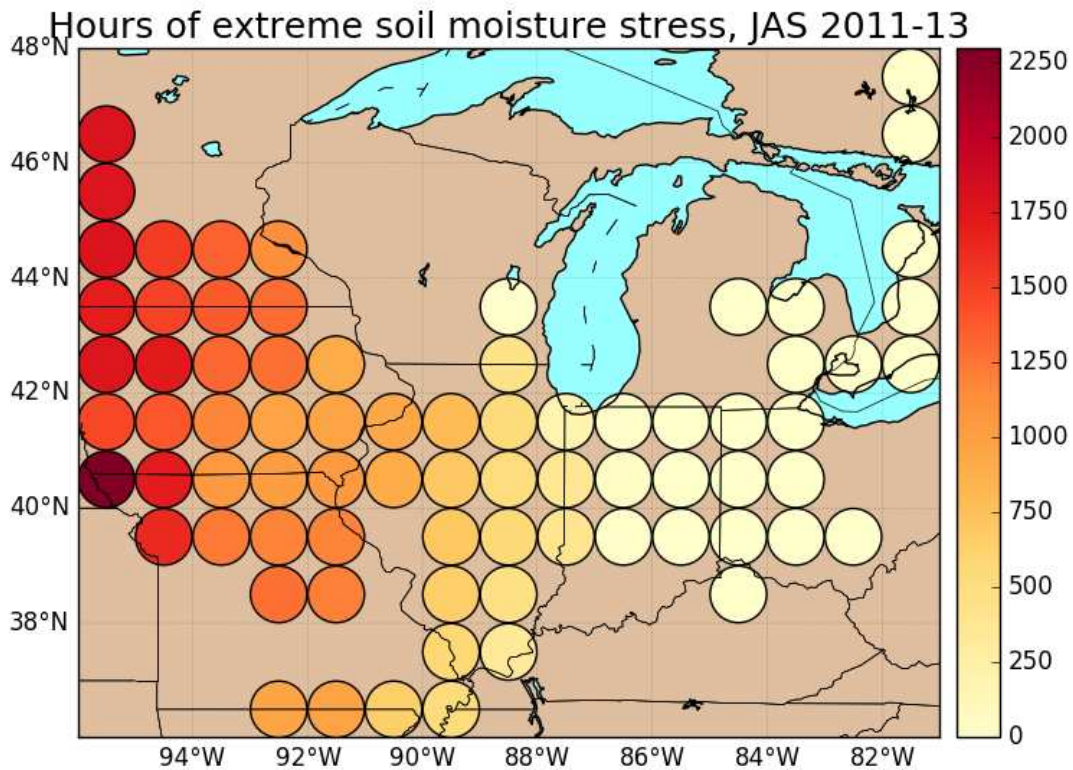


Figure 33: Average hours of extreme soil moisture stress ($\text{rstfac} < 0.3$) experienced by *M. x giganteus* at each site in SiB3 from July through September of 2011-2013. Redder colors indicate more hours of stress. For reference, 2,250 hours, the maximum value, is approximately 94 days.

Well-adapted productive crops may be able to survive periods of drought by strategically closing their stomata (wilting) during times of limited soil moisture. However, as discussed in Joo et al. (2016) and Roy and Baker (Chapter 2), *M. x giganteus*, due to being a recent sterile hybrid plant, may not be as well-adapted, having been observed to keep its stomata open during times of extremely high leaf-level vapor pressure deficit and dry soil. This quickly exhausted the available supply of soil moisture, negatively affecting its survival. These figures indicate that *M. x giganteus* may therefore be physically and economically unsustainable in Illinois and westward in the US Midwest.

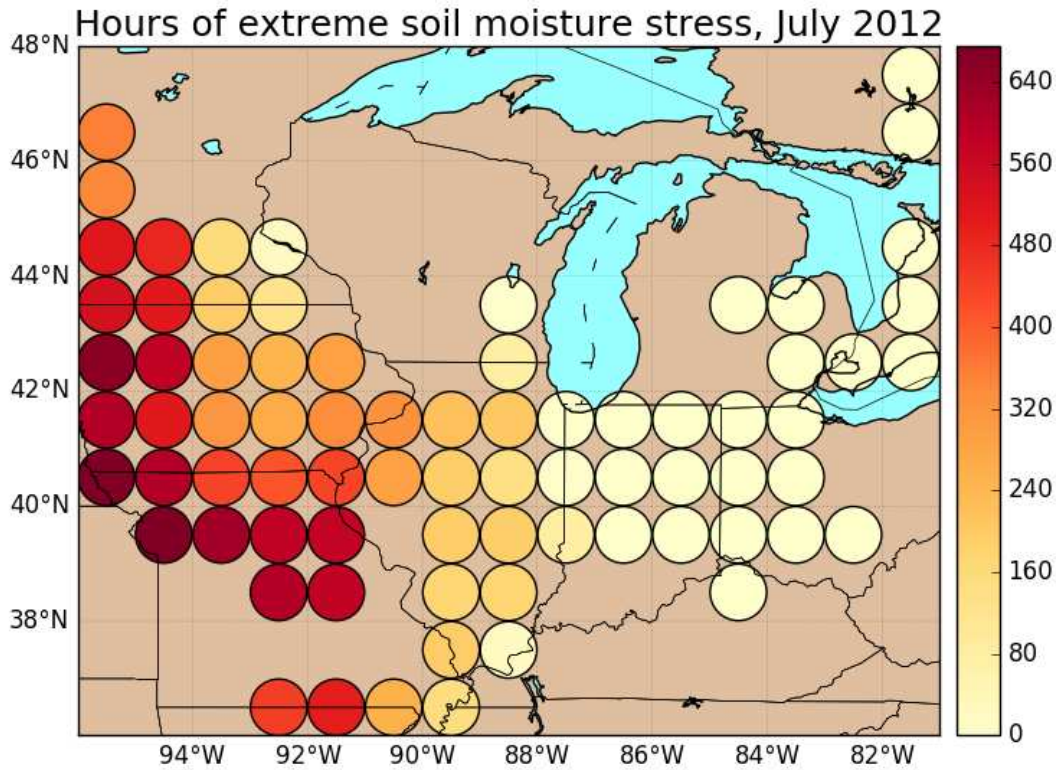


Figure 34: Average hours of extreme soil moisture stress ($\text{rstfac2} < 0.3$) experienced by *M. × giganteus* at each site in SiB3 during July 2012. Redder colors indicate more hours of stress. For reference, 660 hours, the maximum value, is 27.5 days (i.e. nearly the entire month).

To further investigate the soil moisture response to the above changes, the SiB3 soil moisture stress metric rstfac2 of the unmodified and modified *M. × giganteus* simulations was compared from 2011-2013. Four sites were chosen to analyze based on the previously discussed stark differences in simulated soil moisture stress, wintertime soil temperature, and productivity due to location. These sites are numbered in Figure 26 and qualified by rstfac2 , GPP, and wintertime soil temperature in Table 6.

Table 6: Sites characterized by soil moisture stress, GPP, and likelihood of cold soil temperatures 2011-2013. Colors indicate relative favorability of sustainability, where green is favorable and red is unfavorable.

Site number and coordinates	Extreme soil moisture stress	Gross primary productivity (GPP)	Extreme cold soil temperatures
1 (-81.5°, 47.5°)	low	low	low
2 (-84.5°, 38.5°)	low	high	low
3 (-87.5°, 40.5°)	medium	high	medium
4 (-94.5°, 39.5°)	high	medium	medium

The time series of rstfac2 in the unmodified (cropland) and modified (*M. × giganteus*) SiB3 simulations from 2011-2013 is shown in Figure 35. Notable in every series is the drought from approximately June through August 2012, when both parameterized *M. × giganteus* and cropland experienced an increase in soil moisture stress (decrease in rstfac2). This effect was particularly drastic for *M. × giganteus* at sites 3 and 4, which both registered an rstfac2 below 0.1. Site 4, being the driest of the sites, also registered considerable stress during the summer and early fall of 2011. It appears that precipitation in late 2011 and early 2012 was not sufficient to fully recharge the rooting zone soil moisture (i.e. rstfac2 ~ 1.0), exacerbating the stress felt by simulated *M. × giganteus* during the even drier 2012 summer. The unmodified simulation at this site also registered an rstfac2 below 0.3 during 2012, one of only three sites in the domain to do so (the other two were neighboring sites in northwest Missouri and southwest Iowa).

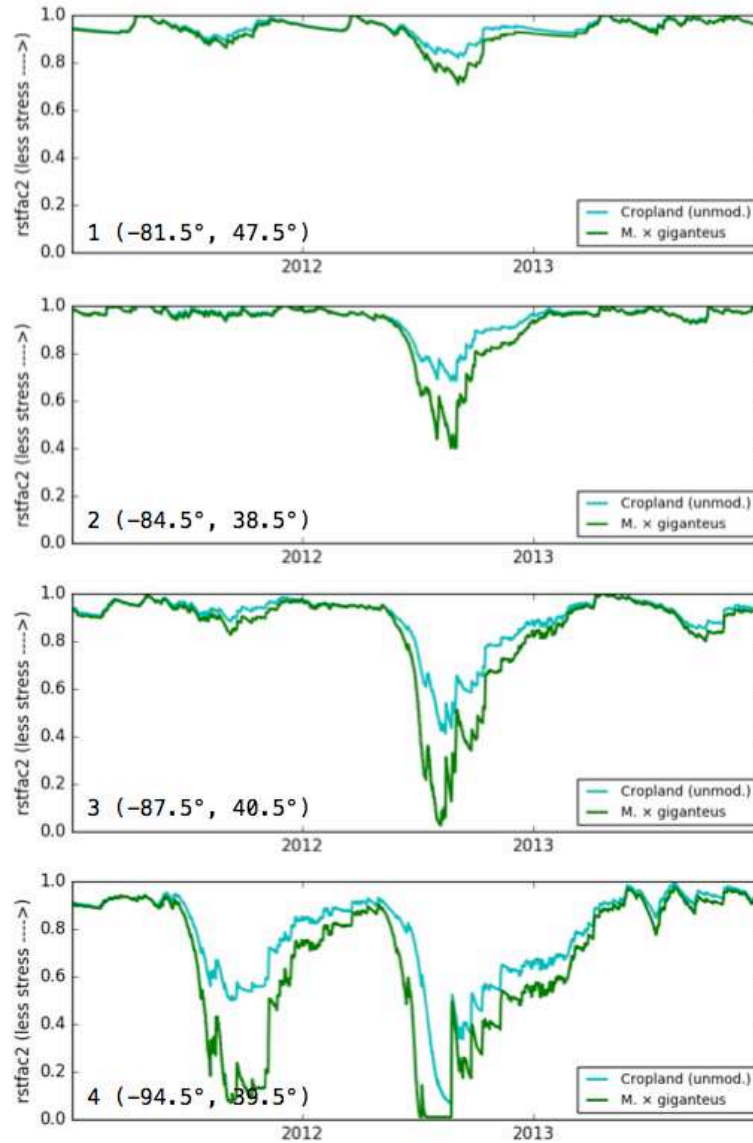


Figure 35: Time series of soil moisture stress (rstfac2) calculated by SiB3 from 2011-2013 at each of the four sites marked in Figure 26. Rstfac2 from the unmodified SiB3 simulation is represented in cyan while the evolution of rstfac2 during the *M. x giganteus* simulation is in green. Rstfac2 is used as an analog for transpiration where an rstfac2 value of 1.0 indicates zero stomatal stress due to ample soil moisture while a value of 0.01, the minimum allowable value, indicates complete stress and no transpiration. Note that each tick along the x-axis represents the beginning of the year, i.e. 0 on the x-axis marks the beginning of 2011. Notable in all four plots are the stress-inducing effects of the 2012 US Midwest drought. In all cases, *M. x giganteus* experienced more stress than simulated unmodified cropland, but the difference was much larger in times of greater stress.

While site 4 was an extreme dry scenario, site 1 in central Ontario was the moistest of the scenarios and shows *M. x giganteus* and cropland hardly decreasing in rstfac2 during

the drought. This was in part due to the drought being less intense in Ontario, but was also hypothesized to be due to a significantly lower GPP than the other sites (Figure 28), resulting in less modeled water usage. Additionally, due to its northern location, the soil there likely freezes more frequently than at the other sites and limits infiltration during the winter, reflected in the “flatlining” of *rstfac2* seen during each of the three winters in Figure 35.

At all sites, *rstfac2* was 20-50% lower for *M. × giganteus* than for the unmodified cropland scenario during the 2012 drought, consistent with previous findings of simulated *M. × giganteus* water usage. In every simulation except for site 4, *M. × giganteus* soil moisture recharged to the same level as the unmodified simulations in SiB3 by the spring of 2013, resulting in a new soil moisture equilibrium which Georgescu et al. (2011) conjectured would occur in these areas. This would indicate sufficient seasonal precipitation to sustain *M. × giganteus* assuming three criteria: 1) extreme soil moisture stress in the summer doesn’t kill *M. × giganteus*, 2) extreme cold soil temperatures in the winter don’t kill *M. × giganteus*, particularly first-year rhizomes, and 3) the 2012 drought and concurrent heat wave is the most extreme such event that could possibly be observed. These strict criteria, particularly the last, make the prospects of a completely risk-free large-scale *M. × giganteus* regime somewhat dubious in terms of biogeophysical and economic sustainability.

CHAPTER 5

Discussion and Conclusions

5.1 Summary

As the production of energy from fossil fuels becomes increasingly contentious, renewable alternatives are have been sought to satisfy increasing energy demands. A recent source of renewable energy interest and optimism has been the cultivation of crops from which cellulosic ethanol can be produced at a high volume. The most productive of these cellulosic ethanol crops is *M. × giganteus*. A decision must be made, and made soon, as to whether or not to fully pursue this cropping and energy strategy on a national scale. This doctoral research sought to provide an updated recommendation on this issue, and benefited from a unique land-surface modeling strategy as well as robust new empirical field observations to use as accurate validation dataset for the first time in such a study.

Within the SiB3 land surface model, a first-of-its-kind surface parameterization for *M. × giganteus* was developed and tested at the field data site in Champaign, Illinois. This parameterization succeeded in not only capturing the average diurnal and annual cycles of *M. × giganteus* growth and senescence but also its behavior during the record warm spring and dry summer of 2012. Because climate extremes will have an outsized impact on the viability of a domestic *M. × giganteus* strategy, should it be implemented, it was crucial that these were represented adequately by SiB3.

Because *M. × giganteus* is a perennial, rhizomatously-propagating crop, extreme cold soil temperatures also had to be factored in as a potential threat to this crop's sustainability. A large segment of this doctoral research was spent addressing this

question. The climatology of soil temperatures at experimental *M. × giganteus* sites in the northern Midwest was analyzed, with a special focus on the effect of snow cover in insulating shallow soil layers and thereby potentially protecting young rhizomes from mortality. While an insulating effect was observed, the research ultimately arrived at a null result: snow cover is too variable to be exclusively relied upon to prevent *M. × giganteus* from wintertime mortality. However, several useful new insights arose from this work. It was empirically discovered in this research that the speed at which cold soil temperatures are reached likely play a role as important as temperature magnitude in determining the survival of the rhizomes (replicated in the laboratory experiments of Peixoto et al., 2015). Because more gradual and damped cooling was found to be associated with higher survival, the importance of effective wintertime field management practices can be quantitatively emphasized to farmers. Such management practices include the post-harvest leaving of plant residue on the field as well as an awareness of the timing of synoptic scale systems, particularly the danger of cold frontal passage during times of no snow cover.

The SiB3 *M. × giganteus* surface parameterization and this new knowledge of wintertime rhizome susceptibility was applied across the US Midwest in a domain that included 75 individual simulations in varying climates. Over the course of three years, the behavior of *M. × giganteus* was tracked and compared to the unmodified simulation at these sites. In doing so, many expected results were seen: for example, the water needs of *M. × giganteus* are impossible farther west in the US Midwest due to insufficient seasonal precipitation, and the proposed mortal soil temperature thresholds were surpassed every single winter in the north of the domain. In addition to these expected results, however, this exercise allowed a new areal bounds of sustainability to be recommended, again

benefitting from the first-time use of a third-generation land surface model accurately tuned to represent *M. × giganteus* thanks to a new robust validation dataset.

5.2 *M. × giganteus* viability; limitations

The recommendation here calls for *M. × giganteus* no further west than 87°W and no further north than 40°N. In the US Midwest, this is approximately southern Indiana, southern Ohio, and Kentucky. These bounds are more limited and less optimistic than the estimates of previous research, and align most closely with the agronomic simulations of Song et al., (2014), shown in Figure 2. The drought of July 2012 played a significant role in defining the western bounds, which was defined based on crop survival and productivity. As seen in Figure 30, areas east of 87°W performed on par with or better than unmodified cropland in the simulation. This implies that, for this extreme event, *M. × giganteus* would not have theoretically been an additional stress on the hydrometeorologic system and would have survived, albeit with a lower productivity. Calculated stomatal stress due to dry soil reflects this (Figure 34) as do the time series of *rstfac2* at sites 2 and 3 (Figure 35): *M. × giganteus* has lower but sustainable soil moisture at site 2 in Kentucky, but reaches beyond the wilting point at site 3 in Illinois, beyond the proposed bounds.

The northward propagation of *M. × giganteus* is limited by low productivity possibilities due to insufficient warmth in the summer (see, for example, average growing season GPP in central Ontario in Figure 27). Cold soil temperatures, prevalent in the simulations, also limit the possibility of successful *M. × giganteus* cropping further north in the regime. While most sites within the recommended bounds still experienced mortal soil temperatures many winters (Figure 31), the time spent below these thresholds was low,

often less than 20 hours (Figure 32). It is hoped that good management practices, such as the timing of field residue application, would further reduce the minimum winter soil temperatures experienced. However, insulation of the near surface soil is not adequately represented in SiB3.

While SiB3 and its surface parameterization have a proven track record, performing at the same level or better than its peers in Model Intercomparison Studies (MIPS; Schwalm et al., 2010), there are limitations to its capabilities that may lessen the extent to which the results and bounds derived here may be fully trusted. Primarily, SiB3 has been shown to have difficulties resolving soil temperatures at times (Philpott et al., 2008; Schafer et al., 2009). Philpott et al. (2008) studied eight sites in the Atmospheric Radiation Measurement (ARM) Climate Research Facility in the US Southern Great Plains and compared turbulent fluxes and soil temperatures to SiB3 model calculations over the course of two years; it was discovered that the sensible heat flux, ground heat flux, and soil temperature were poorly correlated (< 0.7) on average. This was likewise observed in the present research, which can be seen in the average diurnal cycle of turbulent fluxes shown in Figure 6. This was found to be not a vegetation coverage issue (since albedo was not affected) but rather a thermal insulation of the soil (energy flux resistance) that was too low. Therefore, energy flow into and out of the soil was overestimated, making site soil temperatures too warm in the summer and too cool in the winter. This same issue with soil temperatures in SiB3 was observed by Schafer et al. (2009), which assessed SiB3 and attempted to increase its accuracy in calculating wintertime soil temperature at five increasingly cold sites in North America. By implementing a novel, process-interdependent representation (Baker et al., 2008) of snow cover, thereby increasing the thermal inertia of the soil and modifying the

transfer of energy through snowpack, their SiB3 results more closely resembled observations. All together, this may act to explain the conservative bounds of *M. × giganteus* derived by this study compared with the three previous estimates shown in Figure 2 (Miguez et al., 2002; US DoE, 2006; Song et al., 2014), since the unmodified version of SiB3 employed here is likely returning soil temperatures that are colder than observed due to a low thermal insulation.

Another limitation of the present research is the consequence of course-resolution forcing data within SiB3. Schafer et al. (2009) found that one of the greatest manifestations of the discrepancies between SiB3 forcing data (North American Regional Reanalysis) and in situ observations was the resultant soil temperature. Because Schafer et al. (2009) focuses on soil freeze/thaw processes, as does the present research (using NLDAS-2 forcing data at the same resolution), this discrepancy ends up being an important implication to consider. Fortunately, SiB3 allows for the implementation of finer resolution forcing data. As addressed in Future Work, this would be a valuable area to analyze in more depth, ensuring that SiB3 calculations represent reality as closely as possible.

Despite these limitations, the present research will be a valuable supplement to existing studies of *M. × giganteus* viability in the US, particularly given that it implemented the first-ever validation of a *M. × giganteus* parameterization within a land surface model, and also given the extremely important consideration of the possibility of wintertime crop mortality. Also, it is reemphasized that the bounds derived here may still be overly optimistic, as just one year in ten of mortal soil temperatures could catastrophically reduce *M. × giganteus* decadal yield by 20-30%.

5.3 Future work

This work will benefit greatly from future validation of *M. × giganteus* performance across the domain. This could be as simple as binary wintertime survival statistics or summertime yield statistics, which could be used to validate *M. × giganteus* behavior in some regions near the bounds of sustainability delineated here and in other studies. With more instances of validation across the domain, it will almost certainly prove beneficial to employ reanalysis data with finer than one-degree resolution to force the land surface model simulations. Future work could also include expansion of the domain further south and west. Propagation to the south will be limited by the lack of cold wintertime temperatures that provide the biological signal to senesce, an effect which will need to be worked into a future *M. × giganteus* parameterization. It will also be important to consider that the existing land and agricultural infrastructure in this area, essentially the US Southeast, is of poorer quality and less established than in the US Midwest, which will increase production costs. Finally, because this study was the first to employ a LSM with a hydrometeorological focus (rather than an agronomic model with emphasis on phenology and yield), another beneficial future area of research will be the use of this *M. × giganteus* surface parameterization within a similar model that can be coupled to an atmospheric general circulation model. While it is posited here that even a large regime of *M. × giganteus* would not meaningfully increase the rainfall recycling ratio or downstream precipitation, a statistically significant local temperature decrease may still be observed (as in Georgescu et al., 2009) which could in turn lead to a positive feedback cycle through lower stomatal stress and higher transpiration.

5.4 Final remarks

I began this research with an open mind and great enthusiasm about the novel idea of this “miracle plant”, *M. × giganteus*, being able to solve the domestic ethanol production problem of the US. As often happens in research, my opinion changed over the course of my doctoral research and through reading hundreds of articles on the subject. With such an important decision to make, it is summarily important to err on the side of caution when setting the cultivation bounds of a perennial plant whose single-year mortality would have catastrophic effects on the renewable energy sector, particularly if it is relied upon to produce a majority of US domestic ethanol. Given its uncertainty, we must therefore focus on the consequences, not on the probability, of *M. × giganteus* mortality.

Many outstanding researchers and scientists are working on the *M. × giganteus* problem. However, there has been no attempt at releasing a definitive statement as to the viability of a *M. × giganteus* ethanol strategy in the US that would assist decision-makers and politicians in either fully funding or scrapping this idea. There are many agronomic, logistical, and ethanol production problems still to be answered, but more than anything it is my opinion that the science community has been hesitant to enthusiastically back a *M. × giganteus* regime because we’re beginning to understand how finicky, volatile, and poorly understood this new sterile hybrid plant is. Again, I entered into this field incredibly optimistic about the possibilities of cellulosic ethanol, but like increasingly more scientists (ex. Khosla, 2010; Aziz, 2013; Brunner and Robijns, 2016) I find myself pessimistic about the feasibility of such a strategy.

REFERENCES

- Angel, J., 2016: *Climate Observations for Champaign-Urbana, IL*. State climatologist office for Illinois. Digital media.
- Arguez, A., I. Durre, S. Applequist, R. S. Vose, M. F. Squires, X. Yin, R. R. Heim, Jr., and T. W. Owen, 2012: NOAA's 1981-2010 U.S. Climate Normals: An Overview. *Bull. Amer. Meteor. Soc.*, **93**, 1687-1697.
- Arundale, R. A., 2012: The higher productivity of the bioenergy feedstock *Miscanthus* \times *giganteus* relative to *Panicum virgatum* is seen both into the long term and beyond Illinois. Ph.D. dissertation, University of Illinois at Urbana-Champaign, 110 pp.
- Arundale, R. A., F. G. Dohleman, E. A. Heaton, J. M. McGrath, T. B. Voigt, and S. P. Long, 2014b: Yields of *Miscanthus* \times *giganteus* and *Panicum virgatum* decline with stand age in the Midwestern USA. *GCB Bioenergy*, **6**, 1–13.
- Aziz, J., 2013: It's time for America to end ethanol subsidies. *The Week*, 31 July 2013. [Available online at <http://theweek.com/articles/461619/time-america-end-ethanol-subsidies>].
- Baker, I. T., A. S. Denning, N. Hanan, L. Prihodko, P.-L. Vidale, K. Davis and P. Bakwin, 2003: Simulated and observed fluxes of sensible and latent heat and CO₂ at the WLEF-TV Tower using SiB2.5. *Glob. Change Biol.*, **9**, 1262-1277.
- Baker, I. T., L. Prihodko, A. S. Denning, M. Goulden, S. Miller, and H. R. da Rocha, 2008: Seasonal drought stress in the Amazon: Reconciling models and observations. *J. Geophys. Res.*, **113**, G00B01, doi:10.1029/2007JG000644.

- Baker, I. T., A. B. Harper, H. R. da Rocha, A. S. Denning, A. C. Araújo, L. S. Borma, H. C. Freitas, M. L. Goulden, A. O. Manzi, S. D. Miller, A. D. Nobre, N. Restrepo-Coupe S. R. Saleska, R. Stöckli, C. von Randow, and S. C. Wofsy, 2013: Surface ecophysiological behavior across vegetation and moisture gradients in tropical South America. *Agric. For. Meteorol.*, **182**, 177–188, doi: <http://dx.doi.org/10.1016/j.agformet.2012.11.015>.
- Beale, C. V. and S. P. Long, 1997: Seasonal dynamics of nutrient accumulation and partitioning in the perennial C-4-grasses *Miscanthus × giganteus* and *Spartina cynosuroides*. *Biomass Bioenerg.*, **12**, 419–428.
- Benoit, G. R., S. Mostaghimi, R. A. Young, and M. J. Lindstrom, 1986: Tillage-residue effects on snow cover, soil water, temperature, and frost. *T. ASAE*, **29**, 473–479.
- Bland and Wayne, cited 2015: Weather station status and data. University of Wisconsin Extension. [Available online at http://agwx.soils.wisc.edu/uwex_agwx/awon.]
- Bluestein, H. B., 1993: Precipitation systems in the midlatitudes. *Synoptic-Dynamic Meteorology*, Vol. II, Oxford Univ. Press, 426–579.
- Boersma, N. N. and E. A. Heaton, 2014: Does propagation method affect yield and survival? The potential of *Miscanthus × giganteus* in Iowa, USA. *Ind. Crop Prod.*, **57**, 43–51.
- Boersma, N. N. and C. Bonin, 2014: *Miscanthus × giganteus*: experiences in Iowa. 2014 Extension Energy and Environment Summit, Ames, IA, Iowa State Univ. [Available online at <https://www.2014e3.org/files/2013/10/boersman.pdf>.]
- Bonan, G., 2013: Hydrometeorology. *Ecological Climatology*, 5th ed. Cambridge Univ. Press, 418–431.

- Brunner, A. and T. Robijns, 2016: Biofuels – a story without a happy end. *EU Bioenergy*, 12 May 2016. [Available online at <https://eubioenergy.com/2016/05/12/biofuels-a-story-without-a-happy-end/>].
- Christian, D. G., N. E. Yates, and A. B. Riche, 2009: Estimation of ramet production from *Miscanthus × giganteus* rhizomes of different ages. *Ind. Crop Prod.*, **30**, 176–178.
- Clifton-Brown, J. C. and I. Lewandowski, 2000: Overwintering problems of newly established *Miscanthus* plantations can be overcome by identifying genotypes with improved rhizome cold tolerance. *New Phytol.*, **148**, 287–294.
- Climate Source, cited 2015: Mean monthly and annual snowfall, conterminous United States. [Available online at http://www.climatesource.com/us/fact_sheets/fact_snowfall_us.html.]
- Colello, G.D. and Grivet, C., P.J. Sellers, and J.A. Berry, 1998: Modeling of Energy, Water and CO₂ Flux in a Temperate Grassland Ecosystem with SiB2: May-October 1987. *J. Atmos. Sci.*, **55**, 1141-1169.
- Collatz, G.J., J.T. Ball, C. Grivet, and J.A. Berry, 1991: Physiological and environmental regulation of stomatal conductance, photosynthesis and transpiration: A model that includes a laminar boundary layer. *Agr. Forest Meteorol.*, **54**, 107-136.
- Collatz, G.J., M. Ribas-Carbo, and J.A. Berry, 1992: Coupled photosynthesis-stomatal conductance model for leaves of C₄ plants. *Aust. J. Plant Physiol.*, **19(5)**, 519-538.
- Corbin, K.D., A.S. Denning, L. Lu, J.W. Wang, and I.T. Baker, 2008: Possible representation errors in inversions of satellite CO₂ retrievals. *J. Geophys. Res.*, **113(D2)**, Art. No. D02301.

- Corbin, K.D., A.S. Denning, E.Y. Lokupitya, A.E. Schuh, N.L. Miles, K.J. Davis, S. Richardson, and I.T. Baker, 2010: Assessing the Impact of Crops on Regional CO₂ Fluxes and Atmospheric Concentrations. *Tellus*, **62B**, 521-532.
- Dai, Y., X. Zeng, R.E. Dickinson, I. Baker, G.B. Bonan, M.G. Bosilovich, A.S. Denning, P.A. Dirmeyer, P.R. Houser, G Niu, K.W. Oleson, C.A. Schlosser, and Z-L Yang, 2003: The common land model. *B. Am. Meteorol. Soc.*, **84(8)**, 1013-1023.
- Denning, A.S., M. Nicholls, L. Prihodko, I. Baker, P.-L. Vidale, K. Davis, and P. Bakwin, 2002: Simulated and observed variations in atmospheric CO₂ over a Wisconsin forest using a coupled Ecosystem-Atmosphere Model. *Glob. Change Biol.*, **9**, 1241-1250.
- Dohleman, F. G. and S. P. Long, 2009: More productive than maize in the Midwest: how does miscanthus do it? *Plant Physiol.*, **150**, 2104-2115.
- Farquhar, G.D., S. von Caemmerer, and J.A. Berry, 1980: A biochemical model of photosynthetic CO₂ assimilation in leaves of C₃ species. *Planta*, **149**, 78-90.
- Geiger, R., 1965: The climate near the ground. Harvard Univ. Press, 611 pp.
- Georgescu, M., D. B. Lobell, and C. B. Field, 2009: Potential impact of U.S. biofuels on regional climate. *Geophys. Res. Lett.*, **36**, L21806.
- Georgescu, M., D. B. Lobell, and C. B. Field, 2011: Direct climate effects of perennial bioenergy crops in the United States. *Proc. Natl. Acad. Sci. USA*, **108**, 4307-4312.
- Gentine, P., M. Guérin, M. Uriarte, N. G. McDowell, and W. T. Pockman, 2016: An allometry-based model of the survival strategies of hydraulic failure and carbon starvation. *Ecohydrology*, **9**, 529-546, DOI: 10.1002/eco.1654.
- Godfrey, C. M., D. J. Stensrud, and L. M. Leslie, 2007: A new latent heat flux parameterization for land surface models. Preprints, *87th Annual Meeting*, San Antonio, TX, Amer.

- Meteor. Soc., 6A.3. [Available online at <https://ams.confex.com/ams/pdfpapers/118072.pdf>]
- Hanan, N.P., J.A. Berry, S.B. Verma, E.A. Walter-Shea, A.E. Suyker, G.G. Burba, and A.S. Denning, 2005: Testing a model of CO₂, Water and Energy Exchange in Great Plains Tallgrass Prairie and Wheat Ecosystems. *Agr. Forest Meteorol.*, **31**, 162-179.
- Harding, K. J. and P. K. Snyder, 2012a: Modeling the atmospheric response to irrigation in the Great Plains. Part I: general impacts on precipitation and the energy budget. *J. Hydrometeorol.*, **13**, 1667-1686.
- Harding, K. J. and P. K. Snyder, 2012b: Modeling the atmospheric response to irrigation in the Great Plains. Part II: the precipitation of irrigated water and changes in precipitation recycling. *J. Hydrometeorol.*, **13**, 1687-1704.
- Heaton, E. A., F. G. Dohleman, and S. P. Long, 2008: Meeting US biofuel goals with less land: the potential of *Miscanthus*. *Glob. Change Biol.*, **14**, 2000–2014.
- Heaton, E. A., F. G. Dohleman, A. F. Miguez, J. A. Juvik, V. Lozovaya, J. Widholm, O. A. Zabolina, G. F. McIsaac, M. B. David, T. B. Voigt, N. N. Boersma, and S. P. Long, 2010: *Miscanthus*: a promising biomass crop. *Adv. Bot. Res.*, **56**, 75–137.
- Hickman, G. C., A. VanLoocke, F. G. Dohleman, and C. J. Bernacchi, 2010: A comparison of canopy evapotranspiration for maize and two perennial grasses identified as potential bioenergy crops. *GCB Bioenergy*, **2**, 157–168.
- Hinkel, K. M., S. I. Outcalt, and A. E. Taylor, 1997: Seasonal patterns of coupled flow in the active layer at three sites in northwest North America. *Can. J. Earth Sci.*, **34**, 667–678.

- Hoepner, W., 2014: Long term snow cover. National Weather Service Forecast Office, Grand Rapids, MI. [Available online at http://www.crh.noaa.gov/news/display_cmsstory.php?wfo=grr&storyid=101324&source=2.]
- Hsieh, C. I., G. Katul, and T. W. Chi, 2000: An approximate analytical model for footprint estimation of scalar fluxes in thermally stratified atmospheric flows. *Adv. In Water Res.*, **23**, 765-772.
- Huber, D. B., D. B. Mechem, and N. A. Brunsell, 2014: The effects of Great Plains irrigation on the surface energy balance, regional circulation, and precipitation. *J. Climate*, **2014**, 103-128.
- Isard, S. A. and R. J. Schaetzl, 1995: Estimating soil temperatures and frost in the lake effect snowbelt region, Michigan, USA. *Cold Reg. Sci. Technol.*, **23**, 317-332.
- Isard, S. A. and R. J. Schaetzl, 1998: Effects of winter weather conditions on soil freezing in southern Michigan. *Phys. Geogr.*, **19**, 71-94.
- Jain, A.K., M. Khanna, M. Erickson, and H. Huang, 2010: An integrated biogeochemical and economic analysis of bioenergy crops in the Midwestern United States. *GCB Bioenergy*, **2**, 217-234.
- Johnsson, H. and L.-C. Lundin, 1991: Surface runoff and soil water percolation as affected by snow and soil frost. *J. Hydrol.*, **122**, 141-159.
- Joo, E., M. Z. Hussain, M. Zeri, M. D. Masters, J. N. Miller, N. Gomez-Casanovas, E. H. DeLucia, and C. J. Bernacchi, 2016: The influence of drought and heat stress on long term carbon fluxes of bioenergy crops grown in the Midwestern US. *Plant Cell Environ.*, doi: 10.1111/pce.12751.

- Khanna, M., B. Dhungana, and J. Clifton-Brown, 2008: Costs of producing *Miscanthus* and switchgrass for bioenergy in Illinois. *Biomass Bioenerg.*, **32**, 482–493.
- Khosla, V., 2010: Vinod Khosla on corn ethanol: time to move on. *Green Tech Media*, 3 December 2010. [Available online at <https://www.greentechmedia.com/articles/read/corn-ethanol-time-to-move-on>].
- Kiefer, W., cited 2015: Acres in orchards. Central Michigan University. [Available online at <http://www.geo.msu.edu/geogmich/fruit.html>.]
- Kiniry, J. R. and Coauthors, 2013: Perennial biomass grasses and the Mason-Dixon Line: comparative productivity across latitudes in the Southern Great Plains. *Bioenergy Res.*, **6**, 276–291.
- Kucharik, C. J., A. VanLoocke, J. D. Lenters, and M. M. Motew, 2013: *Miscanthus* establishment and overwintering in the Midwest USA: a regional modeling study of crop residue management on critical minimum soil temperatures. *PLoS ONE*, **8**, e68847.
- Lewandowski I., J. C. Clifton-Brown, J. M. O. Scurlock, and W. Huisman, 2000: *Miscanthus*: European experience with a novel energy crop. *Biomass and Bioenerg.*, **19**, 209–227.
- Lu, Y., J. Jin, and L. M. Kueppers, 2015: Crop growth and irrigation interact to influence surface fluxes in a regional climate-cropland model (WRF3.3-CLM4crop). *J. Clim. Dyn.*, **45**, 3347–3363.
- Lynch, H. J., M. Rhainds, J. M. Calabrese, S. Cantrell, C. Cosner, and W. F. Fagan, 2014: How climate extremes—not means—define a species' geographic range boundary via a demographic tipping point. *Ecol. Monogr.*, **84**, 131–149. doi:10.1890/12-2235.1

- Mallya, G., L. Zhao, X. Song, D. Niyogi, and R. Govindaraju, 2013: 2012 Midwest Drought in the United States. *J. Hydrol. Eng.*, **18**, 737-745.
- Maroco, J. P., J. S. Pereira, and M. M. Chaves, 1997: Stomatal responses to leaf-to-air vapour pressure deficit in Sahelian species. *Aust. J. Plant Physiol.*, **24**, 381-387.
- McIsaac, G. F., M. B. David, and C. A. Mitchell, 2010: *Miscanthus* and Switchgrass production in Central Illinois: impacts on hydrology and inorganic nitrogen leaching. *J. Environ. Qual.*, **39**, 1790–1799.
- Miguez, F. E., M. Maughan, G. A. Bollero, and S. P. Long, 2012: Modeling spatial and dynamic variation in growth, yield, and yield stability of the bioenergy crops *Miscanthus × giganteus* and *Panicum virgatum* across the conterminous United States. *GCB Bioenergy*, **4**, 509–520.
- Monti, A. and A. Zatta, 2009: Root distribution and soil moisture retrieval in perennial and annual energy crops in northern Italy. *Agr Ecosyst Environ.*, **132**, 252–259.
- Naidu, S. L. and S. P. Long, 2004: Potential mechanisms of low-temperature tolerance of C₄ photosynthesis in *Miscanthus × giganteus*: an in vivo analysis. *Planta*, **220**, 145-155.
- National Operational Hydrologic Remote Sensing Center (NOHRSC), 2004: *Snow Data Assimilation System (SNODAS) data products at NSIDC*. Boulder, CO: National Snow and Ice Data Center. Digital media.
- Nemiroff and Bonnell, cited 2015: Astronomy picture of the day. [Available online at <http://apod.nasa.gov/apod/ap041130.html>.]
- Nicholls, M.E., A.S. Denning, L. Prihodko, P.-L. Vidale, I.T. Baker, K. Davis, and P. Bakwin, 2004: A multiple-scale simulation of variations in atmospheric carbon dioxide using

- a coupled biosphere-atmosphere model. *J. Geophys. Res.-Atmos.*, **109(D18)**, Art No. D18117.
- Olsen, L., J. Andresen, B. Bishop, T. Aichele, J. Brown, S. Marquie, A. Pollyea, and J. Landis, cited 2015: Enviro-weather data and tools. Michigan State University. [Available online at <http://enviroweather.msu.edu/homeMap.php>.]
- Peixoto, M. M., P. C. Friesen, and R. F. Sage, 2015: Winter cold-tolerance thresholds in field-grown *Miscanthus* hybrid rhizomes. *J. Exp. Bot.*, **2015**, doi: 10.1093/jxb/erv093.
- Pennington, D., 2011: Establishing *Miscanthus* as a bioenergy crop can be challenging. Michigan State University Extension. [Available online at http://msue.anr.msu.edu/news/establishing_miscanthus_as_a_bioenergy_crop_can_be_challenging.]
- Philpott, A. W., A. S. Denning, I. T. Baker, K. Corbin, N. P. Hanan, W. W. Hargrove, J. A. Berry, and K. Schaefer, 2008: Simulated surface energy budget at the site level in the southern Great Plains using the Simple Biosphere Model, version 3 (SiB3). [Available online at <https://www.researchgate.net/publication/229038650>.]
- Pielke, R. A., A. Pitman, D. Niyogi, R. Mahmood, C. McAlpine, F. Hossain, K. K. Goldewijk, U. Nair, R. Betts, S. Fall, M. Reichstein, P. Kabat, and N. de Noblet, 2011: Land use/land cover changes and climate: modeling analysis and observational evidence. *WIREs Clim. Change*, **2**, 828-850.
- Plazek, A., F. Dubert, F. Janowiak, T. Krepski, and M. Tatrzenska, 2011: Plant age and in vitro or in vivo propagation considerably affect cold tolerance of *Miscanthus × giganteus*. *Eur. J. Agron.*, **34**, 163–171.

- Pyter, R. J., F. G. Dohleman, and T. B. Voigt, 2010: Effects of rhizome size, depth of planting, and cold storage on *Miscanthus × giganteus* establishment in the Midwestern USA. *Biomass Bioenerg.*, **34**, 1466–1470.
- Reichstein, M., E. Falge, D. Baldocchi, and coauthors, 2005: On the separation of net ecosystem exchange into assimilation and ecosystem respiration: review and improved algorithm. *Glob. Chang. Biol.*, **11**, 1424-1439.
- RFA, 2016: World Fuel Ethanol Production, 2015. Renewable Fuels Association. [Available online at <http://ethanolrfa.org/resources/industry/statistics/>].
- Rosser, B., 2012: Evaluation of *Miscanthus* winter hardiness and yield potential in Ontario. M.S. thesis, Dept. of Plant Agriculture, The University of Guelph, 101 pp.
- Roy, G. R., 2016: The role of lake effect snow cover in reducing the susceptibility of *Miscanthus × giganteus* to extreme cold soil temperatures in Michigan. *Cold Reg. Sci. Technol.*, **2016**, 37-48.
- Sato, N. P.J. Sellers, D.A. Randall, E.K. Schneider, J. Shukla, J.L. Kinter, Y.T. Hou, and E. Albertazzi, 1989: Effects of implementing the Simple Biophere Model in a General Circulation Model. *J. Atmos. Sci.*, **46(18)**, 2757-2782.
- Schaefer, K., G.J. Collatz, P. Tans, A.S. Denning, I. Baker, J. Berry, L. Prihodko, N. Suits, and A. Philpott, 2008: The combined Simple Biosphere/Carnegie-Ames-Stanford Approach (SiBCASA) terrestrial carbon cycle model. *J. Geophys. Res.*, **113**, G03034, doi:10.1029/2007JG000603.
- Schaefer, K., T. Zhang, A. G. Slater, L. Lu, A. Etringer, and I. Baker, 2009: Improving simulated soil temperatures and soil freeze/thaw at high-latitude regions in the

- Simple Biosphere/Carnegie-Ames-Stanford Approach model. *J. Geophys. Res.*, **114**, F02021, doi:10.1029/2008JF001125.
- Schaetzl, R. J. and D. M. Tomczak, 2001: Wintertime soil temperatures in the fine-textured soils of the Saginaw Valley, Michigan. *Great Lakes Geogr.*, **8**, 87–99.
- Schaetzl, R. J., B. D. Knapp, and S. A. Isard, 2005: Modeling soil temperatures and the mesic-frigid boundary in the Central Great Lakes region, 1951–2000. *Soil Sci. Soc. Am. J.*, **69**, 2033–2040.
- Schill, S. R., 2007: Miscanthus versus switchgrass. *Ethanol Producer Magazine*, 3 October 2007.
- Schwalm, C., C.A. Williams, K. Schaefer, R. Anderson, M.A. Arain, I. Baker, A. Barr, T.A. Black, G. Chen, J.M. Chen, P. Ciais, K.J. Davis, A. Desai, M. Dietze, D. Drag- oni, M.L. Fischer, L.B. Flanagan, R. Grant, L Gu, D. Hollinger, R.C. Izaurralde, C. Kucharik, P. Lafleur, B.E. Law, L. Li, Z. Li, S. Liu, E. Lokupitiya, Y. Luo, S. Ma, H. Margolis, R. Matamala, H. McCaughey, R.K. Monson, W.C. Oechel, C. Peng, B. Poul- ter, D.T. Price, D. M. Riciutto, W. Riley, A.K. Sahoo, M. Sprintsin, J Sun, H.Tian, C. Tonitto, H. Verbeeck, and S.B. Verma, 2010: A model-data intercomparison of CO₂ exchange during a large scale drought event: Results from the North American Carbon Program Site Synthesis. *J. Geophys. Res.*, **115**, G00H05, doi:10.1029/2009JG001229.
- Sellers, P.J. and Y Mintz, Y.C. Sud, and A. Dalcher, 1986: A Simple Biosphere Model (SiB) for use within general circulation models. *J. Atmos. Sci.*, **43(6)**, 505-531.
- Sellers, P. J., W. J. Shuttleworth, J. L. Dorman, A. Dalcher, and J. M. Roberts, 1989: Calibrating the Simple Biosphere Model for Amazonian tropical forest using field and remote sensing data, Part I: average calibration with field data. *J. Appl. Meteor.*, **28**, 727-759.

- Sellers, P. J., J. A. Berry, G. J. Collatz, C. B. Field, and F. G. Hall, 1992: Canopy reflectance, photosynthesis, and transpiration, III: a reanalysis using improved leaf models and a new canopy integration scheme. *Remote Sens. Environ.*, **42**, 187-216.
- Sellers, P.J., D.A. Randall, G.J. Collatz, J.A. Berry, C.B. Field, D.A. Dazlich, C. Zhang, G.D. Collelo, and L. Bounoua, 1996a: A revised land surface parameterization (SiB2) for atmospheric GCMs. Part I: model formulation. *J. Climate*, **9(4)**, 676-705.
- Sellers, P. J., C. J. Tucker, G. J. Collatz, S. O. Los, C. O. Justice, D. A. Dazlich, and D. A. Randall, 1996b: A revised land surface parameterization (SiB2) for atmospheric GCMs. Part II: The generation of global fields of terrestrial biophysical parameters from satellite data. *J. Climate*, **9**, 706-737.
- Sharatt, B. S., D. G. Baker, D. B. Wall, R. H. Skaggs, and D. L. Ruschy, 1992: Snow depth required for near steady-state soil temperatures. *Agr. Forest Meteorol.*, **57**, 243-251.
- Sinclair, T. R., G. L. Hammer, and E. J. van Oosterom, 2005: Potential yield and water-use efficiency benefits in sorghum from limited maximum transpiration rate. *Func. Plant Biol.*, **32**, 945-952.
- Skamarock, W. C., J. B. Klemp, J. Dudhia, D. O. Gill, D. M. Barker, W. Wang, and J. G. Powers, 2007: A description of the Advanced Research WRF Version 2. *NCAR Tech. Note*, NCAR/TN-468+STR, 88 pp.
- Song, Y., A. K. Jain, W. Landuyt, H. S. Kheshgi, and M. Khanna, 2014: Estimates of biomass yield for perennial bioenergy grasses in the USA. *Bioenerg. Res.*, doi:10.1007/s12155-014-9546-1.
- Sutinen, R., P. Hänninen, and A. Venäläinen, 2008: Effect of mild winter events on soil water content beneath snowpack. *Cold Reg. Sci. Technol.*, **51**, 56-67.

- Thelen, K., J. Gao, K. Withers, and W. Everman, 2009: Agronomics of producing switchgrass and *Miscanthus × giganteus*. 2009 Bioeconomy eConference, Ames, IA, Iowa State Univ. [Available online at <http://www.bioeconomyconference.org/Documents/Kurt-Thelen-MSU.pdf>.]
- US DoE, 2006.: Breaking the biological barriers to cellulosic ethanol: a joint research agenda. DOE/SC/EE-0095, U.S. Department of Energy Office of Science and Office of Energy Efficiency and Renewable Energy [Available online at https://public.ornl.gov/site/gallery/originals/Geographic_Distributio.jpg.]
- US House, 2007: Energy Independence and Security Act of 2007. 110th Congress, H.R. 6. Government Printing Office.
- VanLooke, A., C. J. Bernacchi, and T. E. Twine, 2010: The impacts of *M. × giganteus* production on the Midwest US hydrologic cycle. *GCB Bioenergy*, **2**, 180-191.
- VanLooke, A., T. E. Twine, M. Zeri, and C. J. Bernacchi, 2012: A regional comparison of water use efficiency for *Miscanthus*, switchgrass, and maize. *Agric. For. Meteorol.*, **164**, 82-95.
- Vidale, P.L. and R. Stöckli, 2005: Prognostic canopy air space solutions for land surface exchanges. *Theor. Appl. Climatol.*, **80**, 245- 257, doi:10.1007/s00704-004-0103-2.
- Wang, J.-W., A. S. Denning, L. Lu, I. T. Baker, K. D. Corbin, and K. J. Davis, 2007: Observations and simulations of synoptic, regional, and local variations in atmospheric CO₂. *J. Geophys. Res.*, **112**, D04108, doi:10.1029/2006JD007410.
- WMO, 2015: Surface Soil Moisture data. Accessed 28 December 2015. [Available online at <http://www.pecad.fas.usda.gov/cropexplorer/description.aspx?legendid=207®ionid=useast>.]

- Xie, L., S. Lewis, M. Auffhammer, D. Jaiswal, and P. Berck, 2013: The not so big squeeze: modeling future land use patterns of *Miscanthus* for bioenergy using fine scale data. [Available online at http://www.vatt.fi/file/torstaiseminaari%20paperit/2014/berck_seminar_paper2.pdf.]
- Young, J., 2015: *Climate Data*. Wisconsin State Climatology Office, Madison, WI. Digital media.
- Zaitchik, B. F., J. A. Santanello, S. V. Kumar, and C. D. Peters-Lidard, 2013: Representation of soil moisture feedbacks during drought in NASA Unified WRF (NU-WRF). *J. Hydrometeorol.*, **14**, 360-367
- Zeri, M., K. Anderson-Teixeira, G. Hickman, M. Masters, E. DeLucia, and C.J. Bernacchi, 2011: Carbon exchange by establishing biofuel crops in central Illinois. *Agric. Ecosyst. Environ.*, **144**, 319-329.
- Zeri, M., M. Z. Hussain, K.J. Anderson-Teixeira, E. DeLucia, and C .J. Bernacchi, 2013: Water use efficiency of perennial and annual bioenergy crops in central Illinois. *J. Geophys. Res. Biogeosci.* **118**, 581–589.